

LIGHT INDUCED OXIDATIVE DEGRADATION
STUDIES OF ORGANIC DYES AND THEIR
INTERMEDIATES

THESIS

**SUBMITTED IN FULFILLMENT OF THE REQUIREMENT
FOR THE AWARD
OF
DOCTOR OF PHILOSOPHY**

BY

SUMANDEEP KAUR



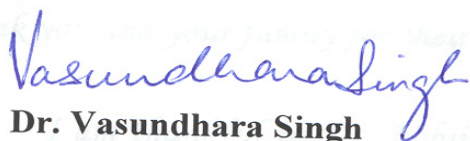
SCHOOL OF CHEMISTRY & BIOCHEMISTRY
THAPAR UNIVERSITY
PATIALA-147004 (PB.)
INDIA

DEDICATED TO MY PARENTS

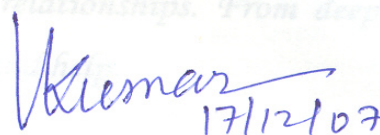
ACKNOWLEDGMENTS

CERTIFICATE

This thesis is the result of many a long hour involving arduous research and the culmination of a process that included the constant assistance, support & guidance afforded. This is to certify that the thesis entitled “**LIGHT INDUCED OXIDATIVE DEGRADATION STUDIES OF ORGANIC DYES AND THEIR INTERMEDIATES**” which is submitted by Ms. Sumandeep Kaur in fulfillment of the requirement for the award of the Degree, Doctor of Philosophy in Chemistry, Thapar University, Patiala is a record of the candidate’s own work carried out by her under my supervision and guidance. The matter embodied in this thesis has not been submitted in part or full to any other University or Institution for the award of any degree.



Dr. Vasundhara Singh
Formerly Asstt. Prof. & Head
School of Chemistry and Bio-Chemistry
Thapar University, Patiala
Presently Asstt. Prof. (Chemistry)
Dept. of Applied Sciences
Punjab Engg. College
Chandigarh



Dr. Vineet Kumar
Head of the Dept.
Dept. of Chemical Engg.
Thapar University
Patiala, 147004

I would like to thank all those members of the laboratory who have contributed to make my stay very pleasant. I am particularly thankful to the...

ACKNOWLEDGMENTS

This thesis is the result of many a long hour involving arduous research and the culmination of a process that included the constant assistance, support & guidance afforded to me by my fellow academicians whom I am deeply indebted. This achievement been accomplished, in no small measure, due to their sheer professionalism and dedication which they demonstrated time after time. It is to them that I owe my heartfelt thanks and the overwhelming sense of satisfaction that I feel at this stage.

A special thank you to Dr. Vasundhara Singh, my supervisor who greatly enriched my knowledge & constantly inspired me and who, in my pursuit of this thesis, had to sacrifice many of her precious hours. She has been able to skilfully manage this research without forgetting the ever essential human relationships. From deep inside thank you and your family for their opportune support and help.

I am thankful to Dr. Abhijit Mukherjee (Director, Thapar University, Patiala) for providing the practical support in allowing me use of their laboratories & facilities. My overwhelming thanks go to Dr. Vineet Kumar for his encouragement and support especially on the administrative grounds. I cannot overstate the importance of his involvement in my doctorate career. I would like to extend my thanks to Dr. Susheel Mittal (Dean – R&SP & HOD, SCBC) for his moral support during the completion of this research work and for providing all possible laboratory facilities to carry out the experimentation.

I would like to thank all those members of the laboratory who have contributed to make my stay very pleasant. I am particularly thankful to Dr. Varinder Saphyia & Mr. Vivek Srivastava for their invaluable help and friendliness. I would like to extend my gratitude to Dr. A.P. Toor & Mr. Anoop Verma for their friendliness, help and other useful discussions about work. I am indebted to the fellow students Ms. Sukhbir Kaur, Ms. Nidhi, Mr. Vineet, Ms. Rajni and Mr. Gulshan for their support and

encouragement. I am also very grateful to Dr. Ashok Kumar for his practical support and assistance.

I would like to offer my heartfelt thanks to Dr. Rakesh Kumar Saini who enabled me to be able to pursue my academic dream. He is an inextinguishable source of encouragement when things did not go so well. Thank you for your unconditional and invaluable support and for your heartfelt help.

A special mention to my parents who through thick & thin were always there for me and never doubted my abilities to achieve my goal. Mom and Dad, thanks for your constant support and enthusiasm.

I would like to thank my husband Mr. Rajdeep Singh Hara & my in laws who enabled me to seamlessly continue my thesis. Huge thanks to my husband for being incredibly understanding, supportive, patient, and for putting up with late hours and my bad temper. Thanks for his editing assistance.

All these thanks are, however, only fraction of what is due to Almighty for granting me an opportunity and strength to successfully accomplish this assignment.

SUMANDEEP

ABSTRACT

Problem Formulation

Reactive dyes are the largest single group of dyes used in the textile industry and have been selected for our study because they are difficult to eliminate by biodegradation and sludge adsorption techniques in the wastewater treatment plants. The work on photocatalytic oxidative degradation studies of reactive dyes in literature is limited as compared to other dyes. Reactive dyes are known to form a covalent bond with the fibre in the dyeing process. This leads to favorable properties such as wash-fastness. However, unfixed dye reacts with water to form hydrolyzed or an oxo-dye intermediate that has lost its bonding capacity and thus cannot be reused. Therefore dye recovery is not an option with reactive dyes and the treatment process must lead to final destruction or disposal of these contaminants. One method to remove reactive dyes from the wastewater is sorption into sorbents in fixed bed filters but no successful regeneration has been reported. Moreover, adsorption transfers the toxic dyes from one medium to the other without converting it to harmless non-toxic substances.

The application of novel treatment methods encompasses investigations of advanced oxidation processes (AOP's), which are characterized by production of the hydroxyl radical (OH) as a primary oxidant. Examples of AOP's include the use of (H₂O₂/UV), semiconductor photocatalysis, ozonolysis and ultrasonic irradiation (sonolysis), (ultrasound/O₃) as important segmental or parallel processes and are found to enhance OH radical production leading to higher oxidation rates and organic matter mineralization. In this work, we investigated the photocatalytic oxidative degradation and discoloration of various reactive dyes and dye intermediates using light (UV/visible)/semiconductor catalyst by optimizing the operational parameters to ensure the rapid and complete transformation of the toxic organic compounds to benign chemicals. Also the simultaneous sonochemical effect along with photochemical oxidation process (light/semiconductor/ultrasound) is used which leads to faster destruction rate.

Work Accomplished

The work done in this study has been presented in **seven chapters** as discussed in the following text. After introducing the problem and its content in **chapter 1**, the study begins with the literature review in **chapter 2**. Literature of various types of toxic pollutants present in the industrial effluents, dyes, photocatalytic degradation, ultrasound, reactor design, mechanism of photosensitization of TiO₂ under visible, UV and solar light have been summarized in this chapter.

In **chapter 3** experimental procedures, description of reactors, instruments used and analytical techniques are discussed in detail. Chapters four, five and six deal with degradation and kinetic studies of Reactive Red 198 (RR dye198), J-acid and industrial effluent respectively. Conclusions are drawn in **chapter seven**.

In **chapter 4**, photocatalytic degradation of Reactive Red 198 (RR 198) has been investigated in aqueous heterogeneous solution using different catalysts (Degussa P25 TiO₂, ZnO, Hombikat UV-100) in immersion well and shallow pond slurry type reactors under UV, visible and solar light. The disappearance of the dye follows approximately pseudo-first order kinetic according to the Langmuir-Hinshelwood model. The adsorption of dye on the semiconductor shows a strong dependence on the pH and follows a Langmuir adsorption model. The studies include dark adsorption experiments at different pH conditions. The degradation was determined by UV-Vis and decrease in COD with time. The acceleration of photocatalytic degradation of RR 198 under visible light using dye sensitized TiO₂ activation by the synergistic effect of ultrasound is also reported. The effect of sonolysis, photocatalysis and sonophotocatalysis under visible light has been examined to study the influence on the degradation rates by varying the initial substrate concentration, pH, catalyst loading, H₂O₂ concentration to ascertain the synergistic effect on the degradation techniques. Further the presence and role of oxidative species, such as singlet oxygen (¹O₂), superoxide (O₂^{•-}) and hydroperoxy (HO₂[•]) radicals was examined with the use of appropriate quenchers of these species. The photocatalytic activity of RR dye 198 dye sensitized TiO₂ is demonstrated by the degradation of phenol in the presence of visible light. A comparative study using TiO₂, Hombikat UV 100 and ZnO was also carried out. GC-MS of the extract left after photocatalytic degradation was done to study the intermediates formed during the reaction and thus to determine the reaction pathway. Recyclability of the photocatalyst was also studied to make the process more economical.

Besides, modification of the catalyst by sensitizers enhances the applicability of the catalyst in utilizing both UV and visible light. This technology was extended to the degradation of dye intermediates under visible light.

In **chapter 5**, degradation of a dye intermediate J-acid has been carried out in the presence of UV and visible light using Degussa P25 TiO₂ and sensitized TiO₂ (TiO₂ sensitized with Rose Bengal) in an immersion well type reactor. Degradation was carried out by varying the parameters like pH, initial concentration, catalyst loading and optimum conditions were determined. Effect of electron acceptors was also determined. Effect of various photocatalysts (ZnO, Degussa P25, Hombikat UV 100) was also studied on the photodegradation rate of J-acid. The degradation was studied by monitoring the change in substrate concentration employing UV-spectroscopic analysis. Photodegradation of J-acid was also carried out in sunlight in a shallow pond type reactor under optimized conditions. To study the synergistic effect of ultrasound, sonophotocatalytic degradation of J-acid was carried out under the optimized conditions. To extend the application of the process to industrial scale and to make the process cost effective, recyclibility of the photocatalyst was also studied under UV light.

In **chapter 6**, the degradation of effluent from a textile industry was done on laboratory scale in a shallow pond type reactor using Degussa P25 under sunlight. The degradation was done by varying conditions like pH, catalyst loading, initial concentration, A/V ratio and electron acceptors such as hydrogen peroxide. The degradation was studied by monitoring the decrease in COD values as a function of irradiation time. Recyclibility of the photocatalyst was also studied so as to make the process cost effective. The optimum degradation parameters for maximum degradation were determined. Total solids, total dissolved solids and total suspended solids in the effluent were also determined.

In **chapter 7**, the conclusions of the entire work are drawn.

CONTENTS

	PAGE NO.
CERTIFICATE	ii
ACKNOWLEDGEMENTS	iii
ABSTRACT	v
LIST OF TABLES	xiv
LIST OF FIGURES	xv
LIST OF ABBREVIATIONS	xix
CHAPTER- 1 INTRODUCTION	1-20
1.1 Dyes and their intermediates, environmental concern	1
1.2 Dye classification	2
1.2.1 Acid dyes	2
1.2.2 Reactive dyes	3
1.2.3 Metal complex dyes	3
1.2.4 Direct dyes	4
1.2.5 Basic dyes	4
1.2.6 Mordant dyes	4
1.2.7 Disperse dyes	4
1.2.8 Pigment dyes	4
1.2.9 Vat dyes	5
1.2.10 Anionic dyes and ingrain dyes	5
1.2.11 Sulphur dyes	5
1.2.12 Solvent dyes	5
1.3 Other dye classes and dye intermediates	6
1.4 Discharge statistics of dyes	7
1.5 Methods for removal of dyes and other organic compounds from wastewater	8
1.6 Advanced Oxidation Processes	8
1.6.1 Homogeneous photocatalysis	9
1.6.2 Heterogeneous photocatalysis	10

1.7	Ultrasound and Photocatalysis	13
1.8	Catalyst	14
1.9	Kinetics	17
1.10	Reactors	18
1.10.1	Concentrating reactors	18
1.10.2	Non-concentrating reactors	19
1.11	Objectives of the work undertaken	19
1.12	Approach adopted	20
CHAPTER- 2	LITERATURE REVIEW	21-53
2.1	AOP's- Homogeneous and Heterogeneous	21
2.2	Degradation of Pesticides, Chloro-organic compounds and Detergents	24
2.3	Degradation of Dyes and Dye Intermediates	25
2.3.1	Review	25
2.3.2	Degradation studies of various classes of dyes	26
2.3.3	Degradation of Dye Intermediates	29
2.4	Catalyst	29
2.4.1	Surface Modifications of TiO ₂	32
2.4.2	Metal modification of TiO ₂	32
2.4.3	Composite semiconductors	35
2.4.4	Catalyst in the Form of Fixed Matrix	37
2.4.5	Catalyst modification for harnessing visible light	38
2.5	Solar technology and textile effluent	41
2.6	Ultrasound and Photocatalysis	43
2.7	Coupled Photocatalytic and Biological treatment	47
2.8	Kinetics and Analytical Techniques	49
2.9	Reactors for Wastewater Treatment	53
CHAPTER- 3	MATERIAL AND METHODS	54-61
3.1	Materials	54
3.1.1	Samples	54
3.1.2	Catalysts used	54

3.1.3	Reagents and Chemicals	55
3.2	Equipment and Instruments	55
3.2.1	Radiometer	55
3.2.2	pH meter	56
3.2.3	UV-Vis Spectrophotometer	56
3.2.4	Filtration	56
3.2.5	Ultrasonic Bath	56
3.2.6	Autoclave	56
3.3	Photoreactors	56
3.3.1	Immersion well type photoreactor	56
3.3.2	Shallow pond slurry reactor	57
3.4	Experimental Procedures	58
3.4.1	Adsorption Experiments	58
3.4.2	Experiments using Immersion well Photoreactor	58
3.4.3	Experiments using Shallow pond slurry reactor under sunlight	59
3.5	Sample collection and storage of wastewater sample	59
3.6	Water Analysis	60
3.6.1	Total Solids	60
3.6.2	Total Dissolved Solids	60
3.6.3	Total suspended solid	60
3.6.4	Estimation of BOD	60
3.6.5	Estimation of COD	60
3.6.6	GC- MS analysis	60
3.6.7	Using UV- Visible Spectrophotometer	61
3.7	Biodegradability of Organic Pollutants	61
CHAPTER-	PHOTOCATALYTIC DEGRADATION OF	62-75
4 (A)	REACTIVE RED 198 UNDER UV LIGHT	
4.1	Overview	62
4.1.1	Structure of Reactive Red 198	62
4.1.2	Adsorption Equilibrium in Dark Conditions	62
4.1.3	Dye Degradation and Decolorization- TiO ₂ suspensions using Immersion Well Reactor	64

4.1.4	Kinetic Studies	65
4.1.5	Mineralization of RR dye 198	65
4.1.6	Effect of catalyst loading	66
4.1.7	Effect of initial substrate concentration	67
4.1.8	Effect of initial pH of the solution	68
4.1.9	Effect of H ₂ O ₂ addition	69
4.1.10	Efficiency of the recycled catalyst	70
4.1.11	Comparison of Photodegradation of RR dye198 under UV light and solar light using Shallow Pond slurry reactor	70
4.1.12	Discussion	71
CHAPTER –	PHOTOCATALYTIC AND	76-90
4 (B)	SONOPHOTOCATALYTIC DEGRADATION	
	OF REACTIVE RED 198 UNDER VISIBLE	
	LIGHT	
4.2	Overview	76
4.2.1	Photocatalytic and Sonophotocatalytic Degradation of RR 198 Using Immersion Well reactor	76
4.2.2	Decolorization and kinetic analysis	77
4.2.3	Effect of catalyst loading	78
4.2.4	Effect of initial substrate concentration	79
4.2.5	Effect of initial pH	80
4.2.6	Effect of H ₂ O ₂ addition	82
4.2.7	Effect of various photocatalysts	82
4.2.8	Effect of radical quenchers	83
4.2.9	Identification of degraded intermediates	84
4.2.10	Decomposition of phenol by dye-sensitized TiO ₂ under visible light	86
4.2.11	Discussion	87
CHAPTER	PHOTOCATALYTIC DEGRADATION OF J-	91-102
5 (A)	ACID UNDER UV LIGHT	
5.1	Overview	91

5.1.1	Structure of J-acid	91
5.1.2	Adsorption Equilibrium under Dark Conditions	92
5.1.3	Photocatalytic Degradation of J-acid Using Immersion Well Reactor	92
5.1.4	Kinetics of J-acid disappearance	92
5.1.5	Mineralization of J-acid	93
5.1.6	Effect of catalyst loading	94
5.1.7	Effect of initial substrate concentration	95
5.1.8	Effect of initial pH of the solution	95
5.1.9	Effect of Electron acceptors	96
5.1.10	Effect of different catalysts	97
5.1.11	Efficiency of the recycled catalyst	98
5.1.12	Comparison of Photodegradation of J-acid under UV light and Solar light using Shallow Pond Slurry Reactor	98
5.1.13	Discussion	99
CHAPTER -	PHOTOCATALYTIC DEGRADATION OF	103-112
5 (B)	J-ACID UNDER VISIBLE LIGHT	
5.2	Overview	103
5.2.1	Photocatalytic Degradation of J-acid Using Immersion well slurry reactor	103
5.2.2	Structure and Absorption Spectra of J-acid with sensitized TiO ₂	103
5.2.3	Kinetics of disappearance of J-acid	104
5.2.4	Influence of the amount of TiO ₂ in suspension	105
5.2.5	Effect of pH on degradation of J-acid	106
5.2.6	Influence of initial substrate concentration on degradation rate of J- acid	106
5.2.7	Effect of H ₂ O ₂ concentration	107
5.2.8	Comparison of degradation efficiency under photocatalytic and sonophotocatalytic conditions	108
5.2.9	Mineralization of J-acid	109
5.2.10	Discussion	109

CHAPTER-6	PHOTOCATALYTIC TREATMENT OF	113-125
	TEXTILE EFFLUENT UNDER SUNLIGHT	
6.1	Photocatalytic Degradation of Textile Effluent Using reactor Shallow pond slurry	113
6.2	Textile Effluent Characteristics	113
6.3	Absorption Spectra for Raw Effluent	114
6.4	Solar Photocatalytic Pretreatment	114
6.4.1	Sample Preparation	115
6.4.2	Radiation Conditions in Punjab(India) during Summers	115
6.4.3	Experiments with TiO ₂	115
6.4.4	Effect of initial pH	116
6.4.5	Effect of Oxidant addition	117
6.4.6	Effluent characteristics after Solar Photocatalytic Pretreatment	118
6.4.7	Color Removal	118
6.4.8	Absorption Spectra of Effluent after Photocatalytic Treatment	119
6.4.9	Effect of different Catalysts	119
6.4.10	Recycling of TiO ₂	120
6.4.11	Effect of A/V ratio of the reactor	121
6.5	Discussion	121
CHAPTER- 7	CONCLUSIONS	126-128
	REFERENCES	129-153
	LIST OF PUBLICATIONS	154

LIST OF TABLES

TABLE NO.	TITLE	PAGE NO.
Table 1.1	Hydroxyl radical generation in different AOP's (Homogeneous)	10
Table 1.2	Band positions of some common semiconductor photocatalysts in aqueous solution at pH=1	15
Table 2.1	Main ranges of pollutants	24
Table 4.1.1	Langmuir equilibrium constants for the adsorption of RR dye 198 on TiO ₂ in dark	63
Table 4.1.2	Effect of TiO ₂ loading on the degradation rate during the photocatalytic oxidation ($C_o = 100 \text{ g L}^{-1}$, pH = 4.6)	66
Table 4.1.3	Langmuir-Hinshelwood constants for the photodegradation of RR dye 198 at different pH values	69
Table 4.2.1	First order rate constants of RR dye 198 degradation under Sonolysis in the presence of dye sensitized TiO ₂ , photocatalysis and sonophotocatalysis	79
Table 4.2.2	Langmuir-Hinshelwood constants for the photodegradation of RR dye 198 at different pH values	81
Table 5.1.1	Effect of TiO ₂ loading on the degradation rate during the photocatalytic oxidation ($C_o = 100 \text{ g L}^{-1}$, pH = 5.7)	94
Table 5.1.2	Effect of initial concentration on the degradation rate during the photocatalytic oxidation ($C_o = 100 \text{ g L}^{-1}$, pH = 5.7)	95
Table 5.2.1	Effect of initial concentration of J-acid on the photodegradation rate	107
Table 6.1	Characteristics of raw textile effluent from S.R. Industries	114
Table 6.2	Showing change in pH values of the treated water by photocatalysis	117
Table 6.3	Characteristics of the wastewater after solar Photocatalytic treatment	118

LIST OF FIGURES

FIGURE NO.	TITLE	PAGE NO.
Fig. 1.1	Principle of cotton dyeing with a triazol reactive dye	3
Fig. 1.2	Molecular structure of few Organic dyes	6
Fig. 1.3	Dye intermediates	7
Fig. 1.4	Scheme showing some of the events that might be taking place on an irradiated semiconductor particle	11
Fig. 1.5	Mechanism of TiO ₂ under UV and visible light	16
Fig. 2.1	Solar spectrum at sea level with sun at zenith	32
Fig. 2.2	Metal-modified semiconductor photocatalyst particle	33
Fig. 2.3	Photo-excitation in composite semiconductor - semiconductor photocatalyst	35
Fig. 2.4	Excitation steps using dye molecule sensitizer	39
Fig. 3.1	Eppley radiometer	55
Fig. 3.2	Laboratory setup for immersion well type reactor	57
Fig. 3.3	Schematic diagram of lab scale set up for shallow pond reactor	57
Fig. 4.1.1	Structure of Reactive Red 198	62
Fig. 4.1.2	Adsorption isotherms of RR dye 198 on TiO ₂ surface at different initial pH	63
Fig. 4.1.3	Laboratory set up for the photocatalytic degradation of RR dye198 under UV light	64
Fig. 4.1.4	Spectral changes in RR dye 198 during UV irradiation	64
Fig. 4.1.5	Photocatalytic degradation of RR dye 198	65
Fig. 4.1.6	Kinetics of photodegradation of RR dye198	65
Fig. 4.1.7	Relationship between $\ln r_0$ and $\ln [TiO_2]$	67
Fig. 4.1.8	Kinetics of photodegradation of RR dye 198 at different initial concentration	67
Fig. 4.1.9	Representation of Langmuir-Hinshelwood equation	68
Fig. 4.1.10	Effect of pH on initial rate of degradation of RR dye 198	68
Fig. 4.1.11	Effect of H ₂ O ₂ concentration on the initial rate	69
Fig. 4.1.12	Recyclibility of TiO ₂	70

Fig. 4.1.13	Photocatalytic degradation of RR dye 198 in presence of sunlight	71
Fig. 4.2.1	Laboratory set up for the sonophotocatalytic degradation of RR dye 198 under visible light	76
Fig. 4.2.2	Spectral changes that occur during the sonophotocatalytic degradation of aqueous solution of RR dye 198	77
Fig. 4.2.3	Color Removal during Photocatalysis	77
Fig. 4.2.4	First order kinetic plots of RR dye 198 degradation under Vis. light, US+TiO ₂ , Vis+TiO ₂ ,US+Vis+TiO ₂	78
Fig. 4.2.5	Rate constants of RR dye 198 degradation under US+TiO ₂ , Vis+TiO ₂ , US+Vis+TiO ₂ as a function of TiO ₂ conc.	79
Fig. 4.2.6	Initial rate of RR dye 198 degradation, r_0 , under US+TiO ₂ +Vis, Vis+ TiO ₂ , US+TiO ₂ , as a function of the initial dye conc.	80
Fig. 4.2.7	Effect of pH on degradation of RR dye 198 under US+TiO ₂ +Vis, Vis+ TiO ₂	80
Fig. 4.2.8	Representation of Langmuir-Hinshelwood equation: [dye] = 50 mg L ⁻¹ , pH = 4.6, [TiO ₂] = 0.3 g L ⁻¹	81
Fig. 4.2.9	Effect of H ₂ O ₂ concentration on the initial rate under TiO ₂ +Vis, TiO ₂ +Vis+US	82
Fig. 4.2.10	Effect of various Photocatalysts on degradation of RR dye 198 under Photocatalytic and sonophotocatalytic conditions	83
Fig. 4.2.11	Effect of radical quenchers on the degradation rate under sonophotocatalytic conditions	84
Fig. 4.2.12	GC-MS analysis of residue of RR dye 198 after sonophotocatalytic degradation	85
Fig. 4.2.13	MS of the major product (phthalic acid derivative) identified with Retention time-39.81min and fragmentation pattern	86
Fig. 4.2.14	Sonophotocatalytic decomposition of phenol by RR dye 198 adsorbed TiO ₂ under visible light	87

Fig. 5.1.1	Structure of J-acid	91
Fig. 5.1.2	Absorption spectra of J-acid showing the changes before (curve A) and after (curve B) irradiation	92
Fig. 5.1.3	Photocatalytic degradation of J-acid under only UV, only TiO ₂ and TiO ₂ +UV light	93
Fig. 5.1.4	Kinetics of photodegradation of J-acid	93
Fig. 5.1.5	Effect of catalyst loading on degradation rate of J-acid	94
Fig. 5.1.6	Rate constant vs reciprocal of initial conc. of J-acid	95
Fig. 5.1.7	Effect of pH on the degradation rate of J-acid	96
Fig. 5.1.8	Effect of H ₂ O ₂ on the degradation rate of J-acid	97
Fig. 5.1.9	Effect of ammonium persulphate on the degradation rate of J-acid	97
Fig. 5.1.10	Effect of different catalysts on the degradation rate of J-acid	97
Fig. 5.1.11	Recyclability of the catalyst	98
Fig. 5.1.12	Photocatalytic degradation of J-acid in presence of sunlight and under artificial UV light	99
Fig. 5.1.13	Structural changes in J-acid with pH	100
Fig. 5.2.1	Absorption Spectra of J-acid with sensitized TiO ₂	104
Fig. 5.2.2	Photocatalytic degradation of J-acid using TiO ₂ and Vis. light, Vis. light only and TiO ₂ only	104
Fig. 5.2.3	Plot of ln (C ₀ /C) vs time for degradation of J-acid using sensitized TiO ₂	105
Fig. 5.2.4	Influence of catalyst concentration on degradation rate	105
Fig. 5.2.5	Effect of pH on degradation rate of J-acid	106
Fig. 5.2.6	Plot of rate constant vs reciprocal of initial concentration of J-acid	107
Fig. 5.2.7	Effect of addition of H ₂ O ₂ addition on the degradation rate constant of J-acid	108
Fig. 5.2.8	Concentration versus time profile for the degradation of J-acid under photocatalytic and sonophotocatalytic conditions	108
Fig. 6.1	Absorption Spectra of Raw Effluent	114

Fig. 6.2	Intensities of solar radiations during experimental days	115
Fig. 6.3	Effect of catalyst concentration on the COD reduction	116
Fig. 6.4	Effect of pH on the % degradation of the effluent	116
Fig. 6.5	Effect of oxidant addition (H ₂ O ₂) on the COD reduction	118
Fig. 6.6	Color removal after photocatalytic treatment	119
Fig. 6.7	Absorption spectra of effluent after photocatalytic Treatment	119
Fig. 6.8	Effect of different catalysts	120
Fig. 6.9	Recyclization of TiO ₂	120
Fig. 6.10	Effect of A/V ratio on COD reduction	121

LIST OF ABBREVIATIONS

AOP's	Advanced Oxidation Processes
A/V	Area to volume ratio
b	Equilibrium parameter
BOD	Biological oxygen demand
BQ	1, 4-Benzoquinone
C	Solute concentration
C ₀	Initial concentration
C _e	Concentration of dye in aqueous solution
CB	Conduction band
C.I	Color index
COD	Chemical oxygen demand
4-CP	4-Chlorophenol
CVD	Chemical Vapor Deposition
DABCO	1, 4-diazabicyclo [2, 2, 2] octane
E _{bg}	Band gap energy
EDTA	Ethylene diaminetetraacetic acid
EPA	Environmental Protection Agency
g	Grams
GC-MS	Gas Chromatography-Mass Spectroscopy
h	hour
HKUST	Hong Kong University of Science and Technology
HOQ	8-Hydroxyquinoline
H&S	Health and Safety
I	Intensity
k ₁	Reaction rate constant
k ₂	Equilibrium adsorption constant
K	Rate constant
k _{app}	Apparent rate constant
k _{act}	Actual rate constant
K _a	Langmuir equilibrium constant
L	Litre

L-H	Langmuir-Hinshelwood
mg	Milligrams
min	Minute
4-NP	4-Nitrophenol
ppm	Parts per million
Q_e	Concentration of dye in the solid
q_m	Maximum amount of dye adsorbed
R^2	Regression value
RB	Rose Bengal
RR dye 198	Reactive Red dye 198
r_o	Initial rate of reaction
t	Time
TFFBR	Thin-film fixed-bed reactor
TDS	Total Dissolved Solids
TOC	Total organic content
TS	Total Solids
TSS	Total Suspended Solids
UV	Ultraviolet light
US	Ultrasound
Vis	Visible light
VB	Valence band

Chapter 1

INTRODUCTION

After oil, what do you think is the most important commodity? Imagine the wars we will get into when the commodity is even more critical than oil, say *Water?* In fact, since it is a basic necessity for life itself, one would be inclined to believe that it is more important than oil or money. By 2010, water shortage in many developing countries is recognized as one of the most serious political and social issues. Steps should be taken for recycling wastewater of the various industries as water has now become a key symbol of protest around the world and is seen as the most serious social and political issue of this generation.

A large number of organic substances are nowadays introduced into the water system from various sources such as industrial effluents, agricultural runoff and chemical spills. Their toxicity, stability to natural decomposition and persistence in the environment has been the cause of much concern to societies and regulation authorities around the world.

Till recently, the discharging of waste into the environment was the way to eliminate them. The permitted discharge levels have been vastly exceeded, causing such environmental contamination that our natural resources cannot be used for certain purposes and their characteristics have been altered. Dyes, phenols, pesticides, fertilizers, detergents, and other chemical products are disposed of directly into the environment, without being treated, controlled or uncontrolled and without an effective treatment strategy. Color removal from the textile wastewater has become an issue of interest during the last few years because of the toxicity of the dyes and more often the colored wastewater from the textile industries also decreases the visibility of the receiving waters.

1.1 Dyes and their intermediates, environmental concern

The textile dyes and dye intermediates with high aromaticity and low biodegradability have emerged as major environmental pollutants (Arslan et al., 2000; Sauer et al., 2002) and nearly 10-15% of the dye is lost in the dyeing process and is released in the wastewater which is an important source of environmental contamination.

Considerable amount of water is used for dyeing and finishing of fabrics in the textile industries.

The wastewater from textile mills causes serious impact on natural water bodies and land in the surrounding area. High values of COD and BOD, presence of particulate matter and sediments, chemicals which are dark in color leading to turbidity in the effluents causes depletion of dissolved oxygen, which has an adverse effect on the marine ecological system. As dyes are designed to be chemically and photolytically stable, they are highly persistent in natural environments. The improper handling of hazardous chemicals in textile water also has some serious impact on the health and safety of workers putting them into the high-risk bracket for contracting skin diseases like chemical burns, irritation, ulcers, etc. and respiratory problems.

1.2 Dye classification

All aromatic compounds absorb electromagnetic energy but only those that absorb light with wavelengths in the visible range (~350-700 nm) are colored. Dyes contain *chromophores*, delocalized electron systems with conjugated double bonds, and *auxochromes*, electron-withdrawing or electron-donating substituents that cause or intensify the color of the chromophore by altering the overall energy of the electron system. Usual chromophores are -C=C-, -C=N-, -C=O, -N=N-, -NO₂ and quinoid rings, while the auxochromes are -NH₃, -COOH, -SO₃H and -OH groups. Based on chemical structure or chromophore, 20-30 different groups of dyes can be discerned. Each different dye is given a C.I. (Color Index) generic name determined by its application characteristics and its color. The Color Index discerns different application classes which are as follows (Abrahart, 1977):

1.2.1 Acid dyes

The largest class of dyes in the Color index is *Acid dyes*. Acid dyes are anionic compounds that find their main application in dyeing nitrogen-containing fabrics like wool, polyamide, silk and modified acryl. They bind to the cationic NH₄⁺ ions of those fibres. Most acid dyes are azo, anthraquinone or triarylmethane, azine, xanthene, nitro and nitroso compounds. Rather than the presence of acid groups (sulphonate, carboxyl) in the molecular structure of these dyes, the term 'acid' refers to the pH of the dyebaths.

1.2.2 Reactive dyes

Reactive dyes are dyes with reactive groups that are capable of forming a covalent bond between a carbon atom of dye molecule and OH-, NH-, or SH- groups in fibres (cotton, wool, silk, nylon). The reactive group is often a heterocyclic aromatic ring substituted with a chloride or fluoride atom, e.g. dichlorotriazine. Another common reactive group is vinyl sulphone. Most (~80%) reactive dyes are azo or metal complex azo compounds but also anthraquinone and phthalocyanine reactive dyes are applied, especially for green and blue color. In the Color Index, the reactive dyes form the second largest dye class. During dyeing with reactive dyes (Fig. 1.1), hydrolysis (i.e. inactivation) of the reactive groups is an undesired side reaction that lowers the degree of fixation. Salt and ureum (up to 60 and 200 g L⁻¹ respectively) is added during the dyeing process to increase the degree of fixation.

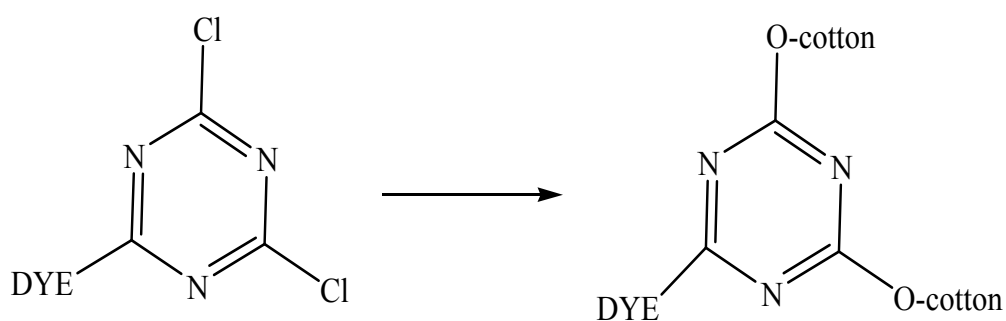


Fig. 1.1 Principle of cotton dyeing with a triazolyl reactive dye

The reactive dyes are commercially available important class of textile dyes for which losses through processing operations are significant and the treatment is problematic. It is estimated that 10 to 50% of the dye will not react with the fabric and remain hydrolyzed or unfixed form in the water phase. The problem of colored effluents is therefore mainly due to the use of reactive dyes.

1.2.3 Metal complex dyes

Among acid and reactive dyes, many metal complex dyes can be found (not listed as a separate category in the Color Index). These are strong complexes of one metal atom (usually chromium, copper, cobalt or nickel) and one or two dye molecules, respectively i.e. 1:1 and 1:2 *metal complex dyes*. Metal complex dyes are usually azo compounds.

1.2.4 Direct dyes

Direct dyes are relatively large molecules with high affinity for cellulose fibres. Vander Waal forces make them bind to the fibre. Direct dyes are mostly azo dyes with more than one azo bond or phthalocyanine, stilbene or oxazine compounds. In the Color Index, the direct dyes form the second largest dye class with respect to the amount of different dyes.

1.2.5 Basic dyes

Basic dyes are cationic compounds that are used for dyeing acid-group containing fibres, usually synthetic fibres like modified polyacryl. They bind to the acid groups of the fibres. Most basic dyes are diarylmethane, triarylmethane, anthraquinone or azo compounds.

1.2.6 Mordant dyes

Mordant dyes are fixed to the fabric by the addition of a mordant, a chemical that combines with the dye and the fibre. Though mordant dyeing is probably one of the oldest ways of dyeing, the use of mordant dyes is gradually decreasing. They are used with wool, leather, silk, paper and modified cellulose fibres. Most mordant dyes are azo, oxazine or triarylmethane compounds. The mordants are usually dichromates or chromium complexes.

1.2.7 Disperse dyes

Disperse dyes are scarcely soluble dyes that penetrate synthetic fibres (cellulose acetate, polyester, polyamide, acryl, etc.). This diffusion requires swelling of the fibre, either due to high temperatures (>120 °C) or with the help of chemical softeners. Dyeing takes place in dyebaths with fine disperse solutions of these dyes. Disperse dyes form the third largest group of dyes in the Color Index. They are usually small azo or nitro compounds (yellow to red), anthraquinones (blue and green) or metal complex azo compounds (all colors).

1.2.8 Pigment dyes

Pigment dyes (i.e. organic pigments) represent a small fraction of widely applied group of colorants. These insoluble, non-ionic compounds or insoluble salts retain their

crystalline or particulate structure throughout their application. Pigment dyeing is achieved from a dispersed aqueous solution and therefore requires the use of dispersing agents. Pigments are usually used together with thickeners in print pastes for printing diverse fabrics. Most pigment dyes are azo compounds (yellow, orange, and red) or metal complex phthalocyanines (blue and green). Also anthraquinone and quinacridone pigment dyes are applied.

1.2.9 Vat dyes

Vat dyes are water-insoluble dyes that are particularly and widely used for dyeing cellulose fibres. The dyeing method is based on the solubility of vat dyes in their reduced (leuco) form. Reduced with sodium dithionite, the soluble leuco vat dyes impregnate the fabric. Next, oxidation is applied to bring back the dye in its insoluble form. Almost all vat dyes are anthraquinones or indigoids.

1.2.10 Anionic dyes and ingrain dyes

Anionic dyes and Ingrain dyes (naphthol dyes) are the insoluble products of a reaction between a coupling component usually naphthols, phenols or acetoacetyl amides and a diazotized aromatic amine. This reaction is carried out on the fibre. All naphthol dyes are azo compounds.

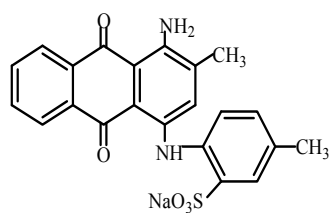
1.2.11 Sulphur dyes

Sulphur dyes are complex polymeric aromatics with heterocyclic S-containing rings. Though representing about 15% of the global dye production, sulphur dyes are not so much used in Western Europe. Dyeing with sulphur dyes involves reduction and oxidation, comparable to vat dyeing. They are mainly used for dyeing cellulose fibres.

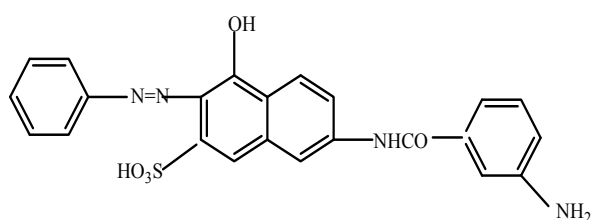
1.2.12 Solvent dyes

Solvent dyes (lysochromes) are non-ionic dyes that are used for dyeing substrates in which they can dissolve, e.g. plastics, varnish, ink, waxes and fats. They are not often used for textile-processing but their use is increasing. Most solvent dyes are diazo compounds that underwent some molecular rearrangement. Also triarylmethane, anthraquinone and phthalocyanine solvent dyes are applied.

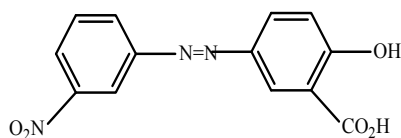
Structures of few organic dyes from various classes are given in Fig. 1.2.



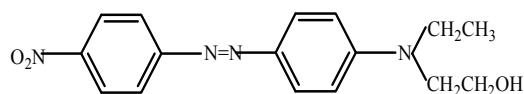
Acid Blue 47



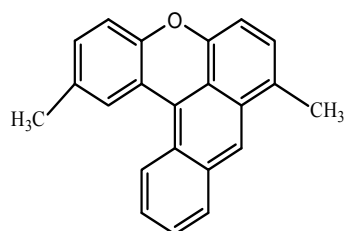
Direct Red 118



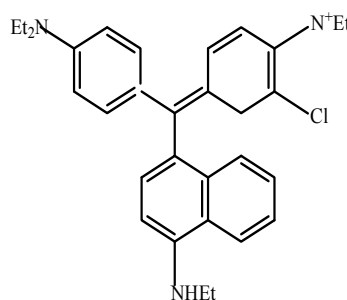
Mordant Yellow 1



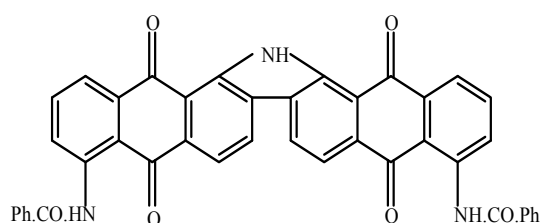
Disperse Red 1



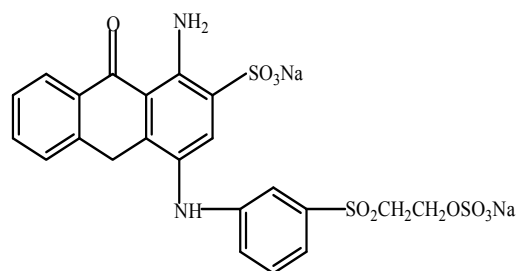
Solvent Green 4



Basic Blue 7



Vat Orange 15



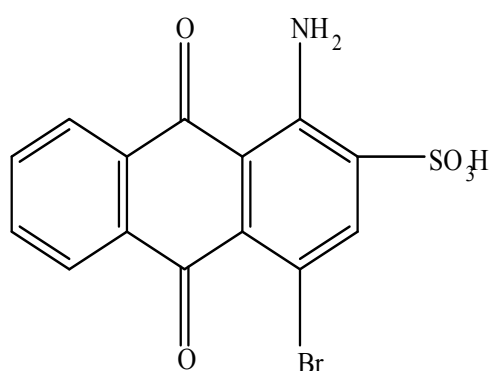
Reactive Blue 19

Fig. 1.2 Molecular Structure of few Organic Dyes

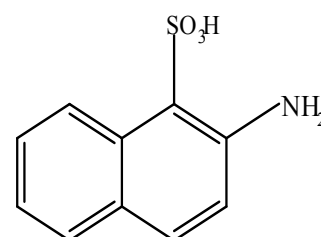
1.3 Other dye classes and dye intermediates

Apart from the dye classes mentioned above, dye intermediates are highly aromatic compounds with low biodegradability which are formed as a result of fragmentation of large dye moieties during the process of degradation. Such organic

compounds being toxic when introduced into the aquatic system cause various health hazards thereby increasing the environmental risks. Various dyes intermediates are found to be chloro or bromo derivatives of naphthalene or sulphonated, hydroxy, amino or nitro aromatic compounds. Few dye intermediates found in the textile wastewater are shown in Fig. 1.3.



1-Amino-4-bromoanthraquinone-2-sulphonic acid
(Bromamine acid)



2-Aminonaphthalene-1-sulphonic acid
(Tobias acid)

Fig. 1.3 Dye intermediates

1.4 Discharge statistics of dyes

As azo dyes represent the largest class of organic colorants listed in the Color Index (60-70% of the total) and their relative share among reactive, acid and direct dyes is even higher, it can be expected that they make up the vast majority of the dyes discharged by textile-processing industries. Anthraquinone dyes are the second largest class (~15%), followed by triarylmethanes (~3%) and phthalocyanines (~2%) of the entries in the Color Index.

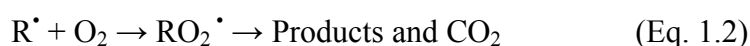
Reactive dyes are known to form a covalent bond with the fibre in the dyeing process. This leads to favorable properties such as wash-fastness. However, unfixed dye reacts with water to form hydrolyzed or oxo-dye intermediate that has lost its bonding capacity and thus cannot be re-used. Therefore dye recovery is not an option with reactive dyes and the treatment process must lead to final destruction or disposal of these contaminants.

1.5 Methods for removal of dyes and other organic compounds from wastewater:

Various physical, chemical and biological pre-treatment and post-treatment techniques have been developed over the last two decades to remove color from dye contaminated wastewaters in order to cost effectively meet environmental regulatory requirements. Chemical and biological treatments have been conventionally followed till now but these treatment methods have their own disadvantages. The aerobic treatment process is associated with production and disposal of large amounts of biological sludge, while wastewater treated by anaerobic treatment method does not bring down the pollution parameters to the satisfactory level and activated charcoal adsorption and air stripping methods simply transfer the pollutants from one medium to another. They either transfer it to the atmosphere, which causes air pollution, or to a solid which is often disposed off in landfills or must be treated in an energy-intensive regeneration process. Merely transferring toxic materials from one medium to another is not a long term solution to the problem of hazardous waste loading on the environment. The recent developments in water decontamination processes are concerned with the oxidation of these bio-recalcitrant organic compounds. These methods rely on the formation of highly reactive chemical species that degrade more number of recalcitrant molecules into biodegradable compounds and are called advanced oxidation processes (AOP's).

1.6 Advanced Oxidation Processes

Advanced oxidation processes (AOP's), uniting together ozone and high output ultraviolet technologies, in conjunction with hydrogen peroxide and catalyst are successfully used to decompose many toxic and bio-resistant organic pollutants in aqueous solution to acceptable levels, without producing additional hazardous by-products or sludge which require further handling. Advanced oxidation processes involve the generation of hydroxyl ($\cdot\text{OH}$) radicals which oxidize the pollutants. After fluorine, the hydroxyl radical is the second strongest known oxidant having an oxidation potential of 2.8 eV. It is able to oxidize and mineralize almost every organic molecule, yielding CO_2 and inorganic ions as shown in Eq.1.1 and 1.2.



Different combinations of homogenous and heterogeneous methods which involve the generation of free radicals are, (i) photochemical irradiation with ultraviolet light (coupled with powerful oxidizing agents like ozone, hydrogen peroxide and /or a semiconductor), (ii) Fenton and Photo-Fenton catalytic processes (iii) Electron Beam Irradiation technique and (iv) Sonolysis.

All these processes use UV range for degradation. The UV spectrum is arbitrarily divided into three bands: UV-A (315 to 400 nm), UV-B (280 to 315nm) and UV-C (100 to 280 nm). Of these bands UV-A and UV-C are generally used in environmental applications. UV-A radiations are referred to as long wavelength radiations or black light and UV-C are referred to as short wave radiations.

Advanced oxidation processes's can be broadly classified into the following groups:

1. Homogeneous photocatalysis
2. Heterogeneous photocatalysis

1.6.1 Homogeneous photocatalysis

The applications of homogeneous photodegradation (single-phase system) to treat contaminated water, involves the use of an oxidant to generate radicals, which attack the organic pollutants to initiate oxidation. The major oxidants used are:

- Hydrogen peroxide (UV /H₂O₂)
- Ozone (UV /O₃)
- Hydrogen peroxide and Ozone (UV /O₃/H₂O₂)
- Photo-Fenton system (Fe⁺³ /H₂O₂)

Table 1.1 Hydroxyl radical generation in different AOP's (Homogeneous)

Method	Key reaction	Drawbacks
UV/H ₂ O ₂	$\text{H}_2\text{O}_2 + h\nu \longrightarrow 2\text{HO}^\bullet$	1) Low molar extinction co-efficient. 2) Absorbs $\lambda < 300\text{nm}$, a lesser component in solar radiation.
UV/O ₃	$\text{O}_3 + h\nu \longrightarrow \text{O}_2 + \text{O}({}^1\text{D})$ $\text{O}({}^1\text{D}) + \text{H}_2\text{O} \longrightarrow \text{HO}^\bullet + \text{HO}^\bullet$	Absorbs $\lambda < 300\text{nm}$, a lesser component in solar radiation
UV/H ₂ O ₂ /O ₃	$\text{O}_3 + \text{H}_2\text{O} + h\nu \longrightarrow \text{O}_2 + \text{H}_2\text{O}_2$	Absorbs $\lambda < 300\text{nm}$, a lesser component in solar radiation
UV/H ₂ O ₂ /Fe (Photo-Fenton)	$\text{H}_2\text{O}_2 + \text{Fe}^{3+} \longrightarrow \text{Fe}^{2+} + \text{HO}^\bullet + \text{OH}^-$ $\text{Fe}^{2+} + \text{H}_2\text{O} + h\nu \longrightarrow \text{Fe}^{3+} + \text{HO}^\bullet + \text{H}^+$	1) Process is expensive. 2) Sludge disposal problem formed during the process. 3) Continuous supply of feed chemicals are required.

Many of the AOP's listed in Table 1.1 utilize the chemical, hydrogen peroxide. The oxidising strength of hydrogen peroxide alone is relatively weak, but the addition of UV light enhances the rate and strength of oxidation through production of increased amounts of hydroxyl radicals. Hydrogen peroxide may also be used to enhance other AOP's if added in low concentrations, as the molecule easily splits into two hydroxyl radicals.

1.6.2 Heterogeneous photocatalysis

Heterogeneous photocatalytic process consists of utilizing the near UV radiation to photo-excite a semiconductor catalyst in the presence of oxygen. Under these circumstances oxidizing species, either bound hydroxyl radicals or free holes, are generated as shown in Fig. 1.4. Using photocatalysis, organic pollutants can be completely mineralized reacting with the oxidizers to form CO₂, water and dilute

concentration of simple mineral acids. The process is heterogeneous because there are two active phases, solid and liquid. This process can also be carried out utilizing the near part of solar spectrum ($\lambda < 380\text{nm}$) what transforms it into a good option to be used (Malato et al., 2002).

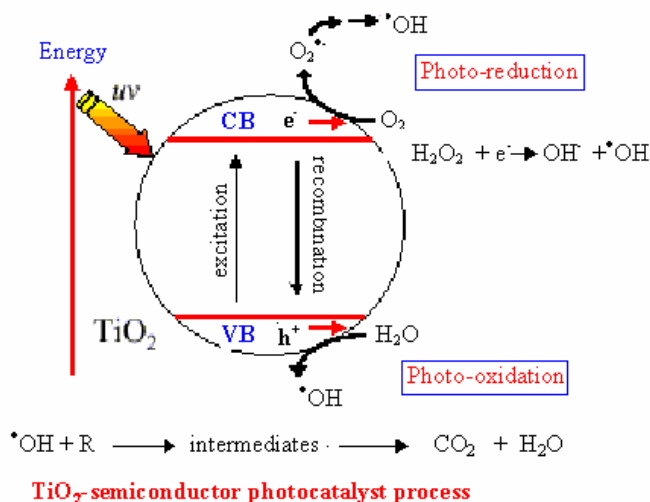
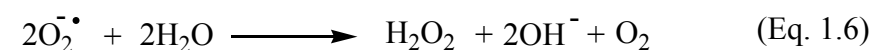
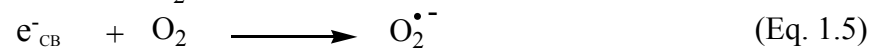
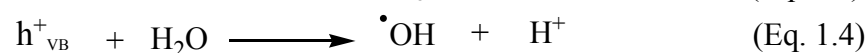
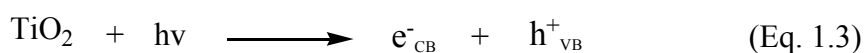


Fig 1.4 Scheme showing some of the events that might be taking place on an irradiated semiconductor particle

The semiconductor may be in the form of a powder suspended in the water or fixed on a support. The most active photocatalyst for this application is the anatase form of TiO₂ because of its high stability, good performance and low cost (Andreozzi et al., 1999). The primary photocatalytic mechanism is believed to proceed as follows:



In solids, the electrons occupy energy bands as a consequence of the extended bonding network. In a semiconductor, the highest occupied and lowest unoccupied energy bands are separated by a bandgap, a region devoid of energy levels. Activation of semiconductor photocatalyst is achieved through the absorption of a photon of ultraviolet bandgap energy which results in promotion of an electron (e^-) from the valence band

(VB) into the conduction band (CB) with the generation of hole in the valence band as shown in the Fig. 1.4. The resulting hole is an oxidizing agent and the electron is a reducing agent. In the generally accepted mechanism for the photocatalytic process, the hole can react with water to generate the hydroxyl radical and the electron can reduce molecular oxygen, hydrogen peroxide or some other oxidizing agent in the solution. This creates the reactive radicals responsible for the removal of hazardous components from the water.

TiO₂/ UV process is known to have many advantages:

- A large number of organic compounds dissolved or dispersed in water can be completely mineralized.
- The rate of reaction is relatively high if large surface area of the catalyst can be used.
- TiO₂ is available at a relatively modest price and can be recycled on a technical scale.
- UV lamps emitting in the spectral region required to initiate the photocatalytic oxidation are well known and are produced in various sizes.
- Absorption cross-section of TiO₂ can be improved by its surface modifications, e.g. by transition metal ion doping.

However, the only drawback in this method is that the liquid-solid separation is expensive, due to the formation of milky dispersions after mixing the powder catalyst in water. To solve this separation problem, fixed TiO₂ is prepared by coating a substrate with a TiO₂ solution and in most cases the catalyst shows a higher photocatalytic activity than the TiO₂ in slurry mode. However in general, the adherence of TiO₂ to support is not by a chemical bond and the heavier catalyst can be worn off easily.

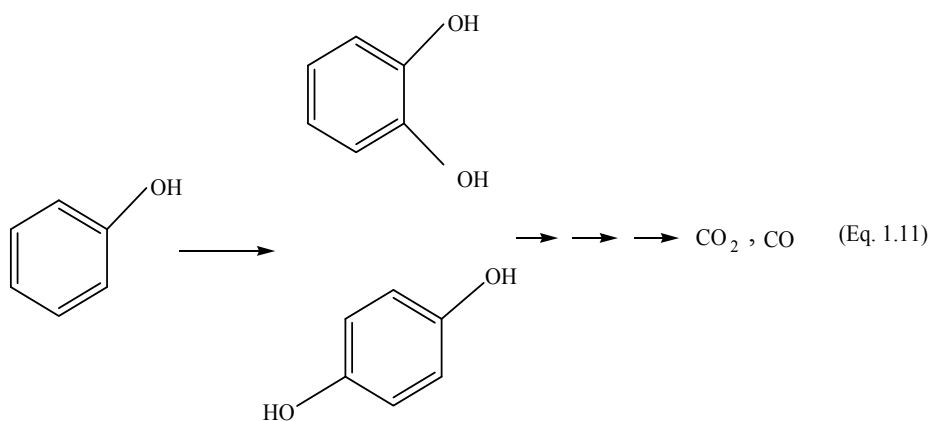
The various combined methods for $\cdot\text{OH}$ radical production mentioned above for the decomposition of a wide variety of organic contaminants have been reported by several authors and are of special interest since some of them can also use solar energy. A common problem of all the AOP's is their high cost, mainly due to high demand of electrical energy for ozonizers and/or UV lamps. Application of solar irradiation to the

photochemical process reduces cost but it is possible only for catalyzed homogeneous and heterogeneous reactions using iron ions and titanium dioxide respectively. These catalysts absorb at wavelengths of the solar spectrum while ozone and hydrogen peroxide do not absorb above 300 nm, which is the most important condition for the use of sunlight.

1.7 Ultrasound and Photocatalysis

Furthermore, an integrated approach of ultrasound and photocatalysis of wastewater is found to be advantageous but has not received much attention until recently. When sonication is added to the photocatalytic system, significant changes are produced. The high energy chemistry generated by ultrasound waves in liquid medium promotes the oxidative destruction of target contaminants. Ultrasonic waves with frequency > 16 KHz are high-energy waves, which are longitudinal and on passing through a liquid medium produce its effects via cavitation bubbles. Formation and behavior of the bubble of cavitations upon the propagation of the acoustic wave in the liquid constitute the essential events that induce the sonochemical effects. The transient cavities in the bubbles, produced using ultrasonic irradiation, exist briefly expanding to at least double their initial size before violently collapsing into smaller bubbles. The collapse of these bubbles can yield local pressures of hundreds of atmospheres and temperatures of thousands of degrees resulting in solute thermolysis and the formation of hydroxyl radical and H₂O₂ by sonolysis of water. Dramatic enhancements in reactivity and rates of chemical processes can arise from the process of cavitation collapse. In this case the transformation of the organic pollutants occurs through reactions with hydroxyl radicals generated from the collapsing bubble Eq. 1.8-1.10. Further, Concentration of the organic material decreases as hydroxylation progresses (Eq. 1.11).





Sonochemical treatment leads to the generation of hydrogen peroxide. Thus, sonochemical effect augments the photochemical process on simultaneous application to photocatalytic degradation with dramatic rate enhancement and is effective for degradation of organic pollutants present in the wastewater.

1.8 Catalyst

Research over the last three decades has not only confirmed the capability of sunlight for detoxification and disinfection but also accelerated the natural process by the use of catalysts. For oxidation reactions to occur the valence band (VB) must have a higher oxidation potential than the material under consideration. The redox potential of the valence band and the conductance band for different semiconductors varies between +4.0 and -1.5 volts versus normal hydrogen electrode (NHE). Therefore, by careful selection of the semiconductor photocatalyst, a wide range of species can be treated *via* these AOP processes. Metal oxides and sulphides represent a large class of semiconductor materials suitable for photocatalytic purposes. Table 1.2 lists some of the selected semiconductor materials, which have been used for photocatalytic reactions, together with the VB and CB potentials, the band gap energy and wavelength required to activate the catalyst that produce this gap, the radiation must be of an equal or lower wavelength than that calculated by that Planck's equation (Eq. 1.12).

$$\lambda = hc / E_{bg} \quad (\text{Eq. 1.12})$$

where E_{bg} is the semiconductor band-gap energy, h is the Planck's constant and c is the speed of light.

Among the listed semiconductors, TiO₂ has proven to be the most suitable for widespread environmental applications. ZnO also seems to be a suitable photocatalyst but it dissolves in acidic solutions and therefore, cannot be used for technical applications. Other semiconductor particles (e.g., CdS) absorb larger fractions of the solar spectrum than TiO₂ and can form chemically activated surface-bond intermediates, but unfortunately, such catalysts are degraded during the repeated catalytic cycles usually involved in heterogeneous photocatalysis.

Table 1.2 Band positions of some common semiconductor photocatalysts in aqueous solution at pH=1

Semiconductor	Valence band (V vs NHE)	Conductance band (V vs NHE)	Band gap (eV)	Band gap wavelength (nm)
TiO ₂	+3.1	-0.1	3.2	387
SnO ₂	+4.1	+0.3	3.9	318
ZnO	+3.0	-0.2	3.2	387
ZnS	+1.4	-2.3	3.7	335
WO ₃	+3.0	+0.2	2.8	443
CdS	+2.1	-0.4	2.5	496
CdSe	+1.6	-0.1	1.7	729

Titanium dioxide is widely used as white paint pigment, sun blocking material, cosmetic, or as builder in vitamin tablets, among many other uses. It is biologically and chemically inert; it is stable to photo and chemical corrosion, and is inexpensive. This semiconductor exists in three crystalline forms: anatase, rutile, and brookite. Anatase and rutile are the most common forms and the former is the most effective in wastewater treatment. The band gap energies are approximately 3.2 eV for anatase and 3.0 eV for rutile but the driving force for oxidative processes are similar. Anatase is thermodynamically less stable than rutile, but its formation is kinetically favored at lower temperature (<600°C), which could explain its higher surface area and its higher surface density of active sites for adsorption and catalysis. Furthermore, TiO₂ is of special interest since it can use natural (solar) UV radiation. This is because TiO₂ has an appropriate

energetic separation between its valence and conduction bands, which can be surpassed by the energy of a solar photon.

One of the disadvantages of the particulate excitation of the semiconductors is the high degree of recombination between the photo-generated charge carriers. As a result of this electron-hole recombination, the efficiency of the semiconductors decreases thereby, decreasing the quantum yield of the redox processes.

The other limitation of TiO_2 is that it utilizes only about 4-6% of the solar energy reaching the earth's surface which is in the UV region. This limitation is overcome by its modification. It has been modified by doping of metal ions and photosensitization by various colored organic and inorganic compounds, in order to extend the photo-response of large bandgap semiconductors into the visible region to use them for the degradation of colored organic contaminants and other organic pollutants. The metal ions added into polycrystalline TiO_2 or photo-deposited metals increase the absorption. Therefore, research on catalyst improvement has been done on the following points:

1. Physical and chemical modification of TiO_2 to improve the catalyst performance.
2. Dye sensitization to increase the useful wavelength range of the solar radiation.

The principle of photosensitized degradation on the semiconductor particle is illustrated in Fig. 1.5.

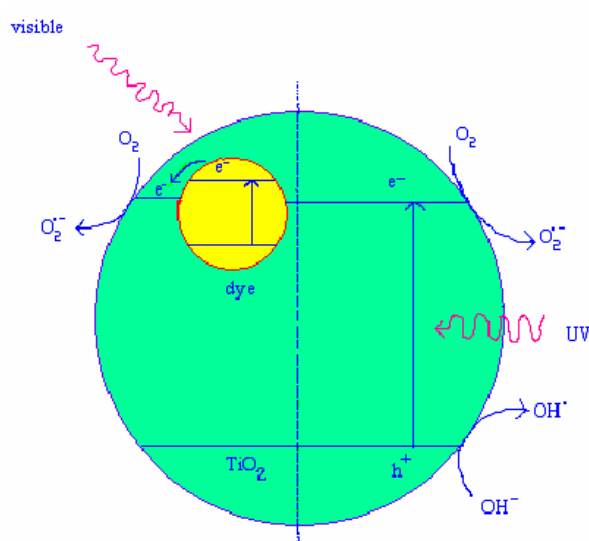
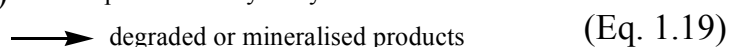
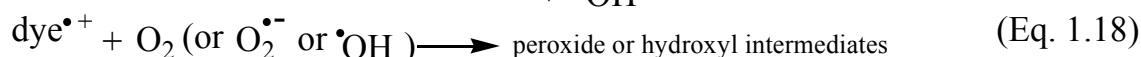
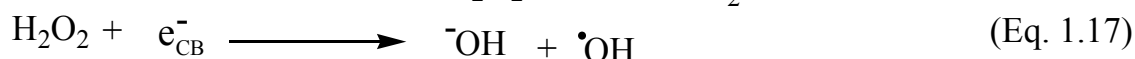
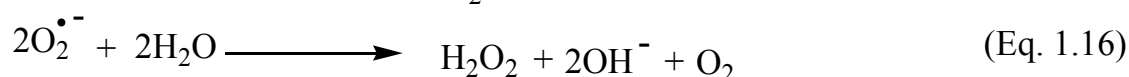
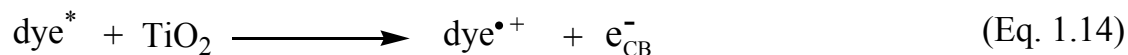


Fig. 1.5 Mechanism of TiO_2 under UV and visible light

The mechanism of photosensitization approach for degrading dye molecules on TiO₂ surface is shown as under:



If the oxidation potential of the sensitizer is higher than the conductance band of the TiO₂, following initial excitation of the adsorbed dye under visible light irradiation, electron is injected from the excited dye to the conduction band of TiO₂. By carefully eliminating the regeneration step, it is possible to initiate the oxidative degradation of the dye. A variety of colored compounds have been investigated to act as photosensitizers. In recent studies it has been suggested that photosensitized degradation on semiconductor surfaces can have important applications for treating a particular class of colored pollutants such as textile dyes.

1.9 Kinetics

An understanding of reaction rates and how the reaction rate is influenced by different parameters is important for the design and optimization of an industrial system. The rate of photocatalytic degradation depends on several factors including illumination intensity, catalyst type, oxygen concentration, pH, presence of inorganic ions and the concentration of organic reactant. The destruction rates of organics in photocatalytic oxidation have been modeled by different kinetic models. Langmuir-Hinshelwood (L-H) kinetics seems to describe many of the reactions fairly well. The rate of destruction is given by Eq.1.20:

$$-dC/dt = k_1 k_2 C / (1 + k_2 C) \quad (\text{Eq. 1.20})$$

In the ideal case, for which the L-H model is derived, C is the bulk solute concentration, k_1 the reaction rate constant, k_2 the equilibrium adsorption constant and t represents time. The L-H reaction rate constants are useful for comparing the reaction rate under different experimental conditions. Once the reaction constants k_1 and k_2 have been evaluated, the disappearance of the reactant can be estimated if all other factors are held constant. For low solute concentration C , the L-H expression reduces to a pseudo first order expression:

$$- dC/ dt = k_1 k_2 C = k C \quad (\text{Eq. 1.21})$$

This equation has been shown to apply to many photocatalysed reactions. The industrial pollutants levels are typically of the order of ppm, which are low enough for the reaction rate to follow pseudo first order kinetics. Besides this 'k' reaction rate constant is not a traditional rate-constant used in reaction engineering due to the nature of the photocatalytic reaction, it is also a function of external system parameters such as UV intensity, pH, catalyst loading, geometry of photoreactor and initial concentration.

1.10 Reactors

The reactors used for the solar photocatalytic treatment are categorized as follows:

1. Concentrating reactors
2. Non-concentrating reactors

1.10.1 Concentrating reactors

Since the photochemical processes depend on the collection of only high energy short wavelength photon to promote photochemical reactions, these are reactors based on the collection of large quantities of photons of all wavelengths. These are based on the focus line parabolic trough concentrators which make use of direct solar radiation and as an additional advantage, the thermal energy collected from the concentrated radiation could simultaneously be used for other applications, so that the handling and control of liquid to be treated is simple and cheap. The main disadvantages are that the collectors use only direct radiations which are expensive and have low optical and quantum efficiencies, resulting in a reaction rate constant dependence on the intensity (I) of UV radiation as follows:

$$k \propto I^{1/2} \quad (\text{Eq. 1.22})$$

These disadvantages tend to favor the use of non-concentrating reactors.

1.10.2 Non-concentrating reactors

Non-concentrating reactors are cheaper as compared to the concentrating reactors. Their maintenance is also easy and is of low cost due to their simple structure and design. They do not concentrate radiations, so that efficiency is not reduced by factors associated with concentration and solar tracking. A disadvantage of the non-concentrating reactors is the requirement of much larger reactor area. Researchers have proposed a number of different designs of non-concentrating solar reactors which are as follows:

- Flat plate
- Tubular
- Falling film
- Shallow solar ponds

Pond reactors can be constructed on-site especially for industrial treatment. Since industries already use ponds for biological treatment of wastewater, shallow solar ponds can be used for the front end or the back end of a combined solar/ biological treatment of wastewater. Thus, these reactors have the best chance of commercialization for wastewater treatment in industries such as pulp and paper, textiles, pharmaceuticals and chemicals. For shallow pond type reactor, the intensity dependence of the reaction rate constant is given by

$$k/k_0 = m [I(A/V) / I_0(A/V)_0]^n \quad (\text{Eq. 1.23})$$

where 'm' and 'n' are empirical constants, A is the aperture and V is the volume irradiated.

1.11 Objectives of the work undertaken

- 1) Photodegradation studies of various dyes and their intermediates using semiconductor catalysts under UV light.

- 2) Modification of TiO₂ by adsorbing dye sensitizers to perform degradation studies under visible light.
- 3) Optimization of the photodegradation process by varying operational parameters like pH, initial concentration of substrate, catalyst loading etc. for improving effectiveness of the process.
- 4) Kinetic studies of the degradation process.
- 5) To study the effect of ultrasound on the photodegradation process.

1.12 Approach Adopted

- 1) Control experiments were done in the absence of TiO₂ and in dark.
- 2) Mainly water-soluble reactive dyes, dye intermediates and textile effluent were photodegraded by varying the initial concentration of dye, catalyst loading, pH (adding HCl or NaOH) by UV light.
- 3) Different catalysts like TiO₂, ZnO and UV-100 were tried for the above mentioned compounds to find the most effective catalyst.
- 4) Surface modification of TiO₂ was done with different dye sensitizers and used as a catalyst under visible light.
- 5) The kinetic studies were carried out by analyzing the samples using UV/visible spectrophotometer, COD analysis to observe the complete degradation/mineralization.
- 6) The combined effect of ultrasound and visible light was also studied.

Chapter 2

LITERATURE REVIEW

2.1 AOP's- Homogeneous and Heterogeneous

In the last 15 years or so, a rather fast evolution of research activities devoted to environment protection has been recorded as a consequence of the special attention paid to the environment by social, political and legislative international authorities, leading in some cases to the delivery of very severe regulations (Legrini et al., 1993).

Gogate and Pandit (2004a, 2004b) in their review aimed at highlighting different processes (belonging to the class of advanced oxidation processes) and the basics of these processes including the optimum parameters and design aspects with a complete overview of the various applications to wastewater treatment in recent years. Destructive oxidation of organic compounds by a variety of homogenous and heterogeneous AOP's has been done effectively thereby increasing the biodegradability of the pollutants (Balchioglu et al., 2003).

The use of AOP's for wastewater treatment has been studied extensively (Andreozzi et al., 1999; Chiron et al., 2000; Esplugas et al., 2002) and it has been concluded that UV radiation by lamps is expensive. Therefore, research is presently focused more and more on the two AOP's i.e. homogeneous catalysis with photo-Fenton and heterogeneous catalysis with UV/TiO₂, with and without addition of oxidants, which can both be powered by solar irradiation i.e. light of wavelength longer than 300 nm. (Goswami, 1997; Konstantinou and Albanis, 2003; Robert and Malato, 2002). The principles and the advantages of several typical homogeneous and heterogeneous AOP's system were summarized by Wu (1999a); Vogelpohl and Kim (2004).

Among the homogeneous oxidation processes, in a recent review by Neyens and Baeyens (2003) they have emphasized the oxidation processes utilizing activation of H₂O₂ by iron salts, classically referred to as Fenton's reagent, known to be very effective in the destruction of many hazardous organic pollutants in water. Few researchers (Modirshahla et al., 2007; Liu et al., 2007; Lucas and Peres, 2006; Muruganandham and Swaminathan, 2004a) have studied the degradation and decolorization of few organic

dyes by Fenton and photo-Fenton processes by varying the various parameters like catalyst loading, initial substrate concentration and pH. The photo-Fenton process proved to be the most efficient and occurs at a much higher oxidation rate than Fenton process. Studies have been done on treatment of wastewater using UV/H₂O₂, UV/O₃ and photo assisted Fenton degradation techniques (Shu, 2006; Shen and Wang, 2002; Wang et al., 2000; Venkatadri and Peters, 1993). Modirshahla and Behnajady (2006) investigated the decolorization of Malachite Oxalate Green (MG) dye using UV radiation in the presence of H₂O₂ in a batch photoreactor at different light intensities. The semi-logarithmic graphs of the concentration of MG versus time were linear, suggesting pseudo-first order reaction. Shu and Chang (2005) studied the decolorization of six azo dyes by means of O₃, UV/O₃ and UV/H₂O₂ processes. He reported that dyes with di-azo links were more difficult to decolorize than mono-azo dyes and the results showed that UV/H₂O₂ used maximum energy which was 5-11 times that of UV/O₃ process, and 265-520 times more than that of the ozonation process. Lafi and Al-Qodah (2006) successfully combined advanced oxidation processes (O₃/UV) with biological treatment processes to remove both pesticides and the COD load from aqueous solutions.

Photocatalysis is a rapidly expanding technology for wastewater treatment. The photocatalytic detoxification has been discussed as an alternative method for cleaning up of polluted water in the scientific literature since 1976 (Carey et al., 1976). In his review Bhatkhande et al., (2002) has discussed the applications of photocatalytic degradation and chemical effects of various variables on the rate of degradation of different pollutants. A growing interest in the purification of water by semiconductor photocatalysis especially in the removal of toxic organic pollutants is evident by the ever-increasing number of studies in this area (Inel and Okte, 1996; Mathews, 1988; Ollis et al., 1989, 1991).

Among heterogeneous AOP's TiO₂ – mediated photocatalytic oxidation appears to be a promising alternative. Various investigators (Muruganandham and Swaminathan, 2004b; Styliadi et al., 2003; Kositzi et al., 2004) have demonstrated that solar radiation is a useful UV source for driving photocatalytic processes. There are number of general reviews which cover aspects of the TiO₂ photocatalytic destruction of organic compounds in water (Fox and Dulay, 1993; Hoffman et al., 1995; Kamat, 1993; Linsebigler et al., 1995). In their review, Fujishima et al., (2000) have discussed progress in the area of TiO₂ photocatalysis mainly for photocatalytic air purification, sterilization and cancer

therapy, together with some fundamental aspects and have presented a novel photo-induced super hydrophilic phenomenon involving TiO₂ and its applications. Herrmann (1999) has described the basic fundamental principles as well as the influence of the main parameters like mass of the catalyst, wavelength, initial concentration, temperature and radiant flux governing the kinetics of heterogeneous photocatalysis in wastewater treatment.

Mills and Lee (2002b) reviewed the major commercial applications of semiconductor photochemistry. The basic principles behind the different applications are discussed, including the use of semiconductor photochemistry to photo-mineralize organics, photo-sterilize and photo-demist. The range of companies, and their products, which utilize semiconductor photochemistry are examined and typical examples are listed. They have done an analysis of the geographical distribution of current commercial activity in this area. Blake (2001) published a bibliography listing 1200 publications and patents on photocatalytic processes. He compiled a list of organic and inorganic compounds with references which shows over 300 compounds including about 100 on the US EPA priority list that can be treated by the photocatalytic process. Blake (1994) also listed 42 review articles that cover various aspects of photocatalytic chemistry and technology. In an article entitled "Solar photocatalytic detoxification" published in *Advances in Solar Energy*; Blake et al., (1992) have reviewed in detail the fundamental chemistry of solar photocatalytic detoxification and the preliminaries of engineering system development. The degradation of many different model compounds has been studied and it has been clearly shown that most of the organochlorine compounds as well as many pesticides, herbicides, surfactants and colorings present in water can be completely oxidized into non-toxic products like carbon dioxide, hydrochloric acid and water (Mohamed, 2002; Morsi et al., 2000; Muneer et al., 2001; Oberg et al., 1993; Puma and Yue, 1999; Soana et al., 2000).

In 1998, the US EPA (Environmental Protecting Agency) made an inventory of more than 800 molecules that can be degraded by this process as shown in Table 2.1 (Robert and Malato, 2002).

Table 2.1 Main ranges of pollutants

Source	Products
Chlorinated solvents	Chloroform, carbon tetrachloride, Trichloroethylene, chlorobenzene
Non-chlorinated solvents	Acetone, acetonitrile, benzene, cyclohexane, formaldehyde, phenol, methylbenzene
Insecticides	Aldrin, dichlorvos, lindane, parathion, Monocrotophos
Pesticides	Atrazine, monuron
Dyes	Acid Orange 7, Green Malachite, Naphthol Blue Black, Reactive Blue 19
Detergent	Octoxynol (triton X-100)

2.2 Degradation of Pesticides, Chloro-organic compounds and Detergents

A wide variety of pesticides, detergents and organic compounds, which are toxic and stable to natural decomposition are nowadays introduced into the water system from various sources such as industrial effluents, agricultural runoff and chemical spills and their persistence in the environment is a subject of concern (Muszkat et al., 1994). Various AOP's are used to get rid of such compounds as reported in the literature.

Muneer and Bahnemann (2002) have investigated the photodegradation of two selected pesticide derivatives, 3-tert-butyl-5-chloro-6-methyluracil (terbacil) and 2,4,5-tribromoimidazole in aqueous suspension of titanium dioxide under a variety of conditions employing a pH- stat technique and degradation studies were done by varying different operational parameters. Shankar et al., (2004) fabricated a thin-film reactor with immobilized TiO₂ and this reactor was used for photocatalytic mineralization of common pesticides, 2, 4-dichlorophenoxyacetic acid (DPA) and monocrotophos (MCP). The results clearly demonstrated that the good adsorption capacity of the support, and the effective light utilization by TiO₂, improved the photocatalytic activity of supported TiO₂.

Djebbar et al., (2006) reported that the photocatalytic degradation of many chlorinated organic compounds by semiconductor particles, has been widely recognised as a promising method of water and wastewater treatment process in literature. Pandiyan et al., (2002) have investigated dehalogenation and destruction of halogenated phenols by using photochemical methods. The reactants and products were analyzed by gas chromatography. Dehalogenation was faster for monohalogenated phenols than poly-substituted phenols. Hariharan (2006) investigated the photodegradation of aromatic chloro organic contaminants using the fluorescence emission characteristics of ZnO nanoparticles (ZnO-nano) in aqueous solutions. He concluded that the ZnO nanoparticles served as a better catalytic system compared to bulk ZnO and commercially available Degussa TiO₂ in achieving degradation of the added contaminants.

Horvath et al., (2005) in his study reported that photo-induced oxidative degradation of both anionic (dodecyl sulfate) and cationic (cetyltrimethylammonium) surfactants can be efficiently realized by simultaneous reduction of chromium(VI) to chromium(III) and mercury(II) to its metallic form in aqueous systems containing colloidal titanium dioxide photocatalyst. Oyama et al., (2004) investigated the photodegradation of a commercial detergent whose major components are an anionic surfactant and a fluorescent whitening agent in aqueous TiO₂ dispersions under irradiation with concentrated sunlight in the presence of air. The degradation process followed apparent first-order kinetics. Horvath and Huszank (2003) in another study investigated the Fe (III)-photo-induced oxidation of anionic lauryl sulfate (LS⁻) and cationic cetyltrimethylammonium (CTA⁺) surfactants in aqueous solution. The complete mechanistic studies have been reported which suggest the major role of OH radicals in degradation of the surfactants.

2.3 Degradation of Dyes and Dye Intermediates

2.3.1 Review

Dyes and dye intermediates with high degree of aromaticity and low biodegradability are introduced into the aquatic system resulting in increase of environmental risk. Dye pollutants from the textile industry are an important source of environmental contamination. Several studies of photocatalytic degradation of dyes have been reported (Chatterjee and Mahata, 2002; Herrera et al., 2000; Poullos and Tsachpinis,

1999; Yang et al., 2001). Factors influencing the degradation rate of aqueous systems have been studied such as effect of pH, dissolved oxygen contents and the amount of photocatalyst added (Kiriakidou et al., 1999; Schrank et al., 2002). There are very few studies related to the use of semiconductors in the photodegradation of photo-stable dyes (Muneer et al., 1997). With the aim of elucidating the potential application of advantageous photocatalytic processes, the kinetic and mechanistic aspects of dye degradation have been investigated and reported in literature (Bauer et al., 2001; Galindo et al., 2002; Houas et al., 2001). TiO₂-mediated photocatalytic degradation of various dyes was investigated in aqueous suspensions of titanium dioxide under a variety of conditions by monitoring the change in substrate concentration employing UV spectroscopic analysis and decrease in total organic carbon content as a function of irradiation time (Saquib and Muneer, 2003a; Qamar et al., 2005). Qaradawi and Salman (2002) used titanium dioxide (TiO₂) as a photocatalyst for the detoxification of water containing Methyl Orange (MO), which was used as a model compound using solar radiation as an irradiation source. Khalil et al., (1999) investigated photodegradation processes of two azo dyes at TiO₂/H₂O interface under visible and ultraviolet light irradiation with different experimental techniques (absorption and fluorescence spectroscopy as well as total organic carbon analysis).

Vinodgopal and Kamat (1995) employed thin film semiconductor to enhance the rate of azo dye photocatalytic destruction. Subrahmanyam et al., (1998) have studied the photocatalytic degradation of textile dyes, Vat Blue, Fast Orange GC Base, Drimarene yellow 3 GLI and Bromothymol Blue using a batch reactor. TiO₂ based catalysts immobilized on ceramic beads and SiO₂ were used for many of the water-soluble compounds. Neppolian et al., (2002b) investigated the photocatalytic degradation of three commercial textile dyes with different structures using TiO₂ (Degussa P25) photocatalyst in aqueous solution under solar irradiation as a function of COD reduction. Experiments were conducted to optimize various parameters like amount of catalyst, concentration of dye, pH and solar light intensity.

2.3.2 Degradation studies of various classes of dyes

Photodegradation of various classes of dyes has been a subject of research and is reported in the literature. Reactive dyes have emerged to be the most important class of dyes which are causing environmental pollution as only small amount of it is fixed and

rest remains unfixed (Karcher et al., 2002). Several studies have been reported in the literature for the degradation of the reactive dyes (Arslan et al., 2001; Gouvea et al., 2000; Baran et al., 2003; Zielinska et al., 2003). Photocatalytic degradation of textile dye, Reactive Red M5B has been carried out on TiO₂ and ZnO semiconductor particles by Neppolian et al., (1998). Gopalkrishnan and Mohan (1997) presented the experimental investigations on color removal from reactive dyeing wastes of cotton units using solar energy through photocatalytic process for waste reclamation using locally available Indian inexpensive ISI grade TiO₂, the usage of which has not been reported earlier. Sauer et al., (2002) presented in their work, a detailed investigation of the adsorption and photocatalytic degradation of the Safira HEXL dye, an anionic azo dye of reactive class. H₂O₂ and UV light have a negligible effect when they were used on their own. The adsorption of dye on the semiconductor shows a strong dependence on the pH and follows a Langmuir adsorption model. Sivekumar and Shanthi (2001) reported the photocatalytic studies on some textile reactive dyes, Procion Brilliant Magenta M-B(PBM), Procion Brilliant Yellow M-4G(PBY) and Procion Brilliant Orange M-2R(PBO) using different grades of TiO₂, namely CDH, CERAC and DEGUSSA and they concluded that TiO₂ (Degussa P-25) was superior to any other grade.

Sakthivel et al., (2002) prepared TiO₂ supported on alumina and glass beads and determined their photocatalytic activities by photo-oxidation of commercial leather dye, Acid Brown 14 in aqueous solution illuminated with solar light. Behnajady et al., (2007) studied the photocatalytic degradation of C.I. Acid Red 27 (AR27), an anionic monoazo dye of acid class, in aqueous solutions in a tubular continuous-flow photoreactor with immobilized TiO₂ on glass plates under UV light. Results show that a linear relation exists between pseudo-first-order reaction rate constant and reciprocal of volumetric flow rate. Based on solar-Fenton process, the effect of pH value and the concentration of dye, Fe²⁺ ions, H₂O₂ as well as oxalic acid concentration on acid dye, Eosin Y degradation efficiency were investigated by Zheng et al., (2007).

Pandurangan et al., (2001) carried out the photocatalytic degradation of textile dye, Basic Yellow Auramine O by a batch process using ZnO as the catalyst and sunlight as the illuminant. In addition to removing the color from the dye solution, the COD was also reduced suggesting that the fragments produced from the dye were mineralized. The photocatalytic degradation of Crystal Violet, a triphenyl methane dye (also known as

Basic Violet 3) in aqueous solutions was investigated with Ag⁺ ion doped TiO₂ under UV and simulated solar light by Sahoo et al., (2005). The dye (20 ppm) was found to degrade about 88% after illumination for 10 h. The degradation kinetics fit well to Langmuir–Hinshelwood rate law.

Park and Choi (2005) reported that the visible-light-sensitized degradation of dyes was enhanced with Nf/TiO₂ not only for cationic dyes (Methylene Blue (MB) and Rhodamine B (RhB) whose uptake on Nf/TiO₂ is enhanced, but also for an anionic dye (AO7) that is less adsorbed on Nf/TiO₂. The unexpected behavior in AO 7 degradation seems to be related to the role of the Nafion layer in retarding the charge recombination. Hasnat (2005) studied the photocatalytic degradation of Methylene Blue, a cationic dye and Procion Red, an anionic dye, in TiO₂ dispersions under visible light. Adsorption is a prerequisite for the TiO₂ assisted photodegradation and the extent of degradation has been discussed in terms of the Langmuir–Hinshelwood model. Baran et al., (2003) studied the decoloration of solutions of azo, anionic (Acid Orange 7, Reactive Red 45, Acid Yellow 23) and cationic (Basic Blue 41 and Basic Orange 66) dyes during illumination with UV irradiation in the presence of TiO₂ and FeCl₃. The process of decoloration during illumination of the solutions studied containing FeCl₃ underwent significant intensification in the case of anionic dyes and unfavorable inhibition in case of cationic dyes.

The adsorption and photocatalytic degradation of diazo Direct Yellow 12 and Direct Black 38 in aqueous suspension of semiconductor oxide TiO₂ under UV light has been investigated by Toor et al., (2006) and Regina et al., (2005) respectively. The adsorption was described according to the Langmuir model. The disappearance of the dye follows pseudo-first order kinetics. In another study, Rathi et al., (2003) reported the photodegradation of Direct Yellow 12 using UV/H₂O₂/Fe²⁺ as a function of concentration and COD reduction. The results indicate that dye degradation is dependent upon pH, UV intensity, concentration of Fenton's reagent and dye. Shen and Wang (2002) successfully carried out the treatment of Direct Yellow 86 dye wastewater by UV/H₂O₂ process in continuous annular photoreactors under UV light intensities, influx concentrations of dye, dosages of H₂O₂ and dimensions of photoreactor.

Saquib et al., (2007) have investigated the photocatalytic degradation of a dye derivative, Disperse Blue 1 under UV light and sunlight in the presence of TiO₂ and H₂O₂

under a variety of conditions, such as, different types of TiO₂, reaction pH, catalyst and substrate concentration containing hydrogen peroxide H₂O₂ and molecular oxygen. The degradation rates were found to be strongly influenced by all the above parameters. Alaton (2004) has described a new method for disperse dye decolorization using the photochemically active silicadodecatungstic acid (H₄SiW₁₂O₄₀)⁺ isopropanol (electron donor) redox system. It was also evident that decolorization kinetics were first-order with respect to dye concentration for concentrations up to 75 mg L⁻¹, and the photochemical degradation rate became UV-light penetration limited (zero order) above 100 mg L⁻¹ dye concentration.

2.3.3 Degradation of Dye intermediates

Rao et al., (2003a) focused on the influence of metal salts on the photocatalytic efficiency of TiO₂ for the elimination of two azo dyes, Acid Orange 7 (AO 7), tartrazine and a dye intermediate, 3-Nitrobenzenesulfonic acid (3-NBSA). A beneficial effect of the presence of metallic species was observed only with samples containing silver. Advanced oxidation process utilizing Fenton's reaction was investigated for the decolorization and degradation of two commercial dyes viz., Red M5B, Blue MR and H-acid, a dye intermediate by Swaminathan et al., (2003). He concluded that the initial oxidation reaction was found to fit into first order rate kinetics and the rate of oxidation of H-acid was higher than the other dyes. Oxidative treatment of H-acid and Reactive Black 5 (RB5) using Fenton reagent (Fe²⁺/H₂O₂) and the Electro-Fenton (EF) method was reported by Rao et al., (2006). Noorjahan et al., (2003) in her work focused on the heterogeneous photocatalytic degradation of H-acid, a toxic and non-biodegradable dye intermediate, in TiO₂ suspensions and TiO₂ thin film fixed bed reactor. It was concluded that photocatalytic treatment significantly reduces COD and increases the biodegradability of H-acid.

2.4 Catalyst

There are a number of different semiconducting materials which are readily available, but only few are suitable for sensitizing the photo-mineralization of wide range of pollutants. The semiconductor to be used as photocatalyst for photo-mineralization of wide range of organic pollutants must be (i) photoactive (ii) able to utilize visible and or near UV light (iii) biologically & chemically inert and (iv) photo-stable. Barbeni et al., (1985) performed the photodegradation of pentachlorophenol sensitized by dispersion of

the following semiconductors, TiO₂, ZnO, CdS, WO₃, SnO₂ and showed that of all the different semiconductor photocatalysts tested, TiO₂ appears to be the most active.

Titanium dioxide in the anatase form appears to be the most photo-active (Rao et al., 1980; Nishimoto et al., 1985) and the most practical of the semiconductors for widespread environmental application such as water purification, wastewater treatment, hazardous waste control, air purification, and water disinfection. ZnO appears to be a suitable alternative to TiO₂; however ZnO is unstable with respect to incongruous dissolution (Carraway et al., 1994; Hoffmann et al., 1994; Bahnemann et al., 1987) to yield Zn(OH)₂ on the ZnO particle surfaces and thus leading to catalyst inactivation over time. Photocatalytic degradation of various azo dyes in water using slurry reactor in the presence of ZnO as a photocatalyst under UV light irradiation have been studied and the effects of various process variables on the degradation performance of the process have been investigated (Akyol and Bayramoglu, 2005; Nishio et al., 2006, Lizama et al., 2002). Studies have also been done using catalysts like ZnO under sunlight (Neppolian et al., 1998; Chakrabarti and Dutta, 2004) and good results have been obtained but their applications remain limited only by pH. Jang et al., (2006) compared the photocatalytic activity of ZnO nanoparticles and its nano-crystalline particles using methylene blue under UV light illumination. The photocatalytic degradation capacity of the ZnO nanoparticles was higher than that of the ZnO nano-crystalline particles.

It is generally found that only n-type semiconductor oxides are stable towards photo-anodic corrosion, although such oxides usually have bandgaps, which are sufficiently larger than the semiconductors, which absorb only UV light. CdS is an example of a highly active semiconductor photosensitizer, which has the highly desirable feature that, it can be activated using visible light (thus sunlight could be used). But as is typical for visible light absorbing semiconductors, it is liable to photo-anodic corrosion and this feature renders it unacceptable as a photocatalyst for water purification (Revtergardh and Iangphasuk, 1997; Karunakan and Senthivelon, 2005).

Kohtani et al., (2003) demonstrated that photocatalytic degradation using visible light driven BiVO₄ photocatalysts useful for the higher alkylphenols because the hydrophobic nature of long alkyl chain results in large amount of adsorption by BiVO₄.

Linder et al., (1997) have reported that anatase TiO₂ powder is a highly active photocatalyst. In recent years, Degussa P25 TiO₂ has set the standard for photoreactivity in environmental applications, although TiO₂ produced by Sachtleben, Germany (Martin et al., 1994a & b) show comparable reactivity. Degussa P25 TiO₂ has effectively become a research standard because it has (i) reasonably well defined nature (i.e. typically nonporous 70:30% anatase-to-rutile mixture with a BET surface area of 55±15 m²g⁻¹ and crystallite sizes of 30 nm in 0.1 µm diameter aggregates and (ii) a substantially higher photocatalytic activity than most other readily available samples of TiO₂. Fujishima et al., (2000) gave in his review, current progress and applications in the area of TiO₂ photocatalysis, mainly photocatalytic air purification, sterilization and cancer therapy. The photocatalytic efficiency of several TiO₂ (namely Degussa P25, UV100 and PC500) used as suspensions are compared for the photocatalytic degradation of triphenylmethane dye by Saquib and Muneer (2003a). Degussa P25 was found to be the most efficient photocatalyst for the degradation of the dye. It was explained on the basis of the slow electron-hole recombination in case of Degussa P25. Sivekumar and Shanthi (2001) reported the photocatalytic studies on some textile reactive dyes using different grades of TiO₂ namely CDH, CERAC and DEGUSSA and they concluded that TiO₂ (Degussa P-25) was superior to any other grade.

Many researchers claim that rutile is catalytically inactive (Mills et al., 1993a & b, Martin et al., 1994c) or a much less active form (Karakitsou and Verykios, 1993; Ohtani and Nishimoto, 1993) of TiO₂, while others find that rutile has selective activity toward certain substrates. However, Domenech (1993) has shown that TiO₂ in the rutile form is a substantially better photocatalyst for the oxidation of CN⁻ than is the anatase form; on the other hand, he also showed that Degussa P25 was a better catalyst than rutile for the photo-reduction of HCrO₄⁻ (Peral et al., 1990).

Martin et al., (1994c) reported an increase in photo degradation rates of 4-chlorophenol as the anatase form of TiO₂ is calcined progressively from 100 to 400°C (i.e., the particles calcined at 400°C yield the highest photo degradation rates) and then a decrease in photo degradation rate was noted for samples calcined above 500°C. For comparison, the photonic efficiency was found to be 0.23 for anatase (400°C) and 0.03 for rutile (800°C).

2.4.1 Surface Modifications of TiO₂

As was stated earlier in this review, one of the most active fields of research in heterogeneous photocatalysis using semiconductor particles is the development of a system capable of using natural sunlight to degrade a large number of organic and inorganic contaminants in wastewater (Matthews, 1987; Ollis et al., 1993, 1991). The overall photocatalytic activity of a particular semiconductor system for the stated purpose is measured by several factors including the stability of the semiconductor under illumination, the efficiency of the photocatalytic process, the selectivity of the products and the wavelength range response. For example, small band-gap semiconductors such as CdS are capable of receiving excitation in the visible region of the solar spectrum, but are usually unstable and photodegrade with time (Henglein, 1982). On the other hand, TiO₂ is a quite stable photocatalyst, but since the band gap is large ($E_{bg} = 3.2$ eV) it is only active in the ultraviolet region, which is < 4-6% of the overall solar intensity as shown in Figure 2.1 (Jackson, 1975). The limitations of a particular semiconductor as a photocatalyst for a particular use can be surmounted by modifying the surface of the semiconductor.

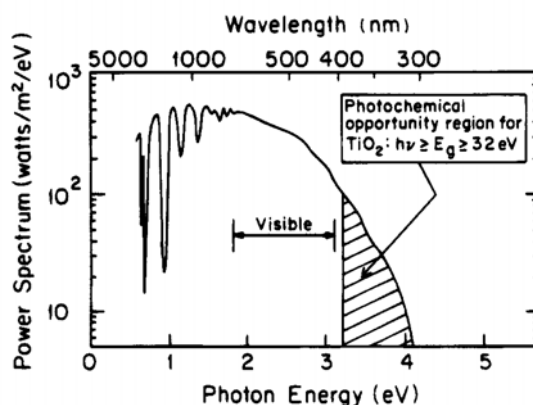


Fig. 2.1 Solar spectrum at sea level with sun at zenith

2.4.2 Metal modification of TiO₂

In photocatalysis, the addition of noble metals to a semiconductor can change the photocatalytic process by changing the semiconductor surface properties thereby enhancing the rate of photocatalytic reaction. Figure 2.2 is an illustration of the electron capture properties at the Schottky barrier of the metal in contact with a semiconductor surface. Transmission electron microscopy measurements have found that the Pt particles form clusters on the surface. After excitation, the electron migrates to the metal where it

becomes trapped and electron-hole recombination is suppressed. The hole is then free to diffuse to the semiconductor surface where oxidation of organic species can occur.

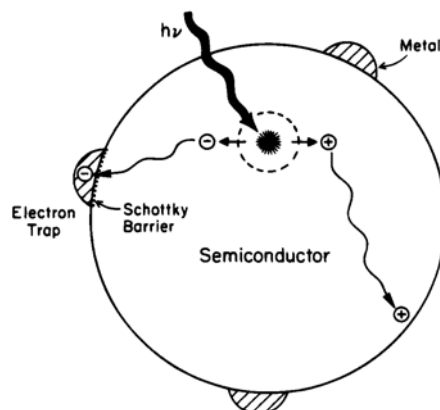


Fig. 2.2 Metal-modified semiconductor photocatalyst particle

Chromium, manganese and cobalt-doped titanium dioxide photocatalysts containing 0.2, 0.5 or 1 % of metal-dopant were investigated by UV–VIS, FT-IR, near-IR and electron paramagnetic resonance (EPR) spectroscopic techniques (Dvoranova et al., 2001). The presence of the doping ions in the titania structure caused significant absorption shift to the visible region compared to pure TiO₂ powder (P25 Degussa).

Crittenden et al., (1995) showed improved performance of platinumized TiO₂ fixed on silica gel. Since platinumized TiO₂ showed the maximum improvement, Magrini et al., (1994) used it to treat Trichloroethylene (TCE) contaminated groundwater and found that the catalyst retained its enhanced activity in a realistic application. He et al., (2006) compared the photocatalytic activity of two platinumized TiO₂ films, Pt-TiO₂/ITO and Pt(TiO₂)/ITO. He concluded that when compared with pure TiO₂/ITO film, the photocatalytic activities of the platinumized TiO₂ films were apparently improved.

Photo-oxidation of oxalic acid over TiO₂ surface in the presence of silver ion was studied by Bardos et al., (2003). It was shown that after the completion of silver deposition, the small metal particles on TiO₂ surface enhance the efficiency of the semiconductor by a factor of 5 for the photo-oxidation of oxalic acid. The dye degradation using untreated TiO₂ and Ag⁺ ion doped TiO₂ was compared and it was found that Ag⁺ ion doped TiO₂ is slightly more efficient (Sahoo et al., 2005; Gupta et al., 2006). Xu et al., (2005) in his paper reported that photocatalysts of Ag-TiO₂/SiO₂/Fe₃O₄ can photodegrade organic pollutants in the dispersion system effectively and can be

recycled easily by a magnetic force. Preparation of TiO₂ photocatalysts loaded with noble metal or transition metal oxide and the influence of preparing procedures on the photocatalytic activity for degradation of formaldehyde has been reported by Yang et al., (2000).

Zhou et al., (2006) prepared highly photo-active nanocrystalline mesoporous Fe-doped TiO₂ powders and their photocatalytic activity was evaluated by the photocatalytic oxidation of acetone in air. The results showed that the photocatalytic activity of the Fe-doped TiO₂ samples prepared by ultrasonic methods exceeded that of Degussa P25 by a factor of more than two times at an optimal atomic ratio of Fe to Ti of 0.25. This could be due to the synergistic effects of Fe-doping, large BET specific surface area and small crystallite size.

The influence of dissolved transition metal impurity ions on the photocatalytic properties of TiO₂ has become another interesting area of semiconductor modification. The benefit of transition metal doping species is the improved trapping of electrons to inhibit electron-hole recombination during illumination. With Fe³⁺ doping of TiO₂, an increase in Ti³⁺ intensity was observed by ESR upon photoirradiation due to trapped electrons (Gratzel and Howe, 1990). Only certain transition metals such as Fe³⁺ (Butler and Davis, 1993) and Cu²⁺ (Fujihira et al., 1982) actually inhibit electron-hole recombination. The concentration of the beneficial transition metal dopants is very small and large concentrations are detrimental.

Other transition metal dopants such as Cr³⁺ (Herrmann et al., 1984) create sites, which increase electron-hole recombination. It is believed that these transition metals create acceptor and donor centers where direct recombination occurs. Negative effects of doping (Luo and Gao, 1992) have been noted for Mo and V in TiO₂, while Gratzel and Howe (1990) noted an inhibition of the electron/hole recombination with the same dopants. Karakitsou and Verykios (1993) reported that doping TiO₂ with cations of higher valency than that of Ti (IV) resulted in enhanced photoreactivity, while Mu et al., (1989) noted that doping with trivalent and pentavalent cations was actually detrimental to the photoreactivity of TiO₂. Titanium dioxide catalysts were implanted with various transition-metal ions by a high-voltage technique, then calcined in O₂ at around 723K to produce photocatalysts capable of absorbing visible light and showed 3-4 times higher

photocatalytic reactivity for the decomposition of NO under sunlight as compared to the original unimplanted TiO₂ photocatalyst (Anpo, 2000).

2.4.3 Composite semiconductors

Coupled semiconductor photocatalysts provide an interesting way to increase the photocatalytic process by increasing the charge separation and extending the energy range of photo-excitation for the system. As illustrated by Fig. 2.3, the energy of the excitation light is too small to directly excite the TiO₂ portion of the photocatalyst, but it is large enough to excite an electron from the valence band across the band gap of CdS ($E_{bg} = 2.5\text{eV}$) to the conduction band. According to this energetic model in Fig. 2.3, the hole produced in the CdS valence band by the excitation process remains in the CdS particle while the electron transfers to the conduction band of the TiO₂ particle. The electron transfer from CdS to TiO₂ increases the charge separation and efficiency of the photocatalytic process. The separated electron and hole are then free to undergo electron transfer with adsorbates on the surface. The quantum yield for the reduction of methylviolet drastically increased and approached an optimum value of 1 when the concentration of TiO₂ was increased in a CdS-TiO₂ system (Gopidas et al., 1990). Transient absorption spectra of the composite CdS- TiO₂ photocatalyst indicates trapping of the electron at Ti⁴⁺ sites on the TiO₂ surface.

The CdS-TiO₂ system exhibits a broad absorption band in the 550-750 nm region after receiving a 355 nm (3.5 eV) picosecond laser pulse. This band is characteristic of chemical changes associated with the trapping of electrons on the TiO₂ surface. The lack of absorption activity in the 550-750 nm regions was tested by using the same laser pulse with the TiO₂ particles alone. Only the CdS portion of the composite photocatalyst exhibited an absorption band in the visible region. The transient absorption spectrum showed no absorption on clean TiO₂.

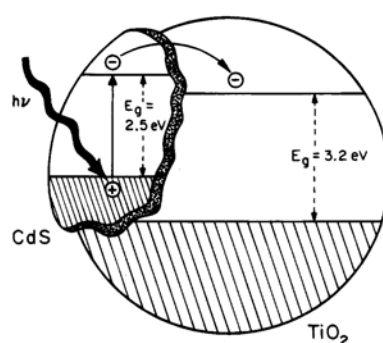


Fig. 2.3 Photo-excitation in composite semiconductor-semiconductor photocatalyst

The experimental results show that the coupling of semiconductors with the appropriate energy levels can produce a more efficient photocatalyst via better charge separation. Bessekhoud et al., (2006) investigated the activity of TiO₂, CdS and coupled CdS/TiO₂ powders. He concluded that under visible light, CdS/TiO₂ exhibit faster degradation rate than both isolated components of the composite photocatalyst.

Zorn et al., (2000) have studied the effect of reaction temperature on the catalytic and photocatalytic oxidation of ethylene on unplatined and platinized versions of a TiO₂/ZrO₂ mixed-oxide thin-film catalyst. Comparison between the thin-film catalyst show a fundamental difference in photocatalytic behavior, mainly due to insufficient utilization of the internal bulk of the particulate catalyst. Tada et al., (2000) have shown that coating TiO₂ with the MgO_x submonolayer increases the point of zero charge from 7.5 to 8.7 and significantly enhances TiO₂ photocatalytic oxidation of sodium dodecylbenzenesulfonate (DBS). Cho and Choi (2001a) have investigated the solid-phase photocatalytic degradation of poly (vinyl chloride) (PVC)-TiO₂ composite films under ambient air in order to assess the feasibility of developing photodegradable polymers. Sun et al., (2002) have prepared titanium dioxide/bentonite clay nanocomposite by acid-catalyzed sol-gel method and used it as a photocatalyst in the reaction of cationic azo dye decomposition in water. Zhang et al., (2004) studied the photocatalytic activity of nanocoupled oxides (ZnO-SnO₂) using Methyl Orange as a pollutant. Experimental results showed that the nanometer coupled oxides mainly consist of nanometer ZnO and SnO₂, and they have the same excellent photocatalytic activity as Degussa P25 TiO₂ for the degradation of methyl orange. Ooka et al., (2003) observed the enhancement in the photocatalytic degradation when TiO₂ pillared clay was applied for the adsorption-photocatalytic degradation of the endocrine disruptors with various hydrophobicities.

Alvaro et al., (2005) determined the photocatalytic activity of iron phthalocyanine adsorbed on silica (FePc/SiO₂) or encapsulated within NaY zeolite (FePc@NaY) towards the degradation of two model compounds using H₂O₂ as oxidant. He found that FePc/SiO₂ exhibits higher photocatalytic activity as compared to FePc@NaY but it cannot be used as a heterogeneous photocatalyst as it undergoes degradation and cannot be recycled. On the other hand FePc@NaY exhibits good recyclability.

2.4.4 Catalyst in the Form of Fixed Matrix

Most of the experimental work on aqueous systems has been carried out using the photocatalyst in the form of fine particles suspended in the liquid phase but the main drawback of this process is that the separation of TiO_2 from the solution is expensive. However to avoid the cost of removing the small catalyst particles from treated water, methods of fixing the catalyst on the support within the reactor has also been investigated which in many cases shows higher photocatalytic activation than parent TiO_2 (Xu and Langford, 1997; Chun et al., 2001). Surface bound-conjugated $\text{TiO}_2/\text{SiO}_2$ was prepared by means of impregnation method for photocatalysis of azo dyes by Chun et al., (2001). This TiO_2 fixed on silica gel showed three times higher photo-activity for the degradation of reactive dye (photodegradation was studied by XRD, FTIR, XPS and BET measurements). Noorjahan et al., (2003) reported the photodegradation of H-acid over a novel TiO_2 thin film fixed bed reactor by immobilized TiO_2 Degussa P-25 in aqueous suspensions using an acrylic emulsion by simple spray technique on inert cuddapah stone. Gopalkrishnan and Mohan (1997) carried out photodegradation of few textile dyes using TiO_2 in fixed mode i.e. by coating TiO_2 on sand and hollow glass beads. Subramanyam et al., (1998) have studied photocatalytic degradation of textile dyes Vat Blue, Fast Orange GC Base by immobilizing TiO_2 on ceramic beads and SiO_2 were used for many of the water soluble compounds. The photocatalytic dye degradation reactions simultaneously reduced COD and TOC, which suggest that dissolved organics have been oxidized.

TiO_2 has been affixed to a variety of surfaces like glass, silica, metals, ceramics, polymers etc. (Heung and Anderson, 1996; Lei et al., 1999; Liu et al., 2000; Miller et al., 1999; Shchukin et al., 1999; Sirisuk et al., 1999; Rao et al., 2003b; Fernandez et al., 2004). Photocatalytic degradation of various dyes using solar light as an irradiation source and immobilized TiO_2 as a photocatalyst showed the potential application for the decolorization of wastewater (Kuo and Ho, 2006; Cancang and Dewan, 1998).

The results of a study for the oxidative mineralization of 4-CP by oxygen, sensitized by thin films of Degussa P25 TiO_2 were reported by Mills and Wang (1998). Using a TiO_2 film, the process goes through the same mechanism as TiO_2 dispersion, generating the same intermediates namely, 4-Chlorocatechol and hydroquinone. Photocatalytic degradation of a few dyes have been successfully done using immobilized ZnO films (Roselin et al., 2002; Comparelli et al., 2004; Sakthivel et al., 2001; Yoshida et al., 2002).

Robert et al., (1999) have presented the preparation of TiO₂ supported on glass-fibre by sol-gel method. The influence of thermal treatment time on specific surface area, crystallinity and photocatalytic activity of the semiconductor for the degradation of a model pollutant compound, benzamide, was investigated. The supported catalysts have a good photocatalytic activity towards benzamide. However, the reduction of total organic carbon (TOC) from the test with TiO₂-FB is very slow. This observation carries out that the degradation process is not the same as that with the classical TiO₂-P25. Mills et al., (2002a) have prepared a novel CVD film of titanium (IV) oxide on glass via the reaction of titanium (IV) chloride and ethyl acetate, using a CVD technique. The film is clear, very robust mechanically and comprises of a thin (24 nm) layer of nanocrystalline anatase titania that absorbs light of $\lambda < 360$ nm. The film is also active photocatalytically and is able to destroy a deposited layer of stearic acid upon exposure to UV light.

2.4.5 Catalyst modification for harnessing visible light

To date, three benefits of modifications to photocatalytic semiconductor systems have been studied: (1) inhibiting recombination by increasing the charge separation and therefore the efficiency of the photocatalytic process; (2) increasing the wavelength response range (i.e., excitation of wide band gap semiconductors by visible light) and (3) changing the selectivity or yield of a particular product. Magrini et al., (1994, 1995) presented a review of the research on the physical and chemical modifications of TiO₂ to improve the catalyst performance and presented comparative data for the modified catalysts tested under the same conditions.

Surface sensitization of a wide bandgap semiconductor photocatalyst (TiO₂) via chemisorbed or physisorbed dyes can increase the efficiency of the excitation process by extending its absorption in the visible region of the spectrum. The photosensitization process can also expand the wavelength range of excitation for the photocatalyst through excitation of the sensitizer followed by charge transfer to the semiconductor (Gerischer and Willig 1976). Some common dyes which are used as sensitizers include Erythrosin B (Kamat and Fox, 1983), Thionine (Patrick and Kamat, 1992), Thionine and Eosin (Chatterjee and Mahata, 2001c) and analogs of Ru(bpy)₃²⁺ (Vlachopoulos et al., 1988; Desilvestro et al., 1986).

Fig. 2.4 illustrates the excitation and charge injection steps involved for the regenerative dye sensitizer surface process. Excitation of an electron in the dye molecule occurs to either the singlet or triplet excited state of the molecule. If the oxidative energy level of the excited state of the dye molecule with respect to the conduction band energy level of the semiconductor is favorable (i.e. more negative), the dye molecule can transfer the electron to the conduction band of the semiconductor. The surface acts as a quencher accepting an electron from the excited dye molecule. The electron in turn can be transferred to reduce an organic acceptor molecule adsorbed on the surface. Photosensitization of semiconductors by various dyes, monitored by nanosecond and picosecond flash photolysis, has provided valuable information on the mechanism of interfacial electron transfer on the semiconductor surface (Brown and Darwent, 1984; Kamat and Fox, 1983). Upon pulsed excitation of a dye-sensitized semiconductor, a shift in the flat-band potential caused by localization of electric charge on the semiconductor surface also occurs (Warman et al., 1991). Furthermore, very highly efficient sensitization of high area metal oxides has been attained with transition metal cyanides, presumably by surface pre-complexation or electrostatic association with metal complexes bearing carboxylate groups (Vrachnou et al., 1987).

Dye sensitization of the photochemical oxidation has been found to be a new pathway of pollutant degradation in visible light. Ross et al., (1994) have decomposed terbutylazine by applying visible light using Rose Bengal as a sensitizer and TiO_2 as a photocatalyst and the degradation was more than 50%.

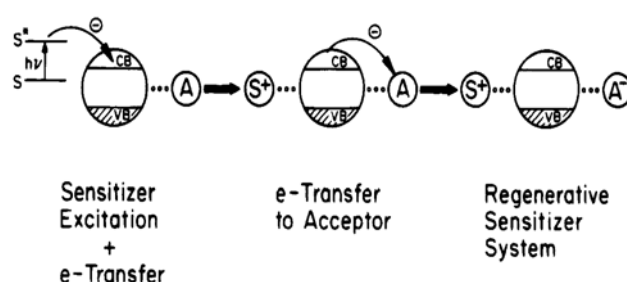


Fig. 2.4 Excitation steps using dye molecule sensitizer

Nasr et al., (1996) carried out visible light induced degradation of the textile diazo dye Naphthol Blue Black (NBB) on TiO_2 semiconductor nanoparticles. Chen et al., (2002a) studied the formation and identification of intermediates in the visible light

assisted photodegradation of Sulforhodamine-B dye in aqueous TiO₂ dispersion. Photodegradation of dyes has been achieved by illuminating the reacting system containing dye and flyash with visible light (Chatterjee et al., 2001b). The activation of TiO₂ photocatalyst for photocatalysis of Acid Red 44 under visible light is described by Moon et al., (2003).

Visible light assisted degradation of aromatics, like phenol, chlorophenol, 1,2-dichloroethane, trichloroethylene and surfactants, like cetyl pyridinium chloride (CPC; cationic), sodium dodecylbenzene sulfonate (DBS, anionic) and neutral Triton-X 100 in air-equilibrated aqueous mixtures has been achieved on the surface of TiO₂ semiconductor modified with Methylene Blue and Rhodamine B (Chatterjee and Mahata, 2002). Photo-assisted decomposition of phenol, chlorophenol and trichloroethylene in wastewater has been achieved on the surface of TiO₂ semiconductor modified with 8-Hydroxyquinoline (HOQ) by using visible light (Chatterjee and Mahata, 2001a). The dye sensitized TiO₂ nanoparticles fabricated onto the mesoporous silica material showed enhanced photocatalytic efficiency for decomposing Indigo Carmine than anatase TiO₂ by using visible light irradiation. The photocatalytic oxidation of various dyes and halocarbons by surface modified TiO₂ have been successfully achieved under visible light (Bauer et al., 2001; Hu et al., 2006; Zhao et al., 1998; Wu et al., 1999b; Mrowetz and Selli, 2004; Hasnat et al., 2005; Chatterjee et al., 2006).

Cho and Choi (2001b) investigated an application of TiO₂ photocatalyst sensitized with tris (4, 4'-dicarboxy-2-2' -bipyridyl) ruthenium (II) complex for CCl₄ degradation under visible light irradiation. The photo-oxidation of phenol, catalyzed by superficially modified with phthalocyanine complex oxide supports has been studied upon irradiation with visible light (Iliev, 2002). Ma and Chu (2001) studied that the use of an additional hydrogen source (NaBH₄) and photosensitizer (acetone) to improve the degradation rates of chlorinated aromatic dye in non-ionic surfactant solutions. Cheng et al., (2006) prepared an organic-inorganic layered hybrid by intercalation of Fe(bpy)₃²⁺ into laponite clay which upon visible light irradiation was found to be highly effective for the degradation of non-biodegradable cationic organic pollutants such as Rhodamine B and N,N-dimethylaniline, but was found to be inactive towards anionic organic compounds such as Orange II and Sulforhodamine B.

Bessekhouad et al., (2006) investigated the activity of TiO₂, CdS and coupled CdS/TiO₂ powders. He concluded that under visible light, CdS/TiO₂ exhibit faster degradation rate than both isolated components of the composite photocatalyst. Xiaodan et al., (2006) prepared photoactive ZnS/TiO₂ nanocomposites which exhibited enhanced visible-light photocatalytic activity as compared to solitary anatase TiO₂ for the aqueous parathion-methyl degradation.

2.5 Solar technology and textile effluent

In an article entitled “Solar photocatalytic detoxification” by Blake et al., (1992), they have reviewed in detail the fundamental chemistry of solar photocatalytic detoxification and the preliminaries of engineering system development. Goswami (1997) in his paper reviewed the engineering developments of the solar photocatalytic detoxification and disinfection processes, including system design methodologies. Anielak and Maria (1996) reviewed the research work on the treatment of textile industry wastewater with the application of mechanical, physicochemical, chemical and biological methods. Also the technological systems in operation and suggestions for application in textile industry wastewater treatment have been presented in this paper.

Arslan et al., (2000) investigated the fact that the effluents of textile industries can be treated with solar irradiation instead of UV-A light driven solar simulators which would eliminate major operational costs. Spiewak et al., (1998) had explored the use of concentrated sunlight combined with dissolved photocatalysts to improve water quality. The effectiveness of ZnO mediated solar photocatalytic degradation of three metal complex azo dyes and woolen textile dye house waste was examined (Saha and Malay, 2003). 53-86% degradation of the dyes was achieved by 15 min illumination, increasing BOD₅/COD ratio from 0.43 to 0.66. The aim of the study was to compare the performance of coagulation, Fenton’s oxidation and ozonation for the reduction of chemical oxygen demand under solar treatment of textile wastewater.

The photocatalytic degradation of few organic dyes in aqueous solution with TiO₂ as photocatalyst in slurry form have been investigated under sunlight (Muruganandham and Swaminathan, 2004b; Sivekumar and Shanthi, 2001; Augugliaro et al., 2002; Sauer et al., 2002; Neppolian et al., 2002a). It was concluded that solar light induced degradation of textile dye in wastewater is a viable technique for wastewater treatment. Styliidi et al.,

(2003) and Saquib and Muneer (2002) studied the photocatalytic degradation of an aqueous solutions of dyes in TiO₂ suspensions with the use of a solar light simulating source and the photo degradation pathway was proposed on the basis of quantitative and qualitative detection of intermediate compounds.

The solar photocatalytic degradation of various dyes has been studied over combustion synthesized nano TiO₂ and the activity was compared with that of commercial Degussa P-25 TiO₂ under similar conditions and the effect of various parameters was also studied (Nagaveni et al., 2004). The initial degradation rates with combustion synthesized nano TiO₂ was higher as compared to Degussa P-25.

Various chemical modifications of TiO₂ such as metallizing and doping with other semiconductors have been done for developing photoactive catalysts that out perform TiO₂ for use in solar-based detoxification systems (Magrini et al., 1994). These improvements in photocatalyst performance will ultimately lead to reducing the cost of solar-based detoxification systems for remediating organic contaminated wastewater streams.

A solar photocatalytic cascade reactor (nine stainless steel plates coated with TiO₂ catalyst arranged in cascade configuration) was constructed to study the photocatalytic oxidation of benzoic acid in water under various experimental and weather conditions at HKUST (Chan et al., 2003). The photocatalytic degradation was studied in terms of TOC and the effect of H₂O₂ was also shown to enhance the efficiency of the degradation process. Freudenhammer et al., (1997) during their research project which deals with the technical application of solar photocatalysis for wastewater detoxification found that non-concentrating thin-film fixed-bed reactor (TFFBR) used to study applications and areas where a solar-catalytic treatment or recycling of wastewater is possible. This reactor excels by its low cost and an easy-to-build construction using molecular oxygen in air as the oxidizing agent. The design parameters of the reactor as well as the process itself have been determined from the reaction kinetics of a model substance, the hydrodynamics and the mass transfer. The treatment of different real wastewaters was successfully carried out.

Herrmann et al., (2002) studied the photocatalytic degradation of pollutants with different grades of photocatalysts, Millennium PC-10, PC-25, PC-50 using titania

Degussa P-25 as a reference photocatalyst. After considering the overall rate of TOC disappearance, the relative activity patterns changed and only Millennium PC-50 with a similar surface area could exceed TiO₂ Degussa P25, chosen as a reference catalyst. Neppolian et al., (2002b) investigated the photocatalytic degradation of three commercial textile dyes with different structure using different photocatalysts in aqueous solution under solar irradiation. Experiments were conducted to optimize various parameters like amount of catalyst, concentration of dye, pH and solar light intensity. Degradation of all the dyes was examined by using chemical oxygen demand (COD) method. The experimental results indicate that TiO₂ (Degussa P25) is the best catalyst in comparison with other commercial photocatalysts such as, TiO₂ (Merck), ZnO, ZrO₂, WO₃ and CdS. Though the UV irradiation can efficiently degrade the dyes, naturally abundant solar irradiation is also very effective in the mineralization of dyes. Hence, it may be a viable technique for the safe disposal of textile wastewater into the water streams.

The feasibility of photocatalytic decolorization of real textile dyeing rinse wastewaters (RWW's) collected from the low salt cotton textile dyeing industry was studied by Kanmani and Thanasekaran (2003), using two grades of titanium dioxide (TiO₂) under ultraviolet and solar light sources. The effects of pH in the range of 6 - 10, catalyst concentration in the range of 0.05–0.5 g L⁻¹ for indoor UV studies and 0.25–2.0 g L⁻¹ for outdoor solar studies and catalyst reuse for twenty cycles were studied on photocatalytic decolorization of four batches of industrial RWW's. Since the RWW's contained more than one dye, their color measurements were done at multiple wavelengths of 436, 525 and 620 nm. In order to compare the effect of the operating variables on rinse wastewaters, the reaction time at 436 nm was taken into consideration since the reaction time necessary was maximum at 436 nm. It is concluded that the decolorisation of RWW's could be carried out at the natural pH itself. A catalyst concentration of 1 g L⁻¹ was found to be necessary in solar studies, whereas only one tenth of 1 g L⁻¹ was needed for UV studies. The titanium dioxides were found to maintain their photo activity during reuse for 20 cycles.

2.6 Ultrasound and Photocatalysis

Use of ultrasound as a catalyst for water and wastewater treatment and solar detoxification for environmental applications in materials chemistry is reported in literature (Suslick, 1999; Hua and Hoffmann, 1997; Ince et al., 2001). Vajnhandl and

Marechal, (2005) in his paper reviewed some fundamentals of ultrasound, its broad applications and gathered some new research regarding its applications in textile wet processes, with the emphasis on textile dyeing and the decoloration/mineralization of textile wastewaters. Gogate and Pandit (2005) in a review reflected the current status of the hydrodynamic cavitation reactors discussing the bubble dynamics analysis and optimum design considerations illustrating the utility of these reactors.

Fly ash samples modified by NaOH solution and sonochemical treatment were tested for the adsorption in aqueous solution of a basic dye, Methylene Blue by Wang and Zhu (2005a). He concluded that sonochemical treatment of fly ash could significantly increase the adsorption capacity depending on the concentration of NaOH and treatment time.

Schramm and Hua (2001) studied the sonochemical degradation of dichlorvos in a batch reactor and found that acoustic power and sparge gas are the two factors which greatly affect sonochemical degradation efficiency. Dukkanci and Gunduz (2006) studied the effect of ultrasound power, H_2O_2 , NaCl, external gases on the degradation of oxalic acid. He observed that H_2O_2 had negative contribution on the degradation of oxalic acid and there was an optimum concentration of NaCl for enhancing the degradation degree of oxalic acid. Further, Shemer and Narkis (2005) concentrated on the kinetics of degradation of trihalomethanes ($CHCl_3$, $CHBrCl_2$, $CHBr_2Cl$, $CHBr_3$ and CHI_3) under ultrasonic frequency of 20 kHz. He found that vapor pressure was the most important parameter affecting the sonodegradation kinetics and efficiency. Jiang et al., (2006) investigated the sonolysis of 4-chlorophenol (4-CP) in oxygen saturated aqueous solutions for a variety of operating conditions with the loss of 4-CP from solution following pseudo-first-order reaction kinetics. He concluded that the degradation takes place in the solution bulk at low reactant concentrations. Inoue et al., (2006) studied the degradation of Rhodamine B and Orange II dyestuff solutions using ultrasonic irradiation under different ultrasonic frequencies. He found that decolorization rate increases with the increase in frequency of the ultrasound. Okitsu et al., (2005) studied the sonochemical decolorization and decomposition of azo dyes, such as Reactive Red 22 and methyl orange. He concluded that azo dye molecules were mainly decomposed by OH radicals formed from the water sonolysis.

Mahamuni and Pandit (2006) studied a hybrid technique of ozonation coupled with cavitation for the degradation of phenol. He concluded that this hybrid technology leads to the formation of intermediates that can further be subjected to bio-degradation. Zhang et al., (2006) studied the combination of ultrasound and ozone for the decolorization of methyl orange dye. The results showed that the synergistic effect was achieved by combining ozone with ultrasonic irradiation for the decolorization of methyl orange. Further, it was observed that the decolorization rate increased with the increase of ultrasonic power, ozone gas flow rate and gaseous ozone. Zeng and James (2006) studied the degradation of pentachlorophenol (PCP) in aqueous solution by audible-frequency sonolytic ozonation. The first-order rate constant of PCP degradation by ozonation with sonication was found to be 15 times faster than that with bubbling ozone alone, while the rate constant with mechanical stirring was only four times faster. Martins et al., (2006) in his study aimed at investigating the chemical oxidation of Pararosaniline dye by ozonation and sonolytic processes. Experimental results indicated that ozonation of pararosaniline solution is more efficient than ultrasonic irradiation alone or in combination with O₃. Kang et al., (1999) investigated the kinetics of degradation of methyl tert-butyl ether by ultrasonic irradiation in the presence of ozone as a function of applied frequencies and applied power.

Gultekin and Ince (2006) reported the laboratory scale degradation of Acid Orange 8 with ultrasound, ozone and both. He concluded that the combined operation of ultrasound and ozone improved the rate of bleaching and UV absorption decay and remarkably enhanced the mineralization of the dye. Tezcanli-Guyer and Ince (2004) investigated a comparative degradation of azo dyes by 520 kHz ultrasonic irradiation and its combinations with ozone and/or ultraviolet light was investigated using a probe dye Acid Orange 7. He concluded that the overall degradation process was most rapid under simultaneous operation of the three (UV/US/O₃) in the presence of a continuous flow of a gas mixture made of argon and oxygen.

Guo et al., (2005) studied the influences of ultrasonic output intensity, solution pH, H₂O₂ concentration and addition of Fenton reagent on the degradation of 2, 4-Dinitrophenol (DNP) under ultrasonic irradiation. He observed that sono-oxidation treatment in combination with FeSO₄/H₂O₂ showed a synergistic effect for DNP degradation.

The hybrid effect of the irradiation by light and ultrasonic waves in conjunction with H₂O₂ was first confirmed to achieve the complete mineralization of propyzamide by Yano et al., (2005). Fung et al., (2000) reported the decolorization of reactive dye wastewater with UV radiation and ultrasonic vibration in the presence of hydrogen peroxide by a batch operation system. He found that the degradation of the reactive dye followed a pseudo-first-order kinetic model at different pH and peroxide dosages.

Further combination of ultrasound and photochemistry has been used to degrade an aqueous solution of phenol by Wu et al., (2001). Harada et al., (2001) investigated the role of a photocatalyst in the sonophotocatalytic reaction of water splitting using TiO₂ photocatalyst. Naffrechoux et al., (2000) combined the sonochemical and photochemical action in a 'sonuv' reactor and concluded that there was enhancement in the degradation rate of phenol. Selli et al., (2005) studied the kinetics of degradation of methyl tert butyl ether in water employing either sonolysis at 20 kHz or photocatalysis on TiO₂ or simultaneous sonolysis and photocatalysis as degradation techniques and found that rate enhancement under sonophotocatalytic conditions was stirring dependent. Chen et al., (2002b) observed the synergistic effect from the ultrasound on the photocatalytic degradation of phenol and chlorophenols in the presence of Hombikat TiO₂ suspensions in a sonophotocatalytic reactor. Mrowetz et al., (2003) studied the influence of initial substrate concentration (2-Chlorophenol) and photocatalyst amount on the degradation and mineralization rates which were found to ascertain the origin of the synergistic effect. Hirano et al., (2005) subjected the chlorinated organic compounds to pre-sonication followed by photocatalytic treatment. The pre-sonication effect results in the formation of some intermediate products, which are rapidly oxidized to carbon dioxide on further photocatalysis. Decolorization and COD removal from synthetic wastewater containing Reactive Brilliant Orange K-R dye using sonophotocatalytic technology was investigated by An et al., (2003). He concluded that this hybrid technology could efficiently remove the color and reduce COD from the synthetic dye containing wastewater, and that both processes followed pseudo first-order kinetics. Selli (2002) in another paper reported that photocatalysis and sonolysis exhibit the synergistic effects in the degradation of Acid Orange 8 in aqueous suspensions, when low ultrasound frequency is used. Chen et al., (2003) and studied the mechanistic aspects of the role of 20 kHz ultrasonication in photocatalytic oxidation of dimethyl methylphosphate in a batch reactor. He concluded, the increase or the rate of DMMP photocatalytic mineralization in the presence of

ultrasound was not due to deagglomeration of TiO₂, but was associated with enhanced mass transport of reagents. Wang et al., (2005b) in his study concluded that the sonophotocatalytic degradation ratios of methyl orange in the presence of TiO₂ were much better than the ones without any TiO₂, but the sonophotocatalytic activity of rutile TiO₂ particles was higher than that of anatase TiO₂ particles.

Gogate and Pandit (2004c) aimed at critically evaluating the status of the sonophotocatalytic reactors with a special focus on wastewater treatment applications. Different reactor configurations used for the hybrid technique have been analyzed and recommendations have been made for the design of optimum configuration. Sato and Yao (2006) treated the aqueous solutions of trichloroethylene and tetrachloroethylene in a flow-through reactor equipped with ultrasound and UV light sources. The results suggested that the combined effect of UV and US on the decomposition of TCE and PCE is synergistic in both the simultaneous and sequential UV/US modes. The rate constants of sonolysis and photolysis are greater with the sequential combination than with the simultaneous combination.

2.7 Coupled Photocatalytic and Biological treatment

Biological treatment of wastewaters discharged by the textile industry could potentially be problematic due to the high toxicity and recalcitrance of the commonly used azo dye compounds. Coupling of photocatalytic and biological processes is a good alternative to minimize the treatment cost of wastewater containing bio-recalcitrant and/or toxic pollutants. The chemical process could be used as pre-treatment method in order to increase the bio-degradability of the wastewater or as a post-treatment method to remove the non-biodegradable compounds. Recently, the advanced oxidation processes (AOP's) combined with biological treatment have appeared to be successful in large-scale systems. The general statements about the integration of bio-degradation and chemical oxidation are exemplified by case studies of textile wastewater bio-degradation combined with AOP's, which have been the subject of research for the last few years as reported by Ledakowicz et al., (2001). Scott and Ollis (2006) reviewed the studies which used the combination of chemical and biological degradation of organic contaminants in water.

Sarria et al., (2002) reviewed recent work in coupling advanced oxidation processes (AOP's) and biological systems for wastewater treatment and confirmed the

beneficial effects of such two-step treatment at laboratory scale. The coupled reactor, operating in semi continuous mode, has shown to reach a whole mineralization performance between 80 and 90%.

A combined photo-Fenton and biological flow reactor for the degradation of isoproturon was operated in continuous mode at laboratory scale. In this coupled system, 100% of the initial concentration of isoproturon and 95% of TOC were removed (Parra et al., 2000).

Pulgarin et al., (1999) presented a combined photochemical (Fenton) and biological flow reactor for the degradation of *p*-nitrotolueneortho- sulfonic acid (*p*-NTS), an important dye intermediate present in wastewaters coming from industries manufacturing dyes. The non-biodegradability of *p*-NTS in a fixed bed reactor (FBR) was proved under theoretically favorable conditions such as the presence of co-substrates and adapted bacteria. Afterwards, several experiments for sole photo-Fenton treatment were carried out in a laboratory scale photo-reactor. By way of Dissolved Organic Carbon (DOC) and HPLC techniques, it was found that mineralization of *p*-NTS via Photo-Fenton treatment in continuous or batch mode is not a cost-effective strategy. However, via photochemical treatment the non-biodegradable dye intermediate was converted to biodegradable non toxic product which could now be subjected to biological treatment leading to complete mineralization.

Leachates from municipal waste deposits which were biologically pre-cleaned, were treated subsequently with photochemical oxidation under three different UV sources. The ratio of COD and BOD₅ was reduced from ca. 230 to 3-4 (in the case of low pressure and vacuum mercury lamp) and to 6 (middle pressure mercury lamp). After this in biological stage the values of COD, BOD and AOX decreased further below the threshold values defined in the legislative regulation (Koh et al., 2004).

Lee et al., (2001) have carried out the theoretical and experimental studies and have established that integrated treatment systems (mostly chemical and biological) for various industrial wastewaters can achieve better quality of treatment and can be cost-effective. In this paper the objective is to minimize the use of processed water in the textile industry by an economical recycle and reuse scheme.

Reddy et al., (2003) studied the decolorization and mineralization of common industry effluents with TiO_2 photocatalyst using solar light illumination. The data indicates that the color and COD removal by the photocatalytic treatment is 74% and 62%, respectively (treated under sunlight for 40 h) whereas the COD removal in biological treatment is only 18% after treating for 120 h using Up-flow Anaerobic Sludge Blanket (UASB) reactor. The initial value of BOD_5/COD ratio of common industry effluent is 0.21, whereas the photocatalytic treatment method has improved the BOD_5/COD ratio to 0.56. Also the samples treated after photocatalytic method are further subjected to biological treatment that resulted in improved levels of COD removal of 72%, confirming that the pretreatment of common industry effluent by this method is beneficial.

Chun and Yizhong (1999) studied the photodegradation and biodegradability of few azo dyes using TiO_2 suspensions irradiated with medium pressure mercury lamp. He found that BOD increases while COD and TOC decreases, so that the ratio of BOD_5/COD of the wastewater increased from original zero up to 0.75 which shows that photocatalytic oxidation enhanced the bio-degradability of the dye containing wastewater.

2.8 Kinetics and Analytical Techniques

An understanding of reaction rates and how the reaction rate is influenced by different parameters is important for the design and optimization of an industrial system. The rate of photocatalytic degradation depends on several factors including illumination intensity, catalyst type, oxygen concentration, pH, presence of inorganic ions and the concentration of the organic reactant.

Different kinetic models have modeled the destruction rates of organics in photocatalytic oxidation. Langmuir- Hinshelwood (L-H) kinetics seems to describe many of the reactions fairly well (Abdullah et al., 1990; Al-Ekabi et al., 1989; Matthews, 1990; Turchi and Ollis, 1989). The pseudo first-order equation has been shown to apply to many photocatalyzed reactions (Gemeay et al., 2007; Fung et al., 2000; Behnajady et al., 2006). The order of reaction for H_2O_2 concentration and light intensity in both processes were obtained by linear regression method. A regression model was developed for pseudo-first order rate constant as a function of the H_2O_2 concentration and UV light intensity.

The first attempt at developing an analytical means for determining rate constants for batch type photocatalytic oxidation experiments was performed by Davis and Hao (1991). Xu and Langford (2000) used the Langmuir–Hinshelwood (L–H) kinetic model to describe semiconductor photocatalysis. In this report, the L–H rate constant (k_{L-H}) and the Langmuir adsorption constant (K) have been determined under different light intensity for the photocatalytic degradation of poorly adsorbed acetophenone over TiO_2 of Degussa P25 in aqueous medium (pH 6.2). The result shows that K decreases when the irradiation is performed at higher light intensity, while k_{L-H} increases expectedly. The kinetics of photocatalytic decomposition of low concentrations of trichloroethylene (TCE) in water was modeled and the reaction parameters were evaluated for different catalyst loading by Brandi et al., (2002).

Photocatalytic degradation of tetrahydrofuran, 1, 4-dioxane and their mixture in a slurry photoreactor was studied by Mehrvar et al., (2000). Using both GC/MS and ion chromatography (IC) methods, possible intermediates were detected and the reaction mechanistic pathways for both compounds were proposed. Kinetic models were developed and the kinetic parameters were estimated using a statistical method of non-linear parameter estimation in which all experimental data were utilized. It was shown that tetrahydrofuran disappeared via direct oxidation as well as hydroxyl radical attack.

For the degradation of phenol, a detailed kinetic modeling which describes the degradation of phenol was performed by Kusic et al., (2006). Mathematical models which predict phenol decomposition and formation of primary oxidation by-products by applied processes were developed. The study also consist the modeling of mineralization kinetics of the phenol solution by applied AOP's.

The dye decomposition kinetics by nano-size TiO_2 suspension at natural solution pH was experimentally studied by varying the agitation speed (50-200 rpm), TiO_2 suspension concentration ($0.25-1.71 \text{ g L}^{-1}$), initial dye concentration ($10-50 \text{ mg L}^{-1}$), temperature ($10-50^\circ\text{C}$) and UV power intensity (0-96W). Kinetic models have been developed to fit the experimental kinetic data well by Wu et al., (2006).

Cabrera et al., (1994) observed that one of the major problems lies in the difficulties associated with the proper evaluation of the absorbed radiant energy due to unavoidable system heterogeneities that produce light scattering. They developed a novel

form of reactor, combined radiation distribution model to evaluate the volumetric rate of energy absorption during the photocatalytic oxidation of trichloroethylene in water using a suspension of TiO_2 . The proposed approach permits a correct description of the radiation field inside the heterogeneous reactor and consequently a precise accounting of the absorbed photons. They also used the reactor and the model to evaluate heterogeneous system quantum efficiencies.

Alfano et al., (1997) gave a kinetic model to represent the time evolution of a photocatalytic reaction. It is applied for reacting systems where the catalyst is in suspension form, substrate is a hydrocarbon compound which is attacked by hydroxyl radical for initiation of the oxidative reaction, catalyst activation is produced by radiation energy in the near UV range, in the presence of oxygen and there is no mass transport limitation.

Ray and Beenackers (1997) designed a new two-phase swirl-flow monolithic type reactor to study the kinetics of heterogeneous photocatalytic processes on semiconductor catalysts. The kinetic rate constants for the destruction of textile dye were measured as a function of wavelength of light intensity and angle of incidence, catalyst layer thickness and the effect of absorption of light by liquid film on the overall rate of photocatalytic degradation. Chen and Ray (1998) also used this new two-phase swirl-flow monolithic type reactor to study the kinetics for destruction of 4-nitrophenol (4-NP). Most of the earlier work investigated the effects of various parameters on the initial degradation rate (or the formation of CO_2) of the pollutants. In this study, photo-mineralization of 4-NP sensitized by Degussa P25 TiO_2 in aqueous solution had been investigated as a function of the following different experimental parameters like initial concentration of pollutant light intensity, partial pressure of oxygen, catalyst concentration, pH and temperature. Andreozzi et al., (2000) have studied the photocatalytic oxidation of 4-nitrophenol in the presence of solid TiO_2 using different type of reactors. Zamostny and Belohlav (2002) have conducted three case studies presenting different aspects of the identification of kinetic models in heterogeneous catalysis. There demonstrations were based on the real examples of the laboratory catalytic hydrogenation experiments. This study helps to demonstrate the possibilities of maximizing the reliability of parameter for the application at the industrial scale.

Minero (1995) presented a kinetic model for the early stages of oxidation of an organic compound over irradiated semiconductors considering simple cases having advantage of simplicity and of analytical solutions to the general differential equations. Minero (1999) explored several kinetic models and gave an analytical equation for the rate and quantum yield which retains the principal features of the photocatalytic process, namely the light induced charge separation and recombination, the oxidative and reductive electron transfers, the formation of stable oxidized intermediate. All the previous features and dependence of light intensity were described by him with only three parameters, which collect all kinetic constants and account for experimental concentrations of the substrate and electron scavenger, light intensity and catalytic system characteristics.

Several researchers working in this field have used various analytical techniques to study the mechanism and degradation pathway of pollutants. Prevot et al., (2001) investigated the photocatalytic degradation of the anthraquinonic dye Acid Blue 80 in aqueous solutions containing TiO₂ dispersions. The mechanism has been studied by following either the disappearance of the dye (via HPLC) or the formation of its end-products (IC, GC, and TOC analysis). The identification of various unstable intermediates formed after low irradiation times was performed by HPLC-MS, to give insight into the early steps of the degradation process which mainly involve C-N bonds breaking and substrate hydroxylation.

Muruganandham and Swaminathan (2006) studied the photo-decolorization and degradation kinetics of Reactive Orange 4 in terms of Langmuir-Hinshelwood kinetic model. The degradation intermediates were analysed by GC-MS technique. The decolorization and mineralization of Acid Red 27, was investigated using UV radiation in the presence of H₂O₂. The AR 27 degradation was followed through HPLC, UV-Vis and COD analysis. Zielinska et al., (2003) studied the photocatalytic decomposition of organic dyes using TiO₂ under UV/Vis illumination. The photo-decomposition of these dyes on the photocatalyst surface was monitored by FTIR spectroscopy. Chun and Yizhong (1999) studied the photo-degradation and biodegradability of few azo dyes in terms of COD, TOC and BOD analysis.

Surface bond-conjugated TiO₂/SiO₂ was prepared by means of impregnation method for photocatalysis of azo dyes by Chun et al., (2001). This TiO₂ fixed on silica gel

showed three times higher photoactivity for the degradation of a reactive azo dye and photo-degradation was studied by XRD, FTIR, XPS and BET measurements. Lam et al., (2007) reported that sol-gel nano titanium dioxide thin film can be activated by the UV radiation available in sunlight to perform solar photocatalysis. The properties of the Cr/TiO₂ thin films were fully characterized by X-ray diffraction (XRD), differential scanning calorimetry (DSC), thermal gravity (TG) analysis, scanning-electron microscopy (SEM) and energy dispersive X-ray (EDX) analysis.

2.9 Reactors for Wastewater Treatment

Different reactors for the solar photocatalytic water treatment have been developed and tested in recent years. The reactors most often used are:

- (1) Parabolic trough reactors (PTRs)
- (2) Compound parabolic collecting reactors (CPCRs)
- (3) Tubular reactors with and without reflectors
- (4) Double-skin sheet reactor (DSSR)
- (5) Thin-film fixed-bed reactor (TFFBR)

Birnie et al., (2006) reviewed the existing photocatalytic reactors used in research and commercial applications and the guiding principles of effective reactor design were also discussed. Caliman and Balasanian (2005) after conducting a survey in the field of photocatalytic reactors reported the major issues that should be considered for the development of commercially available photocatalytic systems for different purposes: whether to use suspended or supported catalysts and whether to use concentrated or non concentrated sunlight. The common problems encountered in the design of photocatalytic reactors were also discussed and a few modalities for increasing their performances were proposed.

To implement solar photocatalytic water detoxification in industrial processes, the effluents from paper mills containing non-biodegradable substances like polyphenolic polymer lignin was very effectively degraded by photocatalytic treatment under sunlight, especially in solar reactors like the CPC type reactor, degradation takes place very fast. Total mineralization of the contaminants can be reached (Sattler et al., (2004).

Chapter 3

MATERIALS AND METHODS

This chapter describes the materials used and methods adopted for carrying out the experimental work.

3.1 Materials

3.1.1 Samples

The following chemicals were used for preparing synthetic wastewater:

- a. Commercially available Reactive Red dye 198 (RR dye 198) was gifted from a nearby textile industry, Nahar Fabrics, Derabassi, Punjab, India and was used as such without any purification.
- b. J-Acid (6-Amino naphthol-3-sulfonic acid) was purchased from Sigma Aldrich Company, USA.

Effluent sample was collected from S.R. textile industry, Derabassi, Punjab, India.

3.1.2 Catalysts used

1. **Degussa P25 TiO₂** was procured from Degussa Company, Germany. It has a BET surface area of $50 \pm 15 \text{ m}^2 \text{ g}^{-1}$ and is 70% in anatase crystal form with average particle size of 30 nm.
2. **Hombikat UV 100 TiO₂** was procured from Sachtleben Chemie GmbH, Germany. It consists of 100% anatase with specific BET-surface area of $> 250 \text{ m}^2 \text{ g}^{-1}$ and primarily particle size of 5 nm.
3. **Sensitized TiO₂** was prepared by the following procedure:
To 500 ml of Rose Bengal solution (500 mg L^{-1}) was added 5 g of TiO₂ and then left overnight in dark with stirring for adsorption equilibration. The solution was filtered and the Rose Bengal adsorbed TiO₂ was dried at room temperature. The amount of the sensitizer adsorbed on the TiO₂ surface was calculated from the difference in absorption and it was found to be 90 mg g^{-1} .
4. **ZnO** was purchased from Sigma Aldrich Company, USA having its BET-surface area of $5 \text{ m}^2 \text{ g}^{-1}$.

3.1.3 Reagents and Chemicals

Hydrogen peroxide (30% v/v solution) and Ammonium persulphate obtained from S. D. Fine Chemicals Limited, India, were used as oxidants. Hydrochloric acid and sodium hydroxide (S. D. Fine Chemicals Limited, India) were used to adjust the pH. Rose Bengal was obtained from Aldrich and was used as received. The other chemicals used were NaN_3 (extra pure, Merck), DABCO ($\text{C}_6\text{H}_{12}\text{N}_2$, 98%, Aldrich) 1,4-Benzoquinone, prepared in the laboratory by the literature reported procedure (Singh V. et al., 2003) and recrystallized twice with pet. ether, and phenol (S. D. Fine Chemicals Limited, India).

Reagents used for COD determination were potassium dichromate, mercuric sulphate, silver sulphate, concentrated sulphuric acid, ferrous ammonium sulphate and ferroin indicator. For BOD determination sodium thiosulphate, manganese sulphate, potassium iodide, sodium azide, starch and sulphuric acid were used. All chemicals for COD and BOD analysis were obtained from Ranbaxy Laboratories, India.

All chemicals were used as received. In all the experiments, double distilled water was used.

3.2 Equipment and Instruments

3.2.1 Radiometer

The sunlight intensity was measured by using an Eppley radiometer (model no. 33013).



Fig 3.1 Eppley radiometer

3.2.2 pH Meter

The pH of the solution was varied by adding HCl or NaOH solution as per requirement and measured using ELICO, India, model no. LI 120 pH meter.

3.2.3 UV-Vis Spectrophotometer

For determining the concentration of various compounds, UV-Vis spectrophotometer (Hitachi U-2001) was used.

3.2.4 Filtration

Samples after photocatalytic treatment were filtered through Millipore filter (0.45 μ m) membrane.

3.2.5 Ultrasonic Bath

To study the effect of ultrasound the whole reactor assembly was immersed in Branson Ultrasonic Cleaning Bath model 3150DTH (47 kHz, 130 W).

3.2.6 Autoclave

Semi- automatic autoclave (EQUITRON, India) was used for the digestion of samples in COD determination.

3.3 Photoreactors

Degradation studies were conducted using following two non-concentrating type reactors:

- 1 Immersion well type photoreactor
- 2 Shallow pond slurry reactor

3.3.1 Immersion well type photoreactor

An immersion well type photochemical reactor made of Pyrex glass equipped with a water-circulating jacket maintaining a temperature of 25°C and an opening for supply of oxygen as shown in Fig. 3.2 was used. The photocatalytic reactor is provided with one more inlet (sampling port) through which the samples are taken with the help of syringe from time to time during the experiment. The photoreactor is placed on a

magnetic stirrer. A 50W halogen lamp and 125W medium pressure mercury lamp is placed in the centre of the photoreactor as a source of UV and visible light respectively.

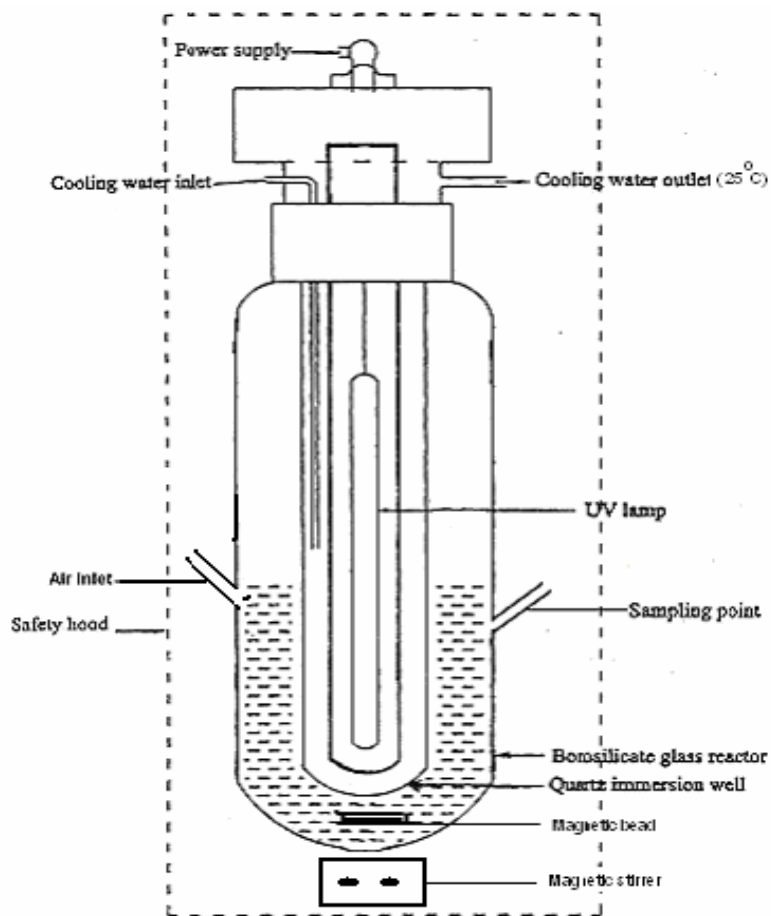
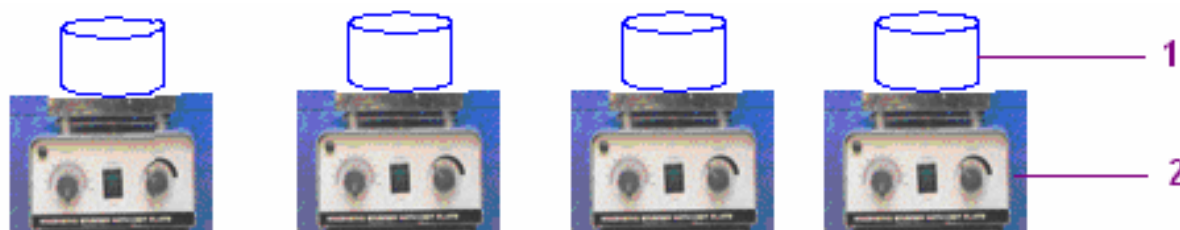


Fig.3.2 Laboratory setup for immersion well type reactor

3.3.2 Shallow pond slurry reactor

A schematic diagram of lab scale set up for shallow pond reactor is shown in Fig. 3.3. A batch type bench scale photocatalytic reactor system was fabricated for conducting experiments. The set up consisted of a batch reactor placed on a platform under sunlight.



*Fig.3.3 Schematic diagram of lab scale set up for shallow pond reactor:
(1) Reactor, (2) Magnetic stirrer*

An Eppley radiometer model no. 33013 was used to measure the UV intensity. A Borosil glass vessel of 1000 ml capacity was used as the shallow pond reactor and it was covered with a thin plastic film through which 98% of UV rays can pass. This reactor is placed on a magnetic stirrer to keep the contents in the reactor well mixed, so that the TiO₂ remains suspended and the concentration of the pollutant within the reactor could be assumed to be constant at any time.

3.4 Experimental Procedures

3.4.1 Adsorption Experiments

The adsorption tests under dark conditions were carried out in order to evaluate the adsorption of dye on the TiO₂ surface at different pH and different initial concentrations of RR dye 198 and J-acid and to calculate the equilibrium constants. These tests were performed using 200 ml aqueous solution of RR dye 198 and J-acid respectively at different initial concentration and pH of the solution put in contact with optimum amount of TiO₂ for 2 h and kept in dark at 25°C. The solution was filtered through a 0.45 µm filter and concentration of the unabsorbed substrate was measured to find the extent of adsorption as a function of initial concentration at different pH.

3.4.2 Experiments using Immersion well Photoreactor

Stock solution of concentration 100 mg L⁻¹ stock solution of the substrate (Reactive Red 198 dye/ J-acid) was prepared in distilled water for all the experiments under UV light which was diluted to 50 mg L⁻¹ while carrying out the irradiation experiments under visible light. 200 ml of solution was taken in the reactor and the catalyst was added to it. The pH of the solution was noted. Oxygen was continuously purged throughout the experiment. The suspension was then irradiated under UV light using 125W medium pressure mercury lamp or visible light using 50W halogen lamp with continuous stirring using a magnetic stirrer for the required period of time. An aliquot of 5 ml was taken from the reactor at regular intervals of time with the help of a syringe. The catalyst was filtered from the sample by using a Millipore filter (0.45 µm). These samples were analyzed using a UV-Vis spectrophotometer/COD analysis. The pH of the final solution was noted. Experiments were repeated in triplicate for getting the reproducibility of results. To study the effect of ultrasound, the entire photoreactor assembly was immersed in an ultrasonic bath. Various experiments were conducted in the

above setup for optimizing the parameters like initial concentration, pH, catalyst loading, and H₂O₂ concentration. To study the effect of radical quenchers on the photocatalytic degradation of RR dye 198, 0.1 g L⁻¹ of three different compounds, NaN₃, DABCO and 1,4-Benzoquinone were added in three individual experiments and the suspension was irradiated under normal conditions as explained above.

3.4.3 Experiments using Shallow pond slurry reactor under sunlight

Stock solution of concentration 100 mg L⁻¹ stock solution of the substrate (Reactive Red 198 dye, J-acid) was prepared in distilled water for all the experiments. Wastewater collected from the textile industry was highly concentrated and therefore to get the values within range, the sample was diluted in the ratio of 1:1. Distilled water was used for all the dilutions. 200 ml of solution was taken in the reactor with A/V ratio of 1.14 cm² ml⁻¹ and the catalyst was added it. The pH of the solution was noted. Oxygen was continuously purged throughout the experiment. The suspension was then irradiated under sunlight (the intensity of which was measured by Radiometer) with continuous stirring using a magnetic stirrer for the required period of time. An aliquot of 5 ml was taken from the reactor at regular intervals of time with the help of a syringe. The catalyst was filtered from the sample by using a Millipore filter (0.45 μm). These samples were analyzed using a UV -Vis spectrophotometer/COD analysis. The pH of the final solution was noted. Experiments were repeated in triplicate for getting the reproducibility of results.

For degradation of effluent with the above mentioned setup, the various experiments were conducted for optimizing the parameters like initial concentration, pH, catalyst loading, H₂O₂ concentration and A/V ratio. Before and after photocatalytic treatment (with optimized conditions), water was filtered and checked for COD, BOD, TSS, TS, TDS and pH.

3.5 Sample collection and storage of wastewater sample

Wastewater sample was collected from the equalization tank in the effluent treatment. The sampling bottle was cleaned and rinsed carefully with distilled water and then with the effluent. About 2.5 cm air space is left in the bottle to facilitate mixing by shaking. Then samples were stored at 4⁰C within one to two hours of sample collection.

3.6 Water Analysis

3.6.1 Total Solids

Total solids were measured by method No. 2540 B, page no. 2-72 of STANDARD METHODS for the examination of Water and Wastewater (Greenberg, 1989)

3.6.2 Total Dissolved Solids

Total dissolved solids were estimated as per the standard method No. 2540 C, page no. 2-74 of STANDARD METHODS for the examination of Water and Wastewater (Greenberg, 1989).

3.6.3 Total suspended solids

Total suspended solids were calculated by method No. 2540 D, page no. 2-75 of STANDARD METHODS for the examination of Water and Wastewater (Greenberg, 1989).

3.6.4 Estimation of BOD

BOD was determined as per standard method No. 5210 B, page no. 5-4 from STANDARD METHODS for the examination of water and wastewater, 1989, 17th edition (Greenberg, 1989). Dilutions for strong industrial effluents are quoted from 0.1% to 1.0%, 0.2% and 0.4%. Tests were repeated for getting the reproducibility of results.

3.6.5 Estimation of COD

COD was calculated as per the standard method No. 5220 C, page no. 5-14 from STANDARD METHODS for the examination of water and wastewater, 1989, 17th edition (Greenberg, 1989). For all the samples 1:1 dilution was done so as to get the COD within range while using the above method. Samples were digested in a semi-automatic autoclave.

3.6.6 GC- MS analysis

GC-MS analysis was done using Hewlett Packard HP 6890 series, GC system with FID detector, 5973 Mass Selective Detector and auto sampler was used. Column DB-5 MS [5% phenyl polysiloxane (30x250x0.25 μm), ID - 0.25 mm, film μm – 0.25]

with temperature limit of $-60-325^{\circ}\text{C}$ purchased from J & W scientific was used. Operating programme was ($100^{\circ}-5^{\circ}-200^{\circ}-15^{\circ}-280^{\circ}$) in splitless mode. An injection volume of $0.5\ \mu\text{l}$ with helium as a carrier gas was used for analyzing the residue.

3.6.7 Using UV- Visible Spectrophotometer

A PC based UV-Vis spectrophotometer was used for determination of concentration of synthetic samples as per following procedure.

The system is switched on and warmed up. Thoroughly cleaned quartz cuvettes are used. One cuvette is filled with the reference compound and the other one with the compound whose absorbance has to be measured at λ_{max} . To get the relationship between concentration and absorbance of the compound, a calibration curve is made. Calibration solutions are made from standard solutions of known concentration. The absorbance is plotted against known concentration of the calibration samples. These calibration curves are stored in the system itself and the concentration of the unknown sample can be calculated directly from the absorbance.

3.7 Biodegradability of Organic Pollutants

The ratio of BOD and COD in wastewater is normally used to express the biodegradability of the wastewater. When the ratio of BOD and COD is more than 0.3, the wastewater has a better biodegradability, whereas if the ratio is less than 0.3, it is difficult to degrade the impurities by biological methods (Chun and Yizong, 1999).

To investigate the biodegradability of dyes solution, COD and BOD of the samples before and after the photocatalytic treatment were measured.

Chapter 4 (A)

PHOTOCATALYTIC DEGRADATION OF REACTIVE RED 198 UNDER UV LIGHT

4.1 Overview

This chapter deals with the adsorption and photocatalytic degradation of Reactive Red 198, commonly used as a textile dye, in the presence of various photocatalysts as an aqueous suspension under UV light in an immersion well type photoreactor. Effect of various operational parameters like catalyst loading, initial substrate concentration, pH and addition of oxidant is studied to determine the optimized conditions for maximum degradation. Under optimized conditions the degradation of RR dye 198 was also carried out under sunlight using a shallow pond slurry reactor.

4.1.1 Structure of Reactive Red 198

The structure of Reactive Red dye 198 (RR dye 198) is as given in Fig 4.1.1. It is a red colored reactive dye containing a suitable group (2,4,6-monochlorotriazinyl amino group and vinyl sulphone group) capable of forming a covalent bond between a carbon atom of the dye ion or molecule and an oxygen, nitrogen or sulphur atom of a hydroxyl, an amino or a mercapto group respectively of the substrate (Abrahart, 1997).

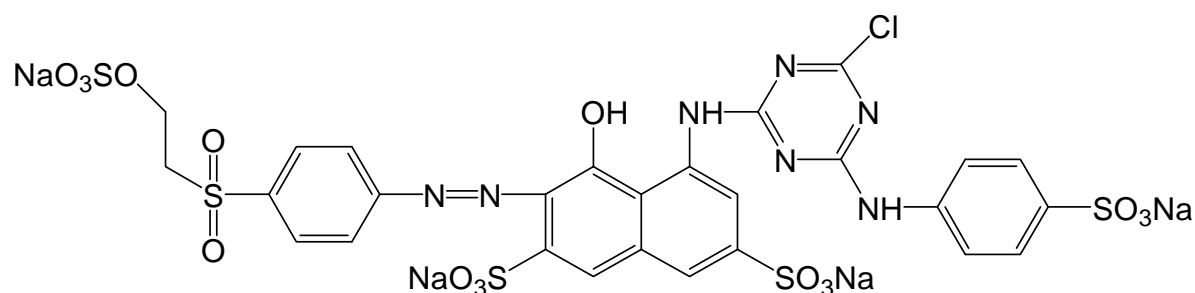


Fig. 4.1.1 Structure of Reactive Red 198

4.1.2 Adsorption Equilibrium in Dark Conditions

The adsorption tests under dark conditions were carried out as per the procedure given in section 3.4.1. All the adsorption isotherms obtained at different pH were L-shaped as shown in Fig 4.1.2.

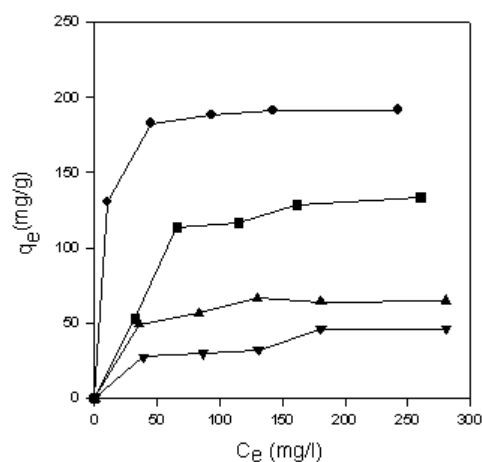


Fig. 4.1.2 Adsorption isotherms of RR dye 198 on TiO₂ surface at different initial pH
 (◆) pH 3.5, (■) pH 4.6, (▲) pH 7, (▼) pH 9

The equilibrium constants were determined by fitting the experimental data to the Langmuir equation (Eq. 4.1.1) to describe the adsorption of the dye on the homogeneous surface of TiO₂:

$$q_e = \frac{q_m b C_e}{1 + b C_e} \quad (\text{Eq. 4.1.1})$$

where q_m is the maximum amount of dye adsorbed forming a complete monolayer, b is the equilibrium parameter, C_e is the concentration of dye in aqueous solution, and q_e is the concentration of dye on the solid. The Langmuir equilibrium constants as per Eq. 4.1.2 are shown in Table 4.1.1.

$$K_a = q_m b \quad (\text{Eq. 4.1.2})$$

Table 4.1.1 Langmuir equilibrium constants for the adsorption of RR dye 198 on TiO₂ in dark

pH	K_a (g L ⁻¹)
3.5	10.55
4.6	1.51
7.0	1.00
9.0	0.50

4.1.3 Dye Degradation and Decolorization- TiO_2 suspensions using Immersion Well Reactor

Photocatalytic degradation of Reactive Red 198 (RR dye 198) was studied with P25 TiO_2 catalyst by varying different parameters in immersion well type photoreactor as shown in Fig 4.1.3. To study the degradation rate, the procedure given in section 3.4.2 was adopted. Reaction rate constant (k) is a function of parameters such as catalyst loading, pH of the solution, initial concentration of the substrate and addition of the oxidant. Therefore, the effects of these parameters on the reaction rate constant have been investigated in the laboratory reactor.

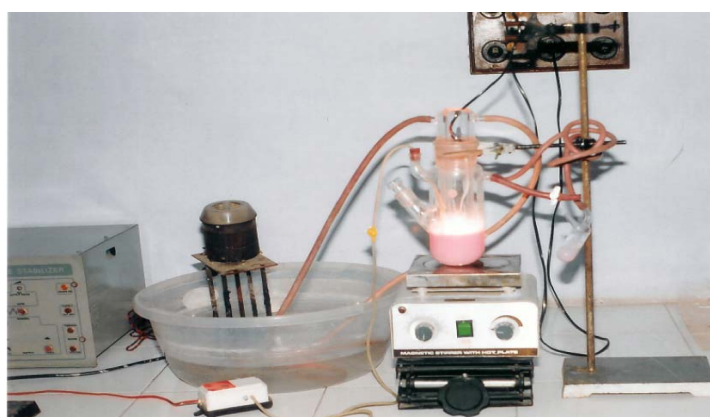


Fig. 4.1.3 Laboratory set up for the photocatalytic degradation of RR dye 198 under UV light

The time dependent electronic absorption spectrum of RR dye 198 is presented in Fig. 4.1.4 during photo-irradiation. The absorption peak height gradually decreases with time and after 45 minutes of irradiation under UV light in a TiO_2 aqueous suspension, the absorption peak of dye disappears totally, which indicates its complete degradation. Besides, no new bands appear in the UV-Vis region due to any reaction intermediate formed during the degradation process.

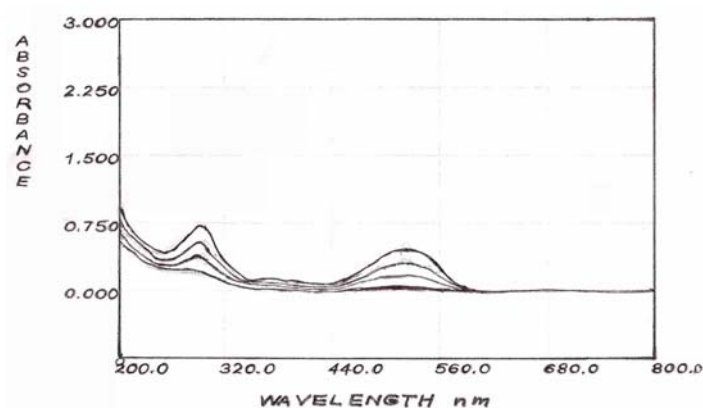


Fig. 4.1.4 Spectral changes in RR dye 198 during UV irradiation

4.1.4 Kinetic Studies

As the photocatalytic mechanism suggests, both TiO_2 and a light source are necessary for the photo-oxidation reaction to occur. A control experiment was conducted on the irradiation of RR dye 198 under only UV light, in the presence of TiO_2 , with and without UV irradiation over a period of 45 min. No degradation was observed in the presence of UV light only. In the presence of TiO_2 , but without irradiation, slight loss was observed due to the adsorption of the dye on to the surface of TiO_2 . However on irradiating the dye with TiO_2 in aqueous dispersion about 99% of the dye was degraded within 45 min of irradiation as shown in Fig 4.1.5.

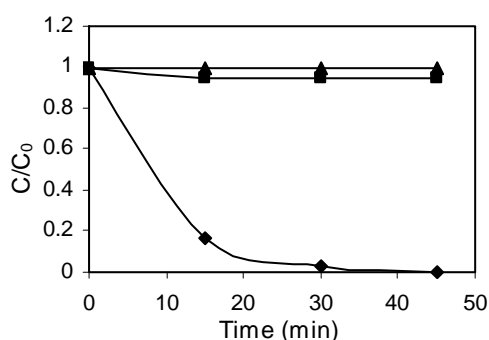


Fig. 4.1.5 Photocatalytic degradation of RR dye 198 (▲) only UV, (◻) only TiO_2 , (0.3 g L^{-1}), (◆) with TiO_2 (0.3 g L^{-1}) and UV light

The degradation, as exemplified by the RR dye 198 photodegradation data, can be approximated as first-order kinetics. Fig. 4.1.6 shows the linear fit between the $\ln(C_0/C)$ and irradiation time that supports this conclusion.

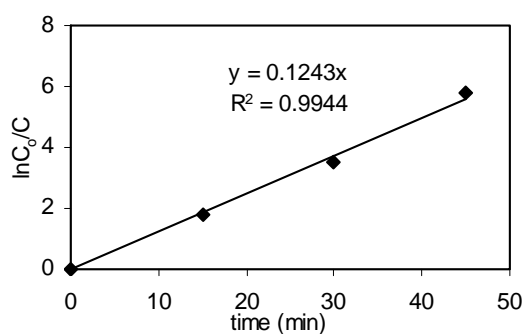


Fig. 4.1.6 Kinetics of photodegradation of RR dye 198; $C_0 = 100 \text{ mg L}^{-1}$, $\text{pH} = 4.6$, $[\text{TiO}_2] = 0.3 \text{ g L}^{-1}$

4.1.5 Mineralization of RR dye 198

Reduction of chemical oxygen demand (COD) reflects the extent of degradation or mineralization of an organic species. The percentage change in COD was studied for

the dye sample having an initial concentration of 100 mg L⁻¹, pH 4.5, and catalyst loading of 0.3 g L⁻¹ under artificial UV light. The COD value decreased from 104 mg L⁻¹ to 5 mg L⁻¹ after 3 h of irradiation which indicates significant mineralization upto 95%.

4.1.6 Effect of catalyst loading

The effect of photocatalyst concentration on the degradation rate of RR dye 198 has been investigated by employing different concentrations of TiO₂ varying from 0.05 to 0.5 g L⁻¹ under UV light. It is observed that the initial rate increases with the increase in catalyst concentration, becomes maximum and remains almost constant thereafter as shown in Table 4.1.2. The optimum catalyst concentration for the degradation of RR dye 198 is 0.3 g L⁻¹.

Table 4.1.2 Effect of TiO₂ loading on the degradation rate during the photocatalytic oxidation (C₀ = 100 mg L⁻¹, pH = 4.6)

[TiO ₂] g L ⁻¹	r ₀ (mg L ⁻¹ min ⁻¹)
0.05	2.4013
0.10	3.5034
0.15	4.3794
0.20	4.6534
0.25	4.8958
0.30	5.4026
0.35	5.3710
0.40	5.3329
0.50	5.2498

Galindo et al., (2002) reported an empirical relationship between the initial decolorization rate and TiO₂ concentration, $r_0 \propto [\text{TiO}_2]^n [\text{dye}]$, where n is an exponent less than 1 for the dye studied (Sauer et al., 2002). In the present work, the dependence of TiO₂ concentration on the initial decolorization rate follows a similar relationship ($r_0 \propto [\text{TiO}_2]^{0.45}$), when catalyst concentration is less than 0.3 g L⁻¹ as calculated from Fig. 4.1.7.

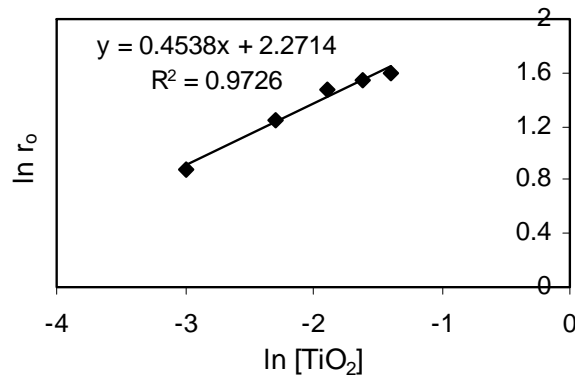


Fig. 4.1.7 Relationship between $\ln r_0$ and $\ln [TiO_2]$; $pH = 4.6$, $C_o = 100 \text{ mg L}^{-1}$

4.1.7 Effect of initial substrate concentration

As pollutant concentration is an important parameter to be studied, the effect of initial concentration of dye solution on the degradation rate of RR dye 198 has been investigated by varying the dye concentrations from 50 mg L^{-1} to 200 mg L^{-1} in the presence of $0.3 \text{ g L}^{-1} TiO_2$ under UV light as shown in Fig 4.1.8. This shows that the photo-oxidation process is more suitable for low concentration of the pollutants.

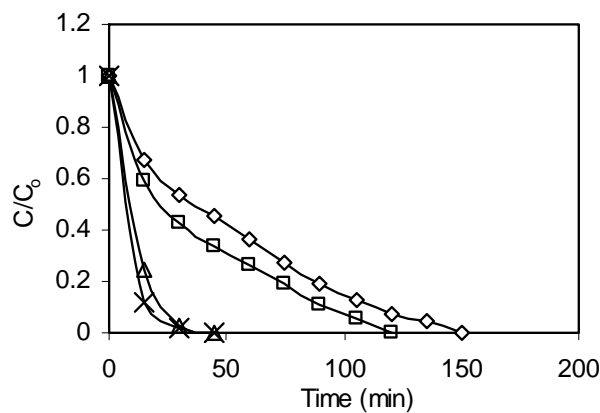


Fig. 4.1.8 Kinetics of photodegradation of RR dye 198 at different initial concentrations:
 $x = 50 \text{ mg L}^{-1}$; $\Delta = 100 \text{ mg L}^{-1}$; $\square = 150 \text{ mg L}^{-1}$;
 $\diamond = 200 \text{ mg L}^{-1}$, $pH = 4.6$, $[TiO_2] = 0.3 \text{ g L}^{-1}$

The influence of the initial concentration of the solute on the degradation rate of most of the organic compounds can be described by a pseudo first order kinetics in terms of Langmuir-Hinshelwood equation (Eq. 4.1.3) modified to accommodate reactions occurring at a solid-liquid interface.

$$r_0 = \frac{-dC}{dt} = \frac{k_v K_e C_o}{1 + K_e C_o} \quad (\text{Eq. 4.1.3})$$

Where k_v reflects the limiting rate of the reaction at maximum coverage under the given experimental conditions. K_e represents the equilibrium constant for adsorption of dye on to illuminated TiO_2 . In Eq. 4.1.3, k_v represents the apparent rate constant because it is also dependent on the source of UV light and the radiation field inside a photocatalytic reactor.

A linear expression can be obtained by plotting the reciprocal initial rate against the reciprocal initial concentration as shown in Fig.4.1.9. The values of K_e and k_v are calculated to be 0.00471 mg^{-1} and 17.699 min^{-1} respectively.

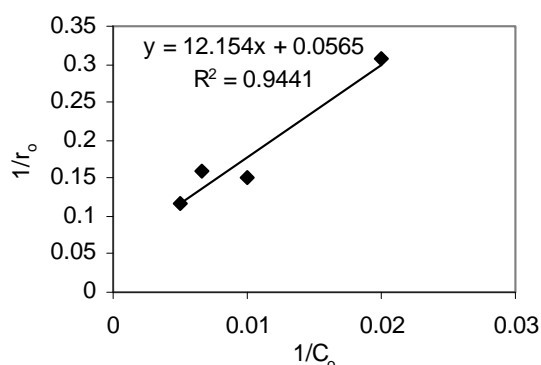


Fig. 4.1.9 Representation of Langmuir-Hinshelwood equation: $\text{pH} = 3.5$, $[\text{TiO}_2] = 0.3 \text{ g L}^{-1}$

4.1.8 Effect of initial pH of the solution

The wastewater pH varies with time and the generation of hydroxyl radicals is also a function of pH. Thus, pH plays an important role both in the characteristics of the wastewater and generation of hydroxyl radicals. Hence, employing Degussa P25 as photocatalyst the degradation of RR dye 198 in the aqueous suspensions of 0.3 g L^{-1} TiO_2 was studied in the pH range between 3.5 and 11 as shown in Fig.4.1.10, the natural pH of dye being 4.6.

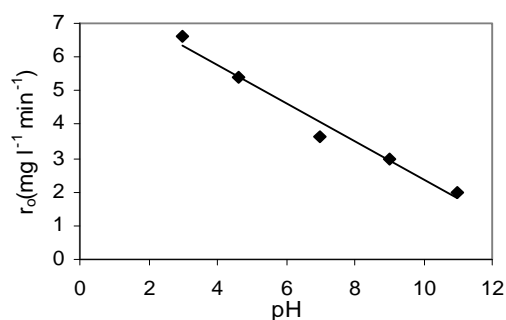


Fig. 4.1.10 Effect of pH on initial rate of degradation of RR dye 198: $[\text{TiO}_2] = 0.3 \text{ g L}^{-1}$, $C_0 = 100 \text{ mg L}^{-1}$

The degradation rate is higher in acidic media and decreases with the increase in pH of the solution upto 11. The photo-oxidation process can, therefore, be carried out in acidic medium. These results are reflected by the k_v and K_e values of the Langmuir-Hinshelwood equation (Eq. 4.1.3) as given in Table 4.1.3.

Table 4.1.3 Langmuir-Hinshelwood constants for the photodegradation of RR dye 198 at different pH values

pH	K_e (img^{-1})	k_v (min^{-1})
3.5	0.004649	17.69912
4.6	0.007372	11.16071
7.0	0.007110	6.747638
9.0	0.011186	3.402518

4.1.9 Effect of H_2O_2 addition

Limitation to the rate of photocatalytic degradation had been attributed to the recombination of photogenerated hole-electron pairs. Since the addition of H_2O_2 may play an important role in accelerating the degradation rate of azo dyes, experiments were conducted to examine its effect on degradation of the dye. The degradation rate increases initially by the addition of H_2O_2 and beyond a certain concentration of H_2O_2 , rate of degradation decreases. The optimum H_2O_2 concentration for degradation of dye with an initial concentration of 100 mg L^{-1} at pH of 4.6 is 5 ml L^{-1} as shown in Fig. 4.1.11.

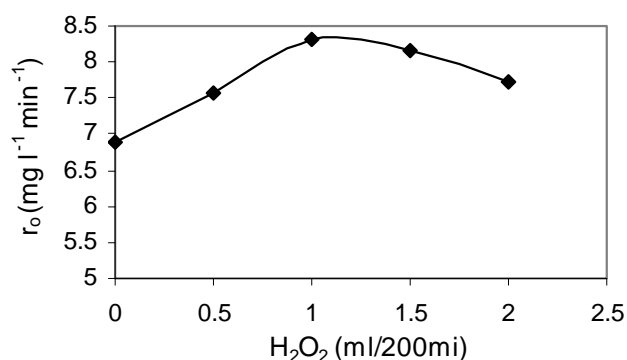


Fig. 4.1.11 Effect of H_2O_2 concentration on the initial rate at $C_0 = 100 \text{ mg L}^{-1}$, $\text{pH} = 4.6$ $[\text{TiO}_2] = 0.3 \text{ g L}^{-1}$

4.1.10 Efficiency of the recycled catalyst

The catalyst's lifetime is an important parameter of the photocatalytic process, due to the fact that its use for longer period of time leads to a significant cost reduction of the treatment. For this reason, the catalyst was recycled four times as shown in Fig. 4.1.12 which shows a drop in efficiency from 98 to 60%. After the optimized conditions for the degradation of the RR dye 198 were determined, the catalyst was recovered by filtration and activated at 100°C and again used to study its recyclability. This is likely due to the fouling of the catalyst and loss due to filtration.

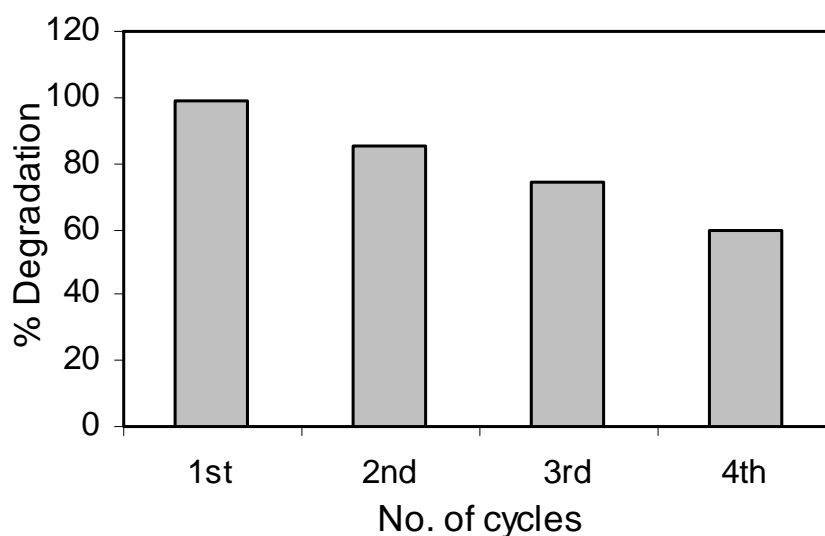


Fig. 4.1.12 Recyclability of TiO₂

4.1.11 Comparison of Photodegradation of RR dye 198 under UV light and solar light using Shallow Pond slurry reactor

After determining the optimum conditions for the degradation of dye under artificial UV light under laboratory conditions, the degradation of this dye was also studied under sunlight in a shallow pond slurry reactor, the procedure of which is given in section 3.4.3 at an average intensity of 29 Wm⁻² in the month of May. It was observed that the degradation of dye under sunlight was 98% in 20 min as compared to 86% under artificial UV irradiation in the same duration of time and similar conditions as shown in Fig. 4.1.13.

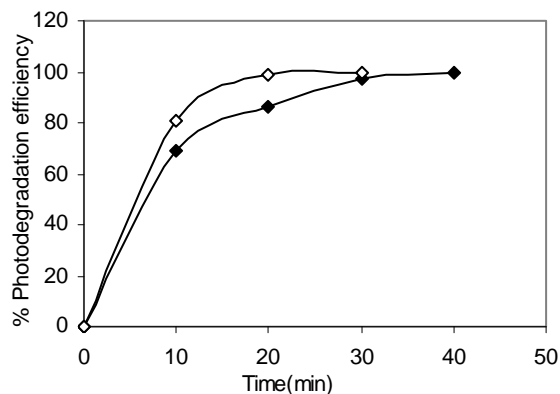


Fig. 4.1.13 Photocatalytic degradation of RR dye 198 in presence of sunlight (◇) and under artificial UV light (◆)

4.1.12 Discussion

Results of the present study clearly show that the photocatalytic treatment of aqueous solution of Reactive Red dye 198 under UV light, leads to decolorization and degradation of dye solution. The results show that significant amount of dye adsorbs on the TiO₂ surface. The adsorption of dye on the surface of TiO₂ at different pH and initial concentrations were studied and equilibrium constant was calculated. All isotherms showed a type of L-shape as shown in Fig 4.1.2. According to the classification of Giles et al., (1974), the L-shape of the isotherms means that there is no strong competition between the solvent and the adsorbate to occupy the adsorbent surface sites.

It is observed that the Reactive Red 198 dye adsorbs in acidic media (pH < 6.8) and negligible adsorption is observed in the alkaline media (pH > 7.0). This can be explained by the point of zero charge of the TiO₂ at pH 6.8. The TiO₂ surface is positively charged in acidic media (pH < 6.8), whereas it is negatively charged under alkaline conditions (pH > 6.8). Therefore the anionic Red dye is readily adsorbed in acidic medium but in alkaline medium (above pH 6.8) the dye is repulsed and, therefore, is scarcely adsorbed.

The photocatalytic decolorization and degradation of RR dye198 containing TiO₂ obeys pseudo-first-order kinetics. At low initial dye concentration the rate expression is given by Eq. 4.1.4.

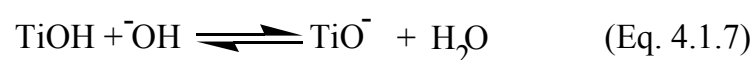
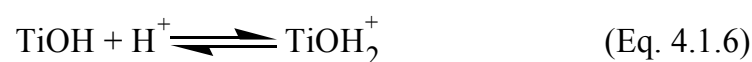
$$\frac{-d[C]}{dt} = k'[C] \quad (\text{Eq. 4.1.4})$$

where k' is the pseudo-first-order rate constant. The dye is adsorbed onto the TiO_2 surface and the adsorption-desorption equilibrium is reached in 30 min. After adsorption the equilibrium concentration of the dye solution is determined and it is taken as the initial dye concentration for kinetic analysis. Integration of the Eq. 4.1.4 (with the limit of $C = C_0$ at $t = 0$ with C_0 being the equilibrium concentration of the bulk solution) gave Eq. 4.1.5.

$$\ln\left[\frac{C_0}{C}\right] = k't \quad (\text{Eq. 4.1.5})$$

where C_0 is the equilibrium concentration of dye and, C the concentration at any time 't'. It appears that a first order fit to data is quite good as the regression value was 0.9944 and rate constant calculated was 0.1243 min^{-1} (from Eq. 4.1.5 and Fig 4.1.6).

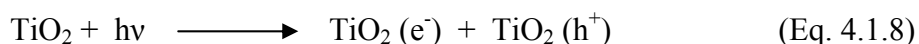
Because of the amphoteric behavior of TiO_2 , an important parameter which affects the reaction rate taking place on the surface of the semiconductor surface is the pH of the dispersions since it affects the surface charge properties on the particles, the size of the aggregates it forms and the position of the conductance and valence bands (Alaton et al., 2001; Saquib and Muneer, 2002).



Three possible mechanisms which lead to the degradation of the dye are hydroxyl radical attack, direct oxidation by the positive hole and direct reduction by the electron in the conducting band depending on the nature of the substrate and pH. In the present experiments the degradation rate is higher in acidic media and decreases with the increase in pH. In acidic pH, the surface of TiO_2 acquires a positive charge thereby attracting the anionic RR dye 198, leading to greater adsorption and hence increasing the degradation rate in the acidic media. However, the reverse effect is observed in the basic medium where the TiO_2 surface is negatively charged which repels the dye thereby decreasing the degradation rate. The adsorption is maximum at pH 3 and so is the degradation rate. This observation confirms the correlation between adsorption and initial rate of degradation,

which are directly related and it further indicates that the degradation is a surface phenomenon.

It is well documented that the absorption of photons possessing energy equal to or higher than that of the semiconductor (3.2 eV for TiO₂), causes charge separation as shown in Eq. 4.1.8:



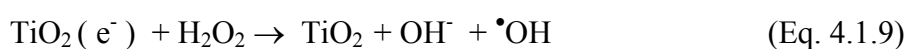
The photo generated holes may then react with adsorbed dye and oxidize the dye molecule by the formation of hydroxyl radicals. The photo-produced electrons in the conduction band react with the adsorbed oxygen to produce reactive radicals to yield the reactive oxygen species as shown in Fig 1.4. Change in COD further confirms the degradation leading to decrease in organic content.

The number of photons absorbed and the number of dye molecules adsorbed increase with the increase in catalyst concentration thereby enhancing the rate of degradation. Above a certain level the number of substrate molecules is not sufficient to fill the surface active sites of TiO₂. Hence, further addition of catalyst does not lead to the enhancement of the degradation rate. The degradation rate also decreases due to the aggregation of TiO₂ particles at higher concentrations causing decrease in the number of surface active sites and also due to the increase in opacity and light scattering of TiO₂ particles at high concentration through the sample. Our results are in good agreement with those reported in literature (Toor et al., 2006; Chen and Ray, 1998; Mills and Morris, 1993b).

One of the important aspects to study is the influence of initial concentration of the dye solution on the rate of degradation. The photodegradation rate is observed to decrease with increasing initial concentration and our results are in accordance with those reported in the literature (Rideh et al., 1997; Chen and Ray, 1998; Nepopolian et al., 2002c). As the concentration increases, the concentration of unadsorbed dye in the solution increases, leading to lesser penetration of light through the solution onto the surface of TiO₂, thereby decreasing the concentration of OH radical which is the most reactive species formed on the surface and hence, decreasing the rate of degradation. Since the relative number of the OH radicals attacking the substrate decreases, the photo-

efficiency of the reaction also decreases. However, the reverse effect is observed at lower substrate concentration, where the light intensity and time of irradiation is same but the interception of the photons to the catalyst surface is decreased leading to the formation of more number of OH radicals, thereby increasing the rate of reaction.

As reported in the literature (Sauer et al., 2002; Saquib and Muneer, 2002; Poulis and Tsacpinis, 1999) increase in concentration of $\cdot\text{OH}$ radicals leads to the increase in the rate of photocatalytic degradation. One of the methods to increase the concentration of the hydroxyl radical is by the addition of hydrogen peroxide, since it inhibits the electron-hole recombination, according to Eq. 4.1.9.



Hydrogen peroxide is considered to have two functions in the process of photocatalytic degradation. It accepts a photo-generated electron from a conduction band and thus promotes the charge separation, and it also forms OH^\bullet radical, according to Eq. 4.1.9. However, at high concentration of H_2O_2 , it also acts as a scavenger as shown in Eqs. 4.1.10 and 4.1.11. Therefore, there is a need to determine the optimum concentration of hydrogen peroxide experimentally.



Degradation studies under sunlight utilize both of its UV and visible components which help in the degradation. In addition to the OH radicals and superoxide radical anions produced under UV light, the dye is also degraded by sensitized photocatalytic mechanism which becomes operable under visible light. In this mechanism the adsorbed dye molecule is excited by visible light and thus acts as a photosensitizer. But the degradation of dye under UV light is mainly due to the generation of electron-hole generation when the TiO_2 particle absorbs photon of light more than its band gap energy (3.2 eV for TiO_2). This electron-hole pair leads to the formation of hydroxyl radical and superoxide radical anion and these radicals are the primary oxidizing species in the photocatalytic oxidation processes. Due to this, the degradation rate is more under similar conditions under sunlight than only UV light as studied in the laboratory.

Photocatalysis is a clean technology, which normally does not involve any waste disposal problem. The process is more economical if the catalyst can be recycled. TiO_2 was recycled efficiently four times with 60% photoefficiency. The decrease in efficiency of the recycled catalyst is due to deposition of photosensitive hydroxides on the photocatalysts surface blocking its active sites also referred to as fouling of the catalyst (Chakrabarti and Dutta, 2004).

Chapter 4 (B)

PHOTOCATALYTIC AND SONOPHOTOCATALYTIC DEGRADATION OF REACTIVE RED 198 UNDER VISIBLE LIGHT

4.2 Overview

In this chapter the accelerated photocatalytic degradation of Reactive Red 198 dye under visible light using dye sensitized TiO₂ activation by the synergistic effect of ultrasound is reported. The effect of sonolysis, photocatalysis and sonophotocatalysis under visible light has been examined to study the influence on the degradation rates by varying the initial substrate concentration, pH, catalyst loading and H₂O₂ concentration to ascertain the synergistic effect on the degradation techniques. Further the presence and role of oxidative species, such as singlet oxygen (¹O₂), superoxide (O₂^{•-}) and hydroperoxy (HO₂[•]) radicals was examined with the use of appropriate quenchers of these species. The photocatalytic activity of RR 198 dye sensitized TiO₂ is demonstrated by the degradation of phenol in the presence of visible light. A comparative study using TiO₂, Hombikat UV 100 and ZnO was also carried out.

4.2.1 Photocatalytic and Sonophotocatalytic Degradation of RR 198 Using Immersion Well Reactor

The experimental procedure adopted to study the degradation rate in case of photocatalysis and sonophotocatalysis is explained in section 3.4.2 and the laboratory setup is as shown in Fig 4.2.1. Reaction rate constant (k) is a function of parameters such as catalyst loading, pH of the solution, initial concentration of the substrate and addition of oxidant and therefore, the effect of these parameters on the reaction rate constant have been investigated.

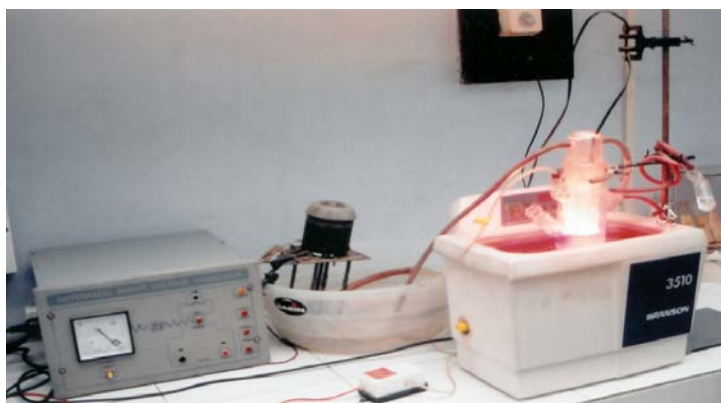


Fig. 4.2.1 Laboratory set up for the sonophotocatalytic degradation of RR dye 198 under visible light

4.2.2 Decolorization and kinetic analysis

Reactive Red 198 is a strongly absorbing dye in the UV-visible region with distinct bands near UV region ($\lambda_{\text{max}} = 294 \text{ nm}$) and another one in the visible region ($\lambda_{\text{max}} = 515 \text{ nm}$). The latter is responsible for the red color arising from aromatic rings connected by azo groups and the former is associated with benzene like structures in the molecule. The disappearance of the visible band as shown in Fig 4.2.2 in a short period is due to the fragmentation of the azo links by immediate OH radical attack (hydroxylation) in the oxidation process.

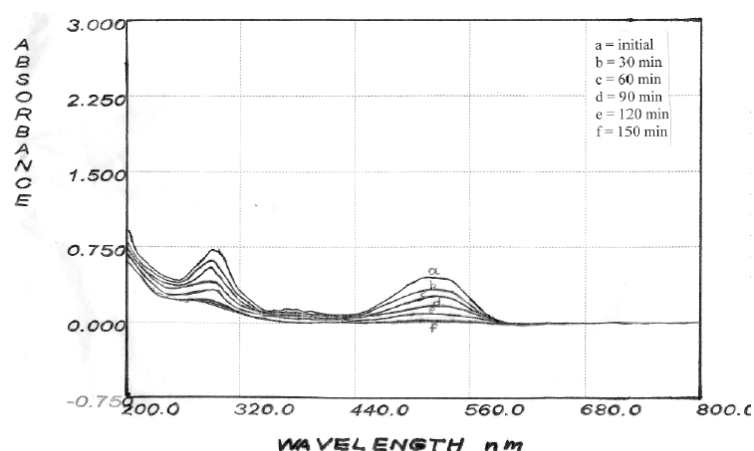


Fig. 4.2.2 Spectral changes that occur during the sonophotocatalytic degradation of aqueous solution of RR dye 198: $\text{pH} = 4.6$, $[\text{TiO}_2] = 0.3 \text{ g L}^{-1}$, $C_0 = 50 \text{ mg L}^{-1}$

In addition to this rapid bleaching effect, the decay of the absorbance at 294 nm is considered as evidence of aromatic fragment degradation in the dye molecule and its intermediates. The color fading during photocatalysis is shown in Fig.4.2.3.



Fig. 4.2.3 Color Removal during Photocatalysis

The degradation rates measured under different experimental conditions could conveniently be compared in terms of first order rate constants, obtained from the slopes

of plots of Fig. 4.2.4. The degradation was negligible in the presence of only visible light without TiO_2 . However, the pollutants underwent relatively slow degradation under ultrasound in the presence of TiO_2 (US+ TiO_2), while under photocatalysis (Vis+ TiO_2) the degradation occurred at higher rate. A further increase in reaction rate was observed on illuminating the sample suspensions simultaneously with visible light and ultrasound in the presence of TiO_2 (Vis+US+ TiO_2). Mainly ultrasound contributes through cavitation to the scission of H_2O_2 produced by both photocatalysis and sonolysis. This increases the amount of reactive radical species inducing oxidation of the substrate and degradation of intermediates and is mainly responsible for the observed synergy.

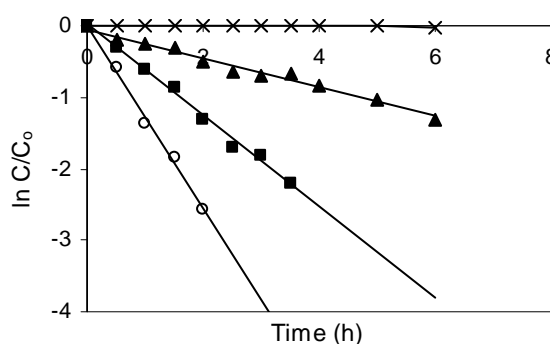


Fig. 4.2.4 First order kinetic plots of RR dye 198 degradation under (x) Visible light (Vis), (▲)Ultrasound in the presence of TiO_2 particles (US+ TiO_2), (■) photocatalysis (Vis+ TiO_2) and (●) sonophotocatalysis (US+Vis+ TiO_2), Initial dye concentration = 50 mg L^{-1} , TiO_2 amount = 0.3 g L^{-1} , pH = 4.6 (natural)

4.2.3 Effect of catalyst loading

The amount of catalyst is one of the main parameters for the degradation studies from economical point of view. In order to avoid the use of excess catalyst it is necessary to find out the optimum loading for efficient removal of dye. Several authors have investigated the reaction rate as a function of catalyst loading in photocatalytic oxidation process. First order rate constants of sonolytic, photocatalytic and sonophotocatalytic degradation of Reactive Red 198 in the presence of different amounts of titanium dioxide (100 mg L^{-1} to 500 mg L^{-1}) are reported in Fig. 4.2.5. The degradation rate under sonolysis was very low and is not influenced by the amount of photocatalyst. Progressively higher $k_{\text{Vis}+\text{TiO}_2}$ and $k_{\text{US}+\text{Vis}+\text{TiO}_2}$ values were measured with increasing TiO_2 concentration with similar change for both the rate constants. The results clearly show that the optimum catalyst loading for degradation of RR dye 198 is 0.3 g L^{-1} .

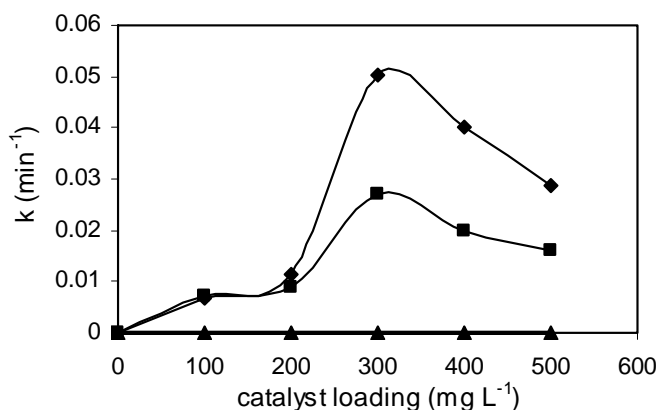


Fig .4.2.5 Rate constants of RR dye 198 degradation under (▲) US+TiO₂, (■)Vis+TiO₂, (●) US+Vis+TiO₂, as a function of the TiO₂ concentration, Initial concentration = 40 mg L⁻¹, pH = 4.6

This can be explained on the basis of synergistic effect which is quantified in Table 4.2.1.

Table 4.2.1 First order rate constants of RR dye 198 degradation under sonolysis in the presence of dye sensitized TiO₂ (US+TiO₂), photocatalysis (Vis+TiO₂) and sonophotocatalysis (Vis+US+TiO₂)

Entry	C ₀	TiO ₂ amt. (mg L ⁻¹)	k _{Vis+us+TiO2}	k _{Vis+TiO2}	k _{us+TiO2}	Synergy
1	50	300	0.0234	0.0145	0.0038	0.2179
2	40	300	0.0466	0.0272	0.0020	0.3733
3	30	300	0.1970	0.0849	0.0012	0.5629
4	20	300	0.3087	0.1257	0.0025	0.5847

4.2.4 Effect of initial substrate concentration

The effect on the degradation rate of different initial substrate concentration was investigated in suspensions containing 0.3 g L⁻¹ of TiO₂ at a normal pH of 4.6. The degradation rate of dye measured under different experimental conditions, are shown in Fig. 4.2.6. Under sonolysis all substrates underwent very slow degradation. Under both photocatalysis and sonophotocatalysis the reaction proceeded much faster, the degradation rate decreases with increase in the initial concentration of the substrate. Our

results are in good agreement with those reported in literature (Mrowetz et al., 2003). The combined action of photocatalysis and sonolysis produced synergistic effects in all the investigated range of initial substrate concentration, however, the effect was more prominent at lower concentrations.

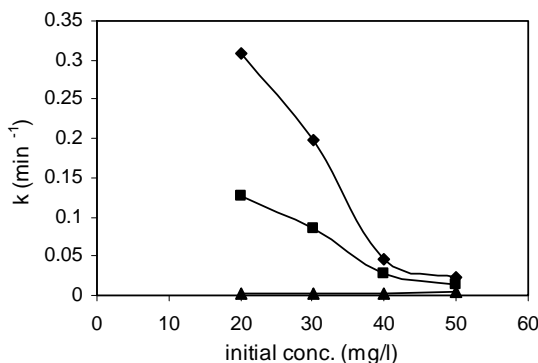


Fig. 4.2.6 Initial rate of RR dye 198 degradation, r_o under (◆) US+TiO₂+Vis, (■) Vis+ TiO₂, (▲) US+TiO₂, as a function of the initial dye concentration, [TiO₂] = 0.3 g L⁻¹, pH = 4.6

4.2.5 Effect of initial pH

Since pH is one of the important parameters for the photocatalytic process and it is of interest to study its influence on the photocatalytic and sonophotocatalytic degradation rate of the Reactive Red 198. The effect of pH on the initial degradation rate of RR dye 198 is given in Fig. 4.2.7.

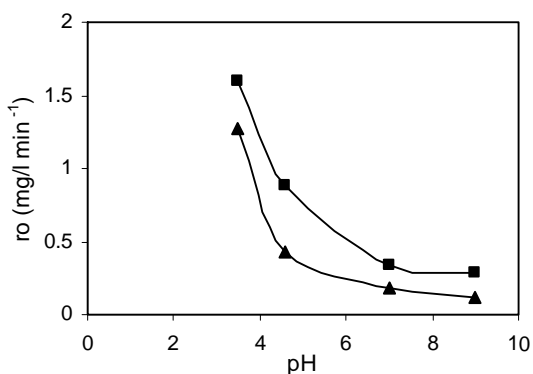


Fig. 4.2.7 Effect of pH on degradation of RR dye 198 under (■) US+TiO₂+Vis, (▲) Vis+ TiO₂, initial dye concentration 50 mg L⁻¹, [TiO₂] = 0.3 g L⁻¹

The influence of the initial concentration of the solute on the photocatalytic degradation derived from the kinetic data can be rationalized in terms of Langmuir-Hinshelwood model (Eq. 4.1.3) modified to accommodate reactions occurring at a solid-liquid interface. A linear expression can be conveniently obtained by plotting the reciprocal initial rate against the reciprocal initial concentration as shown in Fig.4.2.8.

The values of K_e and k_v are calculated to be 0.006 L mg^{-1} and 11.14 min^{-1} respectively during photocatalysis and 0.004 L mg^{-1} and 17.70 min^{-1} respectively during sonophotocatalysis.

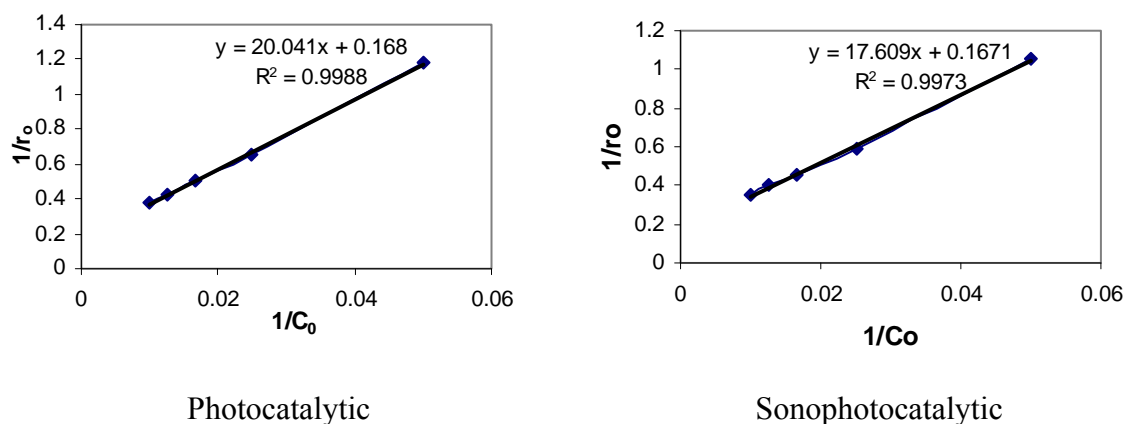


Fig. 4.2.8 Representation of Langmuir-Hinshelwood equation:
 $[dye] = 50 \text{ mg L}^{-1}$, $pH = 4.6$, $[TiO_2] = 0.3 \text{ g L}^{-1}$

In Eq. 4.1.3, k_v represents the apparent rate constant because it is also dependent on the source of visible light and the radiation field inside a photocatalytic reactor.

The results shown in Table 4.2.2, reflect the k_v and K_e values of the Langmuir-Hinshelwood equation (Eq.4.1.1). It is worth noting that the adsorption constant K_a as in Table 4.1.1 obtained from the dark adsorption isotherm is significantly different from the K_e determined from the Langmuir-Hinshelwood equation as in Table 4.2.2 in the photocatalytic and sonophotocatalytic process. The photo adsorption and the fast photoreaction of the substrate on the TiO_2 surface makes the observed K_e under irradiation conditions different from that (K_a) in the dark.

Table 4.2.2 Langmuir-Hinshelwood constants for the photodegradation of RR dye 198 at different pH values

Photocatalysis			Sonophotocatalysis	
pH	$K_e \text{ (l mg}^{-1}\text{)}$	$k_v \text{ (min}^{-1}\text{)}$	$K_e \text{ (l mg}^{-1}\text{)}$	$k_v \text{ (min}^{-1}\text{)}$
3.5	0.006	11.14	0.004	17.70
4.6	0.008	5.95	0.009	5.98
7.0	0.016	1.27	0.035	1.31
9.0	0.004	2.13	0.018	1.10

4.2.6 Effect of H₂O₂ addition

One possible way to increase the reaction rate would be to increase the concentration of the OH radicals which play an important role in the rate enhancement. It is clear from Fig. 4.2.9 that the rate of degradation goes on increasing with the increase in concentration of H₂O₂ and becomes maximum at 0.5 ml L⁻¹ and then starts decreasing with further increase in concentration of H₂O₂. It is observed that the rate enhancement in sonophotocatalytic degradation is more as compared to photocatalytic degradation. This effect has been reported due to the increased production of H₂O₂ under sonophotocatalytic conditions.

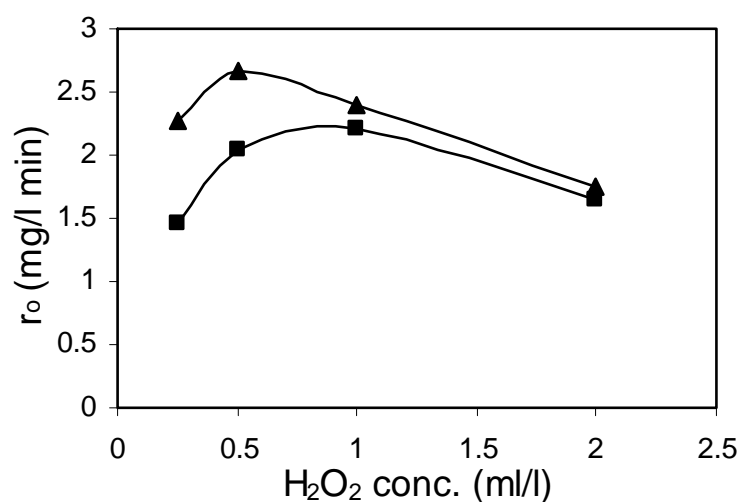


Fig. 4.2.9 Effect of H₂O₂ concentration on the initial rate under (■) TiO₂+Vis, (▲) TiO₂+Vis+US, [dye] = 50 mg L⁻¹, pH = 4.6, [TiO₂] = 0.3 g L⁻¹

4.2.7 Effect of various photocatalysts

The influence of three different photocatalysts, TiO₂-P25, ZnO and UV-100 on the degradation kinetics of RR dye 198 was investigated and results are shown in Fig. 4.2.10. TiO₂ and ZnO are found to be more efficient than UV-100. The order of activities of the photocatalysts are ZnO > TiO₂-P25 > UV-100.

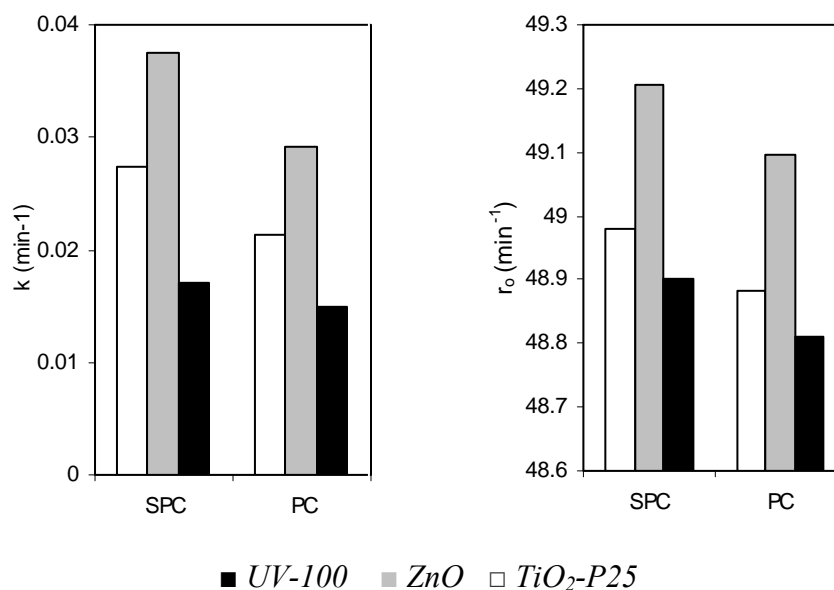


Fig. 4.2.10 Effect of various Photocatalysts on degradation of RR dye 198 under Photocatalytic conditions (PC) and sonophotocatalytic conditions (SPC) [dye] = 50 mg L⁻¹, pH = 4.6, [catalyst] = 0.3 mg L⁻¹

4.2.8 Effect of radical quenchers

The formation of oxidative intermediate species such as singlet oxygen (¹O₂), superoxide (O₂^{•-}) and hydroperoxy (HO₂[•]) radicals under photocatalytic and sonophotocatalytic conditions and their role in the dye degradation process has been investigated indirectly with the use of appropriate quenchers of these species. In these experiments, a comparison is made between the degradation curves of RR dye 198 with TiO₂ dispersions and those obtained after addition of quenchers in the initial solution under otherwise identical conditions. Compounds used for this purpose were 1,4-Diazabicyclo [2,2,2] octane (DABCO), a singlet oxygen quencher, sodium azide (NaN₃), which is also a quencher of singlet oxygen but may also interact with OH[•] radical and 1,4-Benzoquinone (BQ), which is a quencher of superoxide radical.

It is observed from Fig.4.2.11 that in the presence of BQ, which is an O₂^{•-} quencher photobleaching of RR dye 198 is completely suppressed indicating that the superoxide radical is an active oxidative intermediate. The inhibiting effect of NaN₃, which is a ¹O₂ quencher but may also interact with OH[•] radical, becomes significant after 1 h indicating the delayed formation of singlet oxygen (and possibly hydroxyl radical) species. Similar results were obtained after addition of DABCO, which is also a singlet oxygen quencher.

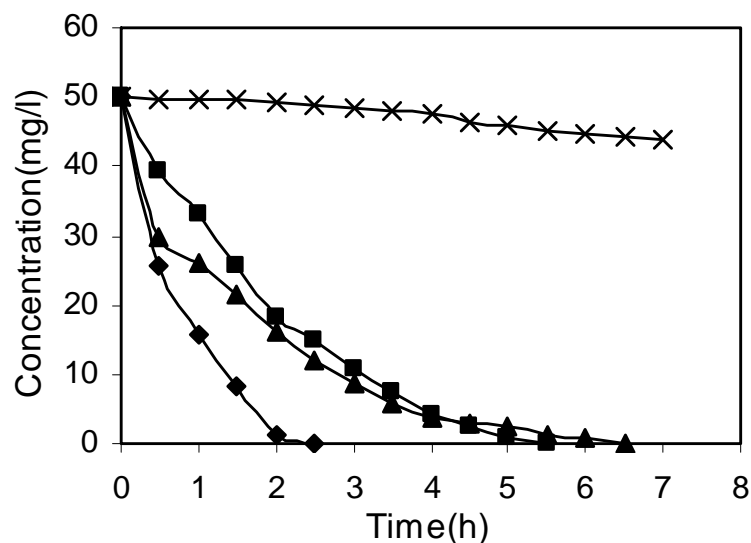


Fig. 4.2.11 Effect of radical quenchers on the degradation rate under sonophotocatalytic conditions ×: 1,4-Benzoquinone, ■: NaN₃, ▲ : DABCO, ◆ : no quencher, [dye] = 50 mg L⁻¹, [TiO₂] = 0.3 g L⁻¹, [quencher] = 0.1 g L⁻¹

4.2.9 Identification of degraded intermediates

For identification of intermediate products, 200 ml of aqueous solution of RR dye 198 containing TiO₂ (0.3 g L⁻¹) was irradiated for 2 h and the photocatalyst was removed by filtration. The filtrate was extracted using chloroform and was subsequently dried over anhydrous sodium sulphate. The solvent was removed under reduced pressure to get the residual mass, which was analyzed by GC-MS analysis.

The GC-MS analysis of the residue after degradation is shown in Fig.4.2.12. Several smaller organic intermediates are formed, out of which, one major product (18%) was formed.

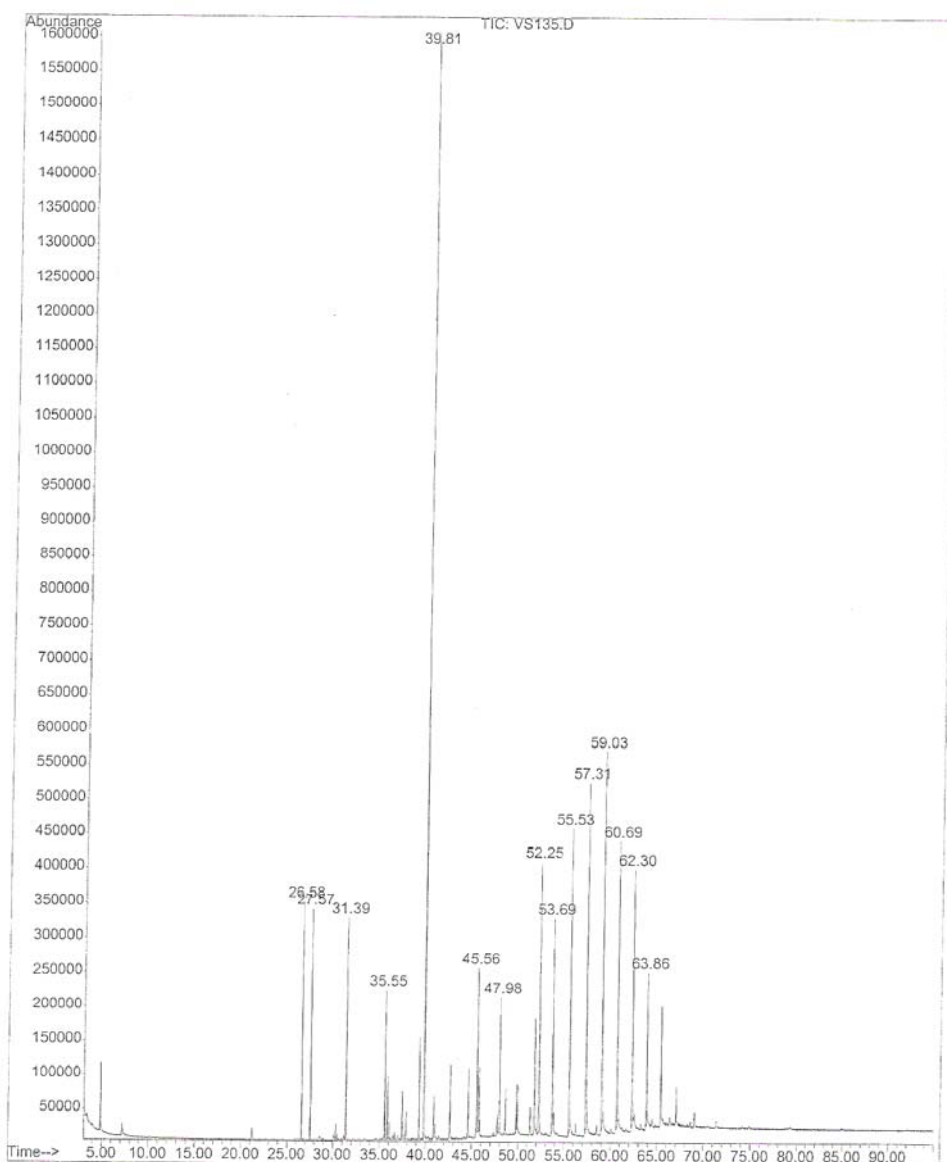


Fig. 4.2.12 GC-MS analysis of residue of RR dye 198 after sonophotocatalytic degradation

The structure of the major intermediate formed is suggested to be a phthalic acid derivative by the molecular ion peak (278) and base peak (M^+) 149 and fragmentation pattern as shown in Fig.4.2.13.

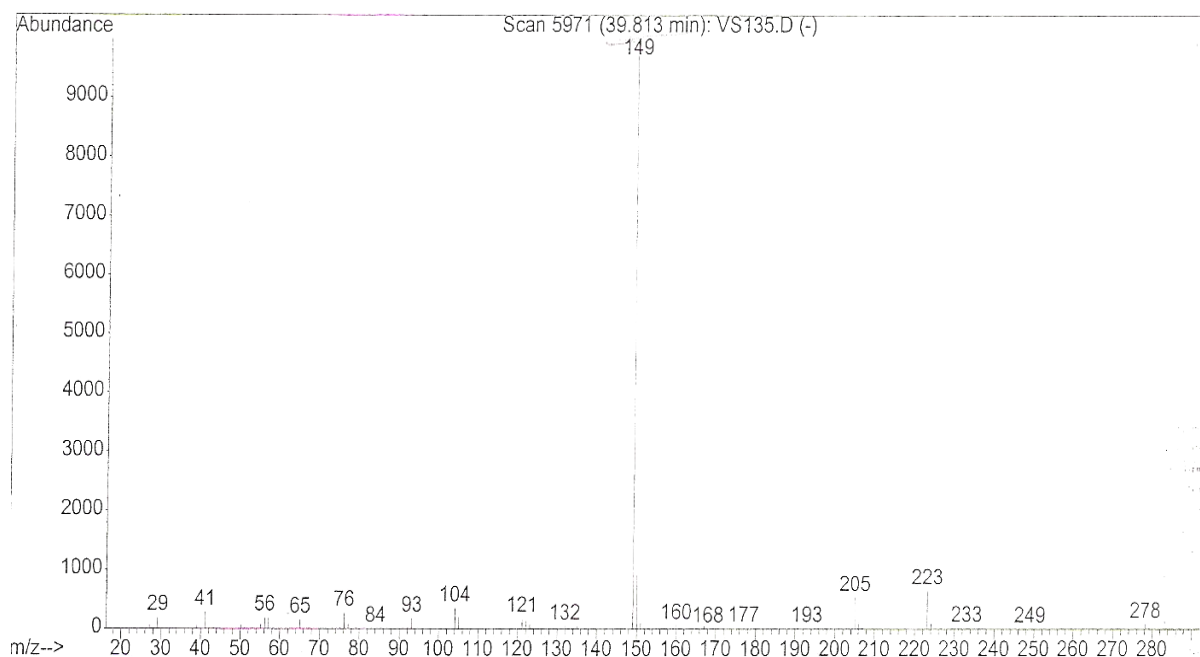


Fig. 4.2.13 MS of the major product (phthalic acid derivative) identified with Retention time-39.81min and fragmentation pattern

4.2.10 Decomposition of phenol by dye-sensitized TiO₂ under visible light

To confirm the action of dye-sensitized mechanism the decomposition of a toxic organic compound, phenol was carried out using RR dye 198 adsorbed TiO₂ as the photocatalyst under visible light. To prepare the catalyst, a saturated solution of RR 198 dye containing TiO₂ (1.0 g) was magnetically stirred for 24 h in dark. The uptake was estimated spectrophotometrically by measuring free dye in the supernatant liquid obtained after filtration and was found to be 374 µeqiv/g. The results of ultrasound mediated phenol degradation by dye-sensitized TiO₂ are shown in Fig. 4.2.14. The specific peak of phenol appeared at 270 nm, and that of the dye at 515 nm. During the process of irradiation, phenol peak disappears with time. This indicates that the dye sensitized TiO₂ attacks phenol first and the decomposition of the dye takes place after the phenol has decomposed.

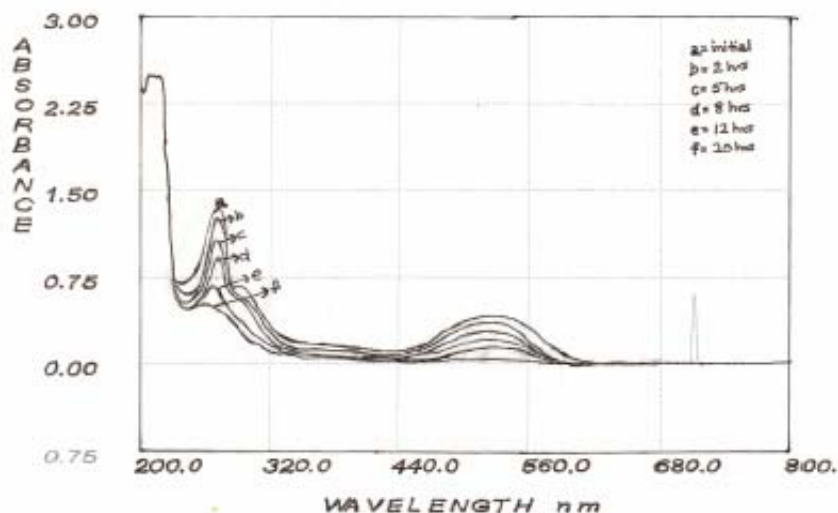


Fig. 4.2.14 Sonophotocatalytic decomposition of phenol by RR dye 198 adsorbed TiO_2 under visible light. $[\text{dye sensitized TiO}_2] = 0.3 \text{ g L}^{-1}$, $[\text{phenol}] = 50 \text{ mg L}^{-1}$, Total solution = 200 ml

4.2.11 Discussion

The adsorption of dye is a pre-requisite for the degradation and it was observed that both adsorption and photo-degradation occur extensively in acidic medium. The point of zero charge (pzc) of the TiO_2 is at pH 6.8. The suitable charge distribution on TiO_2 determines the optimum pH for the adsorption of dye molecule. The anionic nature of dye favors the adsorption in acidic media as TiO_2 is positively charged in acidic media (pH < 6.8) as shown in Table 4.1.1 and K_a is maximum at pH 3.5.

This study reveals that the acceleration of the degradation process of dye sensitized TiO_2 under visible light has been achieved by ultrasonication. Synergistic effect was observed as: the combined effect of sonolysis and photocatalysis led to a degradation rate constant ($k_{\text{US+Vis+TiO}_2}$) which was greater than the sum of the degradation rate constants measured under photocatalysis ($k_{\text{Vis+TiO}_2}$) and sonolysis ($k_{\text{US+TiO}_2}$). The synergy between photocatalysis and sonolysis can be usefully quantified as the normalized difference between the rate constants obtained under sonophotocatalysis and the sum of those obtained under separate photocatalysis and sonolysis as is given in Eq. 4.2.1.

$$\text{Synergy} = \frac{k_{\text{vis+US+TiO}_2} - (k_{\text{US+TiO}_2} + k_{\text{vis+TiO}_2})}{k_{\text{vis+US+TiO}_2}} \quad (\text{Eq. 4.2.1})$$

It is observed that with 60% dilution, the synergy factor increases four fold. Both in photocatalysis and sonophotocatalysis the pollutants in water are degraded mainly through the generation of OH radical attack. In case of sonophotocatalysis, OH^\bullet and other

radicals are generated from scission of water caused under high temperature and pressure conditions created by the collapse of cavitation bubbles. Under photocatalytic conditions the OH^\bullet radicals are generated via photosensitization, which involves initial excitation of dye molecules rather than TiO_2 particles. Charge is then injected from the singlet or triplet excited states of the dye into the conduction band of the semiconductor particle whereas the dye is converted into its cationic radical. The injected electron can reduce surface chemisorbed oxidants, usually O_2 , to yield the oxidizing species like $\text{O}_2^{\bullet-}$, HO_2^\bullet , and OH^\bullet radicals, which cause photodegradation. Sonolysis further enhances the degradation rate by increasing the catalytic activity of the semiconductor catalyst. This could occur through the decrease in size of photocatalyst particles due to the deaggregation of particles leading to an increase in surface area and catalytic performance (Shirgaonkar and Pandit, 1998; Theron et al., 1999; Davydov et al., 2001; Lu et al., 2002).

One of the important parameters studied was the effect of catalyst loading. The degradation rate increases first, becomes maximum at a catalyst loading of 0.3 gL^{-1} and decreases thereafter. Similar trend is observed in both photocatalysis and sonophotocatalysis. The reasons for the decrease in degradation rate are (i) aggregation of TiO_2 particles at high concentrations causing decrease in the number of surface active sites and (ii) increase in opacity and light scattering of TiO_2 particles at high concentration leading to decrease in the passage of irradiation through the sample. Ultrasound induces the increased reaction rate due to the production of more number of photoactive species and due to water splitting leading to the formation of H_2O_2 . Moreover sonication also leads to deaggregation of the TiO_2 particles resulting in the increase of surface area

A decrease in reaction rate with increase in substrate concentration is due to the fixed amount of the substrate adsorbed on the semiconductor. Simultaneous sonolysis did not induce any modification in this trend, indicating that under photocatalytic and sonophotocatalytic conditions, the reaction system exhibits the same dependence on the amount of dye, which determines water-semiconductor interface phenomena. During the course of reaction, due to the formation of intermediates, competition starts between the intermediates and the dye molecules for the surface active sites of TiO_2 leading to the decrease in the degradation rate.

The solution pH is a complex parameter since it is related to the ionization state of the surface as shown in Eq. 4.1.6 and 4.1.7 as well as to that of reactants and products such as acids and amines. Three possible mechanisms can contribute to dye degradation-hydroxyl radical attack, direct oxidation by the positive hole and direct reduction by the electron in the conduction band, depending on the nature of the substrate and pH. In our experiments, any changes in the initial degradation rate with varying pH values must be ascribed to variations of the acid/base properties of the TiO₂ particle surface. Since the photo-oxidation of dyes is accompanied by the release of protons (Poulios and Tsachpinis, 1999), its efficiency may then change because of the reversible protonation of the TiO₂ surface. Photocatalytic activity reached a maximum in acidic conditions, followed by a decrease of r_0 in the pH range from 7-9. Same trend is seen in both photocatalytic and sonophotocatalytic conditions.

The effect of pH on the photocatalytic reaction can be largely explained by the surface charge of TiO₂ (pzc of TiO₂ ~ 6.8) and its relation to the acid dissociation constants of dye. Below pH 6, as pH decreases, a strong adsorption of dye on the TiO₂ particles as a result of electrostatic attraction of the positively charged TiO₂ with the ionized dye is observed. On the other hand, above pH 6, a decrease in the reaction rate has been observed reflecting the difficulty of anionic dye in approaching the negatively charged TiO₂ surface when increasing the solution pH.

Another important parameter which significantly affects the degradation rate of RR dye 198 is H₂O₂. The rate constant increases with the increase in H₂O₂ dosage, becomes maximum and decreases thereafter. These observations can be explained by the fact that hydrogen peroxide is suitable for trapping the electrons (Al-Ekabi et al., 1989) preventing the electron hole recombination and hence increasing the chances of formation of $\cdot\text{OH}$ and $\text{O}_2^{\cdot-}$ radicals on the surface of the catalyst according to Eq. 4.1.9.

Further at higher concentration of H₂O₂ the rate of degradation decreases, as at higher concentration it quenches the OH radicals as shown in Eqs. 4.1.10 and 4.1.11.

The degradation experiments have been conducted using three different catalysts and the best results were obtained when ZnO was used as a catalyst. Although ZnO is the most efficient catalyst but it has the disadvantage of undergoing photocorrosion under

illumination in acidic conditions. The high photoreactivity of TiO₂-P25 as compared to UV-100 is due to the slow recombination of electron-hole pair and its large surface area.

To confirm that sonophotocatalysis takes place via formation of radicals, the irradiation experiments are carried out in the presence of various radical scavengers like DABCO, a singlet oxygen quencher, sodium azide, which is also a quencher of singlet oxygen but may also interact with OH[•] and 1,4-Benzoquinone, which is a quencher of superoxide radical. Significant decrease in the degradation rate in the presence of the radical scavengers supports the fact that sonophotocatalysis takes place via radical formation.

Photosensitized degradation of RR dye 198 has been carried out on TiO₂ where the dye serves as both a sensitizer and a substrate to be degraded. This is an efficient system for the degradation of the organic pollutants in wastewater. The RR 198 sensitized TiO₂ has been successfully used to degrade phenol in visible light. This extends its application for the degradation of organic pollutants on industrial scale.

Chapter 5 (A)

PHOTOCATALYTIC DEGRADATION OF J-ACID UNDER UV LIGHT

5.1 Overview

This chapter deals in detail with the photocatalytic degradation of a dye intermediate J-acid (6-Amino naphthol-3-sulphonic acid) used in chemical industries for the synthesis of various dyes, using an immersion well type photoreactor under UV light by varying operational parameters like catalyst loading, pH, initial concentration of the substrate, addition of electron acceptors like H_2O_2 and ammonium persulphate. The experiments were also carried under sunlight under optimized conditions using a shallow pond slurry reactor.

5.1.1 Structure of J-acid

J-acid is 6-Amino naphthol-3-sulfonic acid as shown in Fig. 5.1.1.

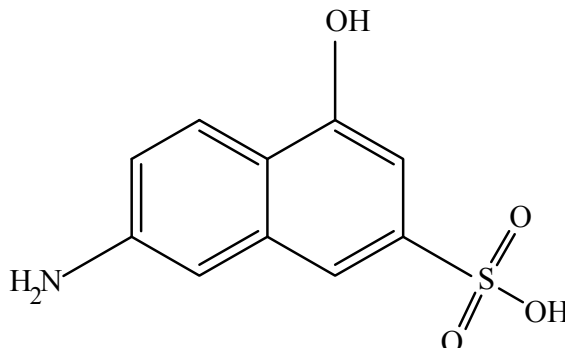


Fig. 5.1.1 Structure of J-acid

It is a strongly absorbing dye intermediate in the UV region with distinct bands near UV region having prominent peaks at $\lambda_{\max} = 294$ nm and another at $\lambda_{\max} = 354.7$ nm as shown in Fig. 5.1.2. The disappearance of these two bands in a short period suggests that the aromatic rings are cleaved by photocatalysis under UV irradiation of the J-acid. The rate of J-acid degradation was quantified by measuring its concentration as a function of time using Hitachi U-2001 UV-Vis spectrophotometer at $\lambda_{\max} 354.7$ nm.

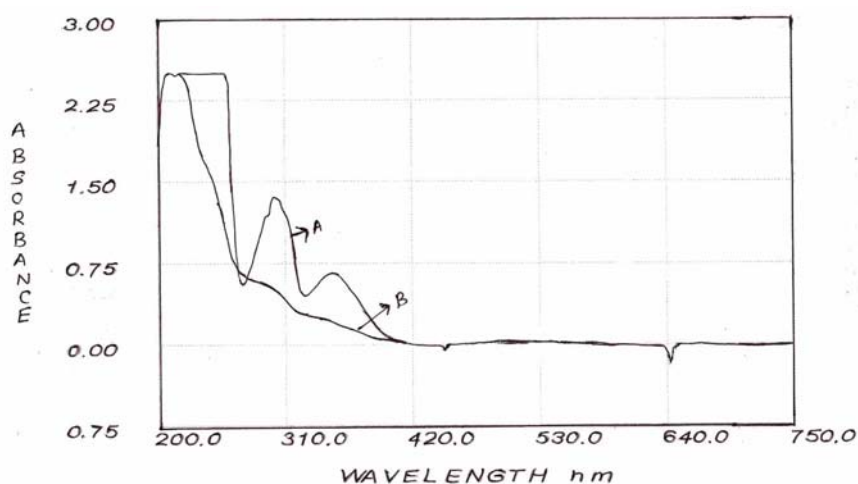


Fig. 5.1.2 Absorption spectra of J-acid showing the changes before (curve A) and after (curve B) irradiation

5.1.2 Adsorption Equilibrium under Dark Conditions

The adsorption tests under dark conditions were carried out in order to evaluate the adsorption of the dye intermediate on the TiO₂ surface at different pH and different initial concentrations and to calculate the equilibrium constants as per the procedure given in section 3.4.1. No significant adsorption was observed.

5.1.3 Photocatalytic Degradation of J-acid Using Immersion Well Reactor

Photocatalytic degradation of J-acid was studied using an immersion well type reactor in the laboratory as shown in Fig.3.2 as per the procedure given in section 3.4.2. Effect of various parameters such as catalyst loading, pH of the solution, addition of oxidant and effect of initial concentration of the pollutant on the reaction rate constant was studied.

5.1.4 Kinetics of J-acid disappearance

To study the kinetics of J-acid degradation, photocatalytic degradation of 100 mg L⁻¹ solution of J-acid was carried out in the presence of only UV light without any catalyst, with catalyst in dark and in the presence of catalyst Degussa P25 TiO₂. No observable loss of J-acid took place when the irradiation was carried out in the absence of TiO₂ and in presence of catalyst in dark. When irradiation was carried for 100 mg L⁻¹ solution of J-acid using 0.3 g L⁻¹ of the photocatalyst under UV light, the degradation was 98% in 75 min as shown in Fig. 5.1.3.

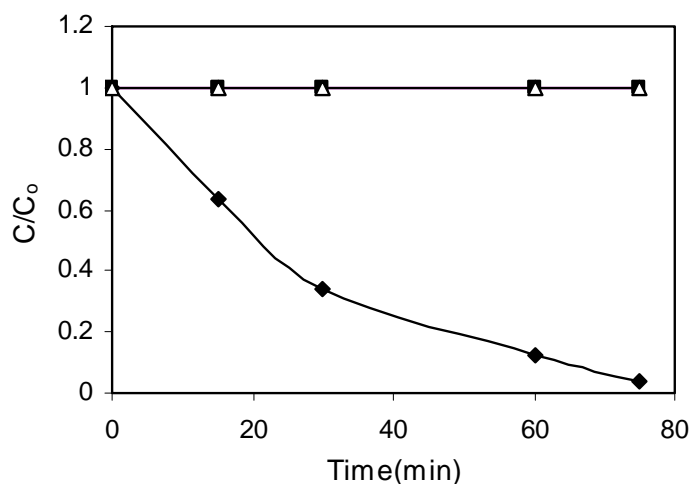


Fig. 5.1.3 Photocatalytic degradation of J-acid (Δ) only UV; (\blacksquare) only TiO_2 (0.3 g L^{-1}), (\blacklozenge) with TiO_2 (0.3 g L^{-1}) and UV light

The first order kinetic model can be used to describe the photocatalytic degradation of J-acid. The semi logarithmic plot of the concentration data gave a straight line as shown in Fig. 5.1.4. The rate constant calculated from the plot was 0.0347 min^{-1} .

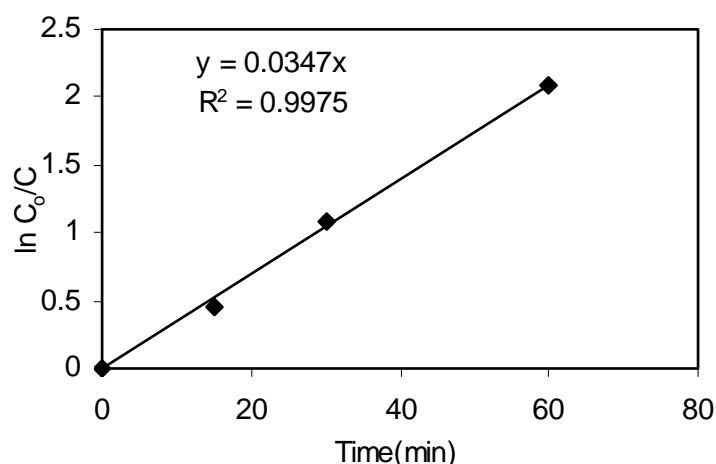


Fig. 5.1.4 Kinetics of photodegradation of J-acid; $C_0 = 100 \text{ mg L}^{-1}$, $\text{pH} = 5.7$, $[\text{TiO}_2] = 0.3 \text{ g L}^{-1}$

5.1.5 Mineralization of J-acid

The initial pH of the 100 mg L^{-1} solution of J-acid was 5.7. Slight change in pH occurred when the photocatalytic degradation of this compound was carried out. The pH of the solution after degradation was found to be 5.9. The COD of the solution decreased from 102 mg L^{-1} to 4 mg L^{-1} which accounts for 95.8% reduction in 2.30 h.

5.1.6 Effect of catalyst loading

The variation in the rate of degradation of J-acid solution (100 mg L^{-1}) was determined by varying the amount of TiO_2 in the range of 0.1 to 0.5 g L^{-1} and irradiating the reaction mixture in the presence of UV light. Fig. 5.1.5 shows that the degradation rate of J-acid increases with increase in the catalyst loading upto 0.3 g L^{-1} and after that it starts decreasing gradually. The optimum catalyst loading as shown in Table 5.1.1 is 0.3 g L^{-1} .

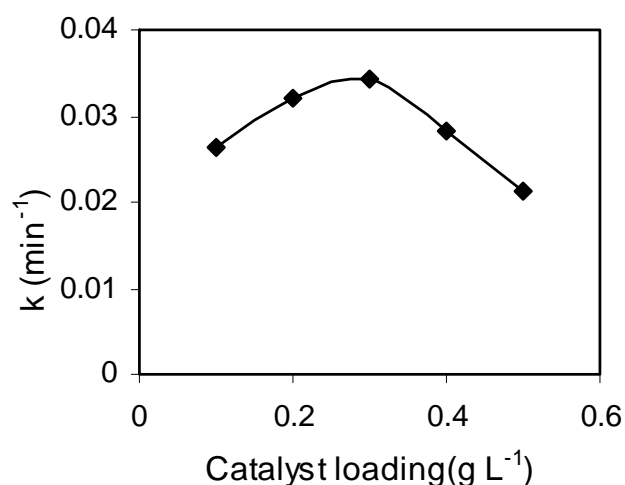


Fig. 5.1.5 Effect of catalyst loading on degradation rate of J-acid

Table 5.1.1 Effect of TiO_2 loading on the degradation rate during the photocatalytic oxidation ($C_0 = 100 \text{ mg L}^{-1}$, $\text{pH} = 5.7$)

$[\text{TiO}_2] \text{ g L}^{-1}$	k ($\text{mg L}^{-1} \text{ min}^{-1}$)
0.10	0.0263
0.20	0.0321
0.30	0.0342
0.40	0.0283
0.50	0.0212

5.1.7 Effect of initial substrate concentration

It is important from application point of view to study the dependence of the photocatalytic reaction rate on the substrate concentration. The photocatalytic degradation of J-acid in the presence of 0.3 g L^{-1} of suspended TiO_2 was examined in the range of 50 mg L^{-1} to 200 mg L^{-1} at pH 5.7 for 2 h. It is observed that the extent of degradation decreases with increase in initial concentration. Fig. 5.1.6 and Table 5.1.2 show that the degradation rate constant is proportional to the reciprocal of the initial concentration of J-acid and follows the Langmuir-Hinshelwood law.

Table 5.1.2 Effect of initial concentration on the degradation rate during the photocatalytic oxidation ($C_0 = 100 \text{ mg L}^{-1}$, pH = 5.7)

$C_0 \text{ mg L}^{-1}$	$k \text{ (min}^{-1}\text{)}$	R^2
50	0.0438	0.9914
100	0.0342	0.9975
150	0.0314	0.9930
200	0.0280	0.9955

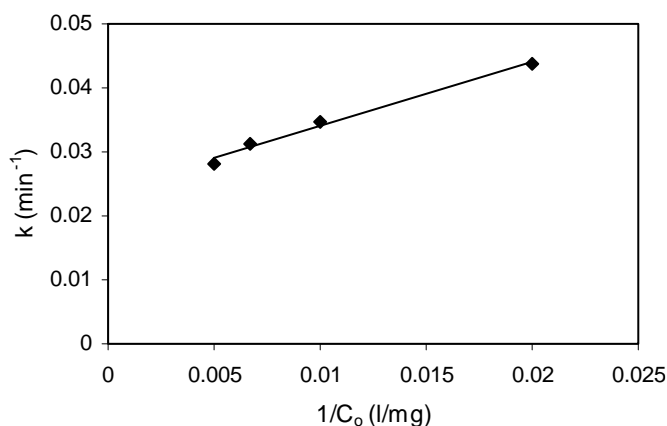


Fig. 5.1.6 Rate constant vs reciprocal of initial concentration of J-acid

5.1.8 Effect of initial pH of the solution

The pH of the solution is an important parameter to be studied for the photocatalysis of the wastewater. It affects the surface charge of TiO_2 thereby, affecting the degradation rate of the pollutants as it affects TiO_2 activity, including the surface

charge on the particles, the size of the aggregates it forms and the position of the conductance and valence bands. Hence, varying the pH of the solution affects the rate of degradation. Results obtained from the experiments by varying the initial pH of J-acid solution from 2.5 to 10.5 on the degradation rate as a function of reaction pH are illustrated in Fig.5.1.7. It is observed that the rate of degradation of J-acid increases with increase in pH from 2.5 to 4.5, beyond which it remains constant up to a pH of 6.5. Above pH 6.5, in basic medium the degradation rate again decreases.

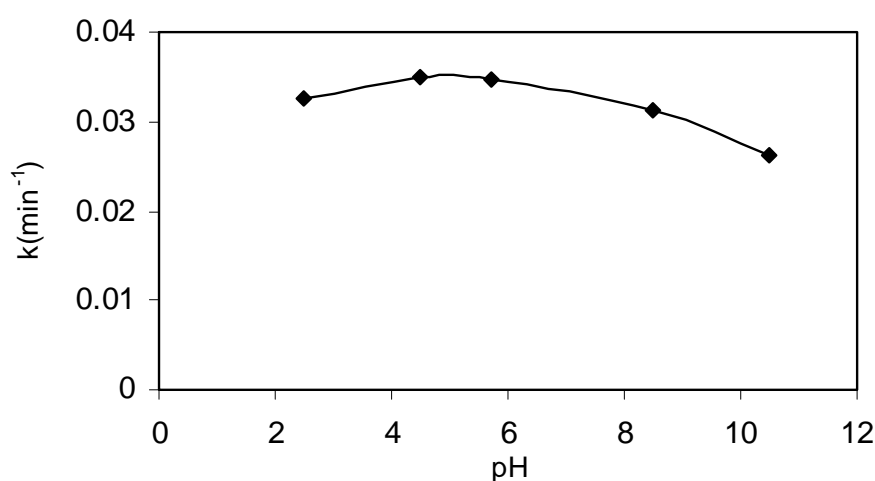


Fig. 5.1.7 Effect pH on the degradation rate of J-acid

5.1.9 Effect of Electron acceptors

Since hydroxyl radicals appear to play an important role in photocatalysis, electron acceptors such as hydrogen peroxide and ammonium persulphate were added into the solution in order to enhance the formation of hydroxyl radicals by preventing the recombination of electron hole. The degradation rates for the decomposition of J-acid in the presence of H₂O₂ by varying the concentration from 1 ml L⁻¹ to 6 ml L⁻¹ and ammonium persulphate from 0.05 g L⁻¹ to 0.4 g L⁻¹ is shown in Fig. 5.1.8 and Fig 5.1.9 respectively. It is observed that both the electron acceptors showed a beneficial effect on the degradation of J-acid under UV light. Optimum H₂O₂ concentration for the effective degradation of the dye intermediate solution is 4 ml L⁻¹. On further addition of H₂O₂, the rate of degradation of J-acid decreases. On the other hand optimum ammonium persulphate concentration for the degradation of J-acid is 0.2 g L⁻¹ and on further addition the degradation rate becomes constant.

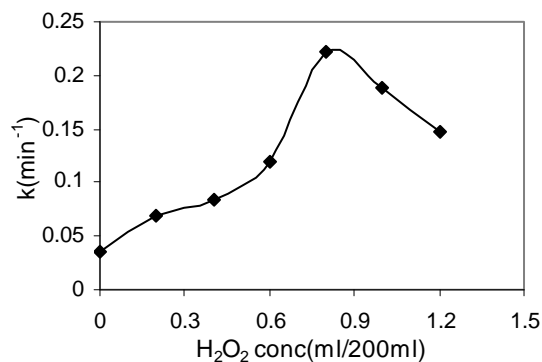


Fig. 5.1.8 Effect of H₂O₂ on the degradation rate of J-acid

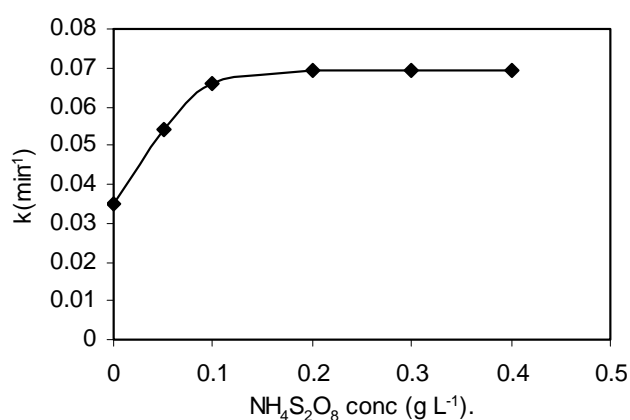


Fig. 5.1.9 Effect of ammonium persulphate on the degradation rate of J-acid

5.1.10 Effect of different catalysts

The effect of various catalysts (TiO₂-P25, ZnO and UV-100) on the photodegradation rate of J-acid is studied and the results are shown in Fig. 5.1.10. TiO₂ and ZnO are found to be more efficient than UV-100. The order of activities of the photocatalysts are ZnO>TiO₂-P25>UV-100.

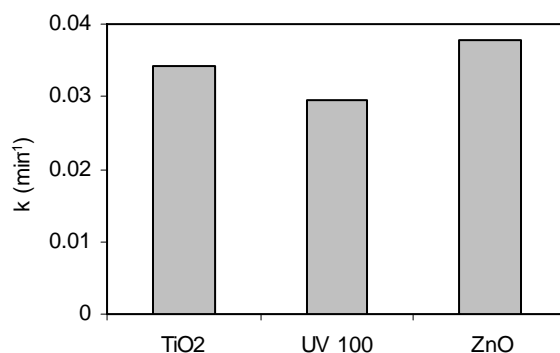


Fig. 5.1.10 Effect of different catalysts on the degradation rate of J-acid

5.1.11 Efficiency of the recycled catalyst

The photocatalytic process should be economical so that it is successfully applicable at the industrial scale and the role of catalyst's lifetime is an important parameter which makes the process cost effective. For this reason, the catalyst was recycled as shown in Fig. 5.1.11 which shows a drop in efficiency from 99 to 52% after four recycles. After the optimized conditions for the degradation of the J-acid were determined, the catalyst was recovered by filtration and activated at 100°C and again used to study its recyclability. This is likely due to fouling of the catalyst and loss due to filtration.

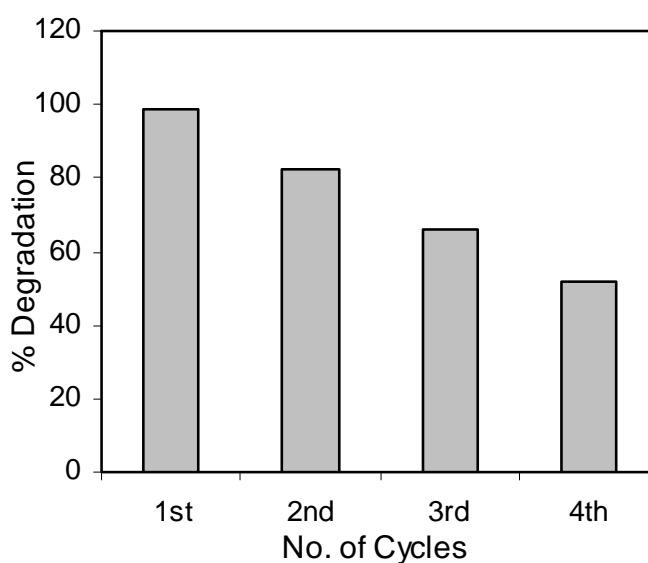


Fig 5.1.11 Recyclability of the catalyst

5.1.12 Comparison of Photodegradation of J-acid under UV light and Solar light using Shallow Pond Slurry Reactor

The degradation of this dye intermediate was also studied under sunlight in a shallow pond slurry reactor at optimum conditions for the degradation of dye intermediate determined under artificial UV light in the laboratory. The experimental procedure adopted for the solar degradation is given in section 3.4.3 and the degradation was carried out at an average sunlight intensity of 30 W m⁻² in the month of June. Fig. 5.1.12 shows that the results of degradation under sunlight were comparable with those under UV irradiation.

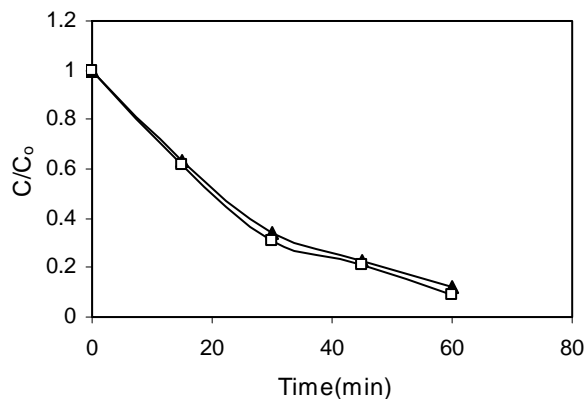


Fig. 5.1.12 Photocatalytic degradation of J-acid in presence of sunlight (■) and under artificial UV light (▲)

5.1.13 Discussion

The photocatalytic degradation of dye intermediate, H-acid under UV irradiation employing TiO₂ is reported by Noorjahan et al., 2003. Photocatalysis by TiO₂ involves under UV light excitation the generation of e⁻ and h⁺ in the conduction and valence band, respectively. These species undergo charge transfer reactions across the interface with oxygen, water and organic pollutants adsorbed on TiO₂ surface. The reaction of h⁺ with ⁻OH or H₂O leads to the generation of reactive. OH radicals having oxidation potential of 2.8 eV, which are powerful oxidants attacking the recalcitrant organic compounds of interest (Blake, 1994; Rachel et al., 2002). Change in COD further confirms the degradation of J-acid leading to decrease in organic content.

Experiments were performed to study the effect of catalyst loading by varying the amount of TiO₂ from 0.1 to 0.5 g L⁻¹. The results show that without catalyst the degradation of J-acid is insignificant. As the concentration of TiO₂ increases, the rate of degradation increases up to certain point and then begins to decrease slowly. The point beyond which the degradation rate starts decreasing is the optimum catalyst concentration i.e. concentration at which maximum degradation takes place. This observation can be explained by the fact that at high TiO₂ concentration, particles aggregate which reduces the interfacial area between the reaction solution and the photocatalyst. This way, the number of active sites on the catalyst surface is decreased. The increase in opacity and light scattering by the particles may be the other reasons for the decrease in the degradation rate. These results are in agreement with those reported in literature (Chen and Ray, 1998; San et al., 2002; Sauer et al., 2002; Saquib and Muneer, 2002).

It is observed in Table 5.1.2, the rate of degradation of J-acid decreases with the increase in initial concentration. On the surface of TiO₂ particles, the reaction occurs between the reactive $\cdot\text{OH}$ and $\text{O}_2\cdot^-$ radicals and J-acid molecules from the solution. With the increase in initial concentration, the number of molecules in contact with the TiO₂ surface increases and hence the penetration of light on the surface of the catalyst decreases and the relative amount of reactive oxidizing species on the surface of the catalyst does not increase, as the intensity and time of illumination remains constant. However, when the initial concentration is low the transfer rate plays an important role. Fig. 5.1.6 shows that the degradation rate constant is proportional to the reciprocal of the initial concentration of J-acid and follows the Langmuir-Hinshelwood equation and the expression for the rate equation is similar to that derived from the L-H model irrespective of whether the process is occurring at the surface, in solution or at the interface as is reported in the literature (San et al., 2002; Chen and Ray, 1998).

The pH of the solution can be one of the most important parameters for the photocatalytic process and so it was of interest to study its influence on the photo-oxidation of J-acid. Since photo-oxidation is accompanied by the release of protons, its efficiency may then change, because of the irreversible protonation of the TiO₂ surface (Hoffman et al., 1995). In the present study, it is observed that the rate of degradation of J-acid increases with increase in pH from 2.5 to 4.5, beyond which it remains constant up to a pH of 6.5. Above pH 6.5, in basic medium the degradation rate again decreases. The result can be explained on the basis of the structural changes of J-acid and nature of surface charges of TiO₂ with the change in pH.

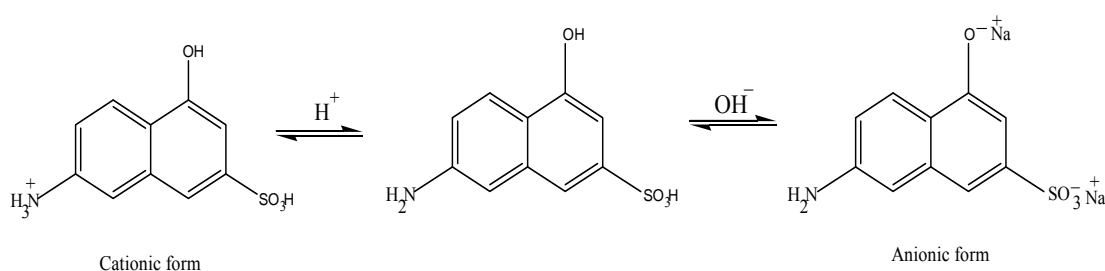
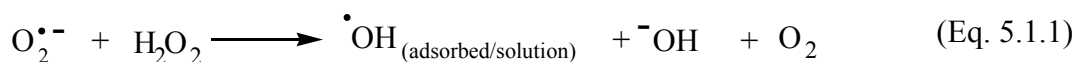


Fig. 5.1.13 Structural changes in J-acid with pH

In acidic media as reported in the literature [Sauer et al., 2002], the surface of TiO₂ is positive and J-acid exists in cationic form as shown in Fig. 5.1.13. This surface charge leads to repulsion thereby, decreasing the surface interactions between the two and

thus decreasing the rate of degradation. However at pH 4.5 to 6.5, J-acid acquires a partial anionic form which increases the surface interactions between the photocatalyst and the dye intermediate leading to maximum degradation rate in this pH range. At pH above 6.5, TiO₂ surface becomes negative and J-acid also acquires an anionic form. This leads to repulsion between the two thereby decreasing the degradation rate at higher pH.

Addition of the various electron acceptors significantly affects the degradation rate of the organic pollutants. Hydrogen peroxide as reported by Sauer et al., 2002 traps the electrons by preventing the recombination of electron and hole pairs, and thus increasing the chances of formation of $\cdot\text{OH}$ and $\text{O}_2^{\cdot-}$ ion. Many investigators (Tanaka et al., 1989; Peterson et al., 1991) have explained the photocatalytic oxidation rate enhancement in the presence of hydrogen peroxide by the following reactions:

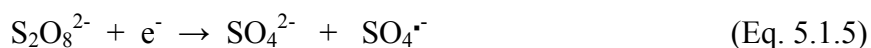


Eq. 5.1.1 and 5.1.2 suggest that the superoxide or conduction band electrons can initiate radical formation from H₂O₂. Since H₂O₂ is photosensitive the illumination of light of wavelength 254nm will also produce OH radicals (Eq. 5.1.3). The rate constant decreases with high concentration of hydrogen peroxide. The negative effect of H₂O₂ of higher concentration may be due to the OH radical quenching by the excess hydrogen peroxide. When hydrogen peroxide concentration is higher the amount of OH radical formed on the surface of the catalyst increases rapidly and hence the annihilation ($\text{OH}^{\cdot} + \text{OH}^{\cdot} \rightarrow \text{H}_2\text{O}_2$) rate is much faster than the reaction rate of OH radical and organic contaminants. Hydroxyl radicals are annihilated before the reaction of OH radical with organic contaminants. Wang et al., (2000) have reported that H₂O₂ sorbed on the catalyst surface can effectively scavenge not only the catalyst surface formed OH radical (Eq. 4.1.10 and 4.1.11) but also the photogenerated holes (h^+_{VB}) and thus inhibit the major pathway for heterogeneous generation of OH radicals (Eq. 5.1.4).

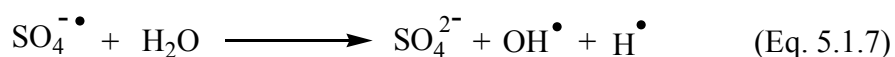
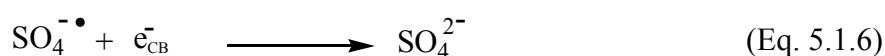


The effect of persulphate ion (electron scavenger) on the photocatalytic degradation of the dye intermediate was investigated by varying the amount from 0.05 to

0.4 g L⁻¹. Ammonium persulphate traps the photogenerated conduction band electrons, according to Eq. 5.1.5, producing simultaneously the sulphate radical, a very strong oxidant (standard potential of persulphate reduction, E⁰ = 2.6 V), which can participate in the degradation process.



In addition, it can trap the photo-generated electrons and generated hydroxyl radicals as shown in Eq. 5.1.6 and 5.1.7.



The production of hydroxyl radical and sulphate radical anion are powerful oxidizing agents and can degrade the dye intermediate at a faster rate. The sulphate anion has a unique property of attacking the pollutant molecule at various positions thus leading to rapid fragmentation and degradation.

The degradation experiments have been conducted using three different catalysts and the best results are obtained when ZnO was used as a catalyst. Although ZnO is the most efficient catalyst but it has the disadvantage of undergoing photocorrosion under illumination in acidic conditions. Zinc oxide is a more efficient catalyst than TiO₂ in degradation of J-acid but its use is limited only by pH. The high photoreactivity of TiO₂-P25 as compared to UV-100 is due to the slow recombination of electron-hole pair.

Photocatalytic processes can be made cost effective if the catalyst can be successfully recovered and recycled. TiO₂ was recycled efficiently four times with 52% photoefficiency. The reason for the drop in efficiency of the recycled catalyst is similar to that reported for RR dye 198 in chapter 4. Further, the studies conducted under sunlight show that these experiments can be performed successfully in the open atmosphere as the results under UV and sunlight are quite comparable.

Chapter 5 (B)

PHOTOCATALYTIC DEGRADATION OF J-ACID UNDER VISIBLE LIGHT

5.2 Overview

The work done in this chapter is focused on the influence of dye sensitized TiO₂ for the elimination of a dye intermediate J-acid (6-Amino naphthol-3-sulphonic acid). Effect of catalyst concentration, pH, initial concentration, H₂O₂ and ultrasound on the photocatalytic degradation of the dye intermediate was studied using immersion well slurry reactor. The degradation studies in slurry form were investigated using TiO₂ Degussa P25, UV 100 and ZnO under visible light illumination.

5.2.1 Photocatalytic Degradation of J-acid Using Immersion well slurry reactor

In the present chapter, we have dealt with the degradation rate of J-acid under visible light using sensitized TiO₂. The effect of ultrasound is also reported under optimized conditions. The procedure adopted to study the degradation rate in case of photocatalysis and sonophotocatalysis is explained in section 3.4.2. Reaction rate constant (k) is a function of parameters such as catalyst loading, pH of the solution, initial concentration of the substrate and addition of oxidant. Therefore, the effects of these parameters on the reaction rate constant have been investigated in the laboratory reactor as shown in Fig.3.2.

5.2.2 Structure and Absorption Spectra of J-acid with sensitized TiO₂

Fig. 5.2.1 shows the absorption spectra of J-acid in the presence of Rose Bengal sensitized TiO₂. J-acid shows absorption bands at $\lambda_{\max} = 294$ and $\lambda_{\max} = 354.7$ nm along with another band in the visible region at $\lambda_{\max} = 559$ nm corresponding to that of Rose Bengal. The rate of J-acid degradation was quantified by measuring the concentration as a function of time using Hitachi U-2001 UV-Vis spectrophotometer at $\lambda_{\max} = 354.7$ nm.

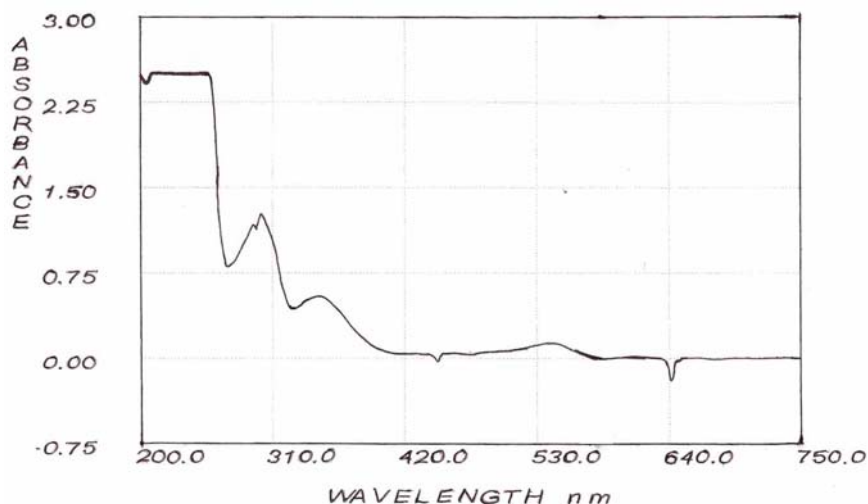


Fig. 5.2.1 Absorption Spectra of J-acid with sensitized TiO_2

5.2.3 Kinetics of disappearance of J-acid

Kinetics of disappearance of J-acid was studied for an initial concentration of 50 mg L^{-1} using 0.25 g L^{-1} of sensitized TiO_2 as shown in Fig. 5.2.2. It is observed that 99% of degradation of the compound takes place after irradiating for 150 min.

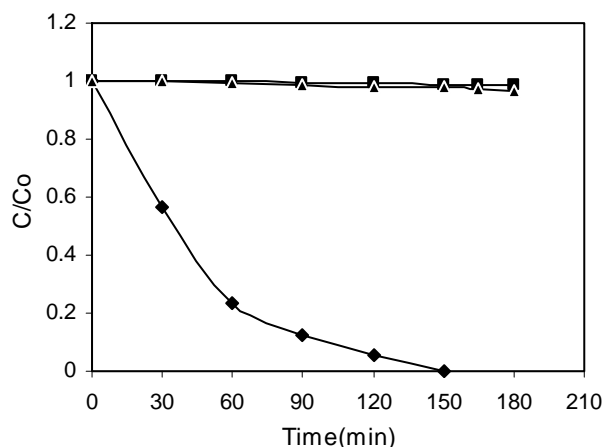


Fig. 5.2.2 Photocatalytic degradation of J-acid (\square) TiO_2 and visible light; (\blacksquare) visible light only; (\blacktriangle) TiO_2 only

The results show that the photocatalytic degradation of J-acid in aqueous TiO_2 slurry can be described by the first order kinetic model, $\ln(C_0/C) = kt$, where ' C_0 ' is the initial concentration and ' C ' is the concentration at any time ' t '. The semi logarithmic plots of concentration data gave a straight line as shown in Fig 5.2.3. The correlation constant for the fitted line was calculated to be $R^2 = 0.9958$. The rate constant was calculated to be 0.0234 min^{-1} . In blank experiments, there was no observable loss of J-

acid when the irradiation was carried out in the absence of TiO₂. In case of non-irradiated suspension, there was a slight loss due to adsorption on the photocatalyst.

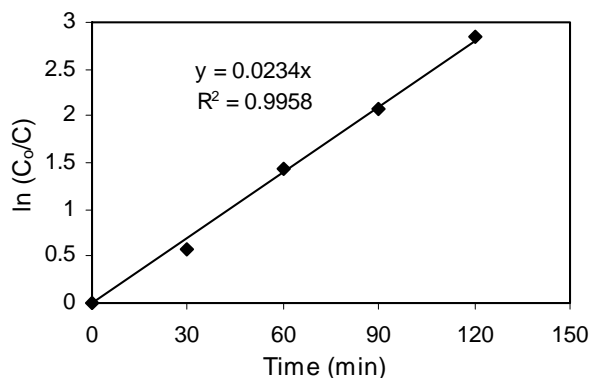


Fig. 5.2.3 Plot of $\ln (C_0/C)$ vs time for degradation of J-acid using sensitized TiO₂

5.2.4 Influence of the amount of TiO₂ in suspension

To investigate the effect of the amount of catalyst on the percentage degradation, experiments were performed over Rose Bengal sensitized Degussa P25 TiO₂ by varying the catalyst concentration from 0.05 g L⁻¹ to 0.35 g L⁻¹. It was observed that with the increase in catalyst concentration up to 0.25 g L⁻¹ the percent degradation of J-acid increases, but thereafter, there is a decrease in the degradation rate as shown in Fig. 5.2.4. Maximum degradation rate is observed with catalyst concentration of 0.25 g L⁻¹. The degradation rate is reduced due to the shielding effect of the suspended sensitized TiO₂ particles hindering the penetration of light (Noorjahan et al., 2003). All other series of experiments were carried out using 0.25 g L⁻¹ of sensitized TiO₂.

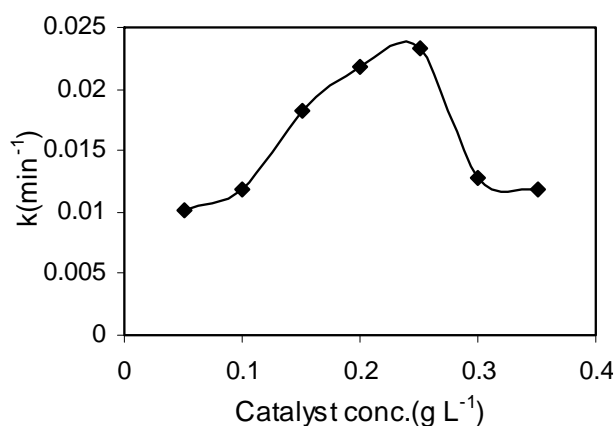


Fig. 5.2.4 Influence of catalyst concentration on degradation rate

5.2.5 Effect of pH on degradation of J-acid

The pH of the solution significantly affects the activity of TiO_2 including the surface charges on the particles and the position of the conductance and valence bands. Experiments are carried out in the presence of visible light by varying the initial pH range from 3 to 11. It is observed that as pH of J-acid is decreased from normal pH 5.7 to 3, the degradation rate decreases but in alkaline medium the degradation rate increases and becomes maximum at pH 9.

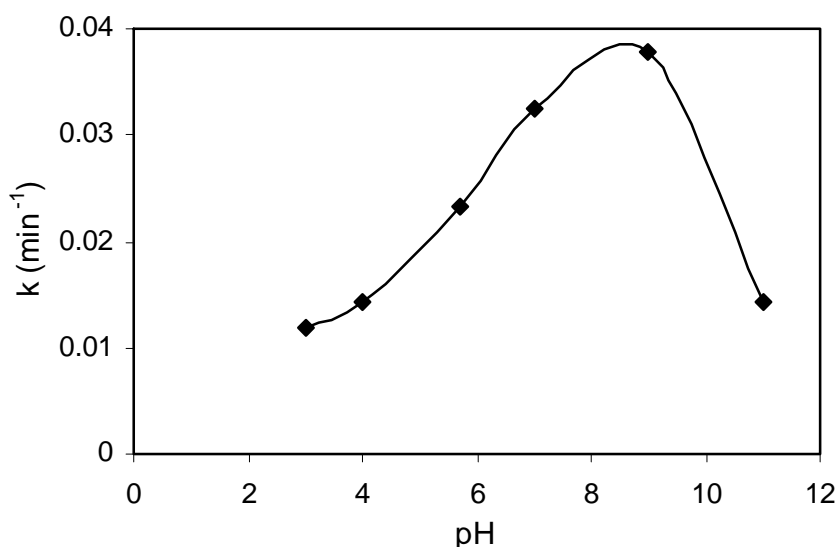


Fig. 5.2.5 Effect of pH on degradation rate of J-acid

5.2.6 Influence of initial substrate concentration on degradation rate of J-acid

Photodegradation reactions of J-acid were carried by varying the dye intermediate concentrations from 10 mg L^{-1} to 50 mg L^{-1} in the presence of 0.25 g L^{-1} of sensitized TiO_2 under visible light. The photodegradation rate is observed to decrease with increasing initial concentration and our results are in accordance with those reported in the literature (Toor et al., 2006, Chen and Ray, 1998). For initial concentration 10 mg L^{-1} , the degradation is 99.9% in 30 min. whereas for 50 mg L^{-1} the degradation is 47.3% during the same time of irradiation. Table 5.2.1 and Fig. 5.2.6 show that the degradation rate constant is proportional to the reciprocal of the initial concentration of J-acid and follows the Langmuir-Hinshelwood equation.

Table 5.2.1 Effect of initial concentration of J-acid on the photodegradation rate

C_o (mg L ⁻¹)	k (min ⁻¹)	R^2
51.98	0.0232	0.992
40.65	0.0251	0.9893
30.54	0.0311	0.9898
21.48	0.0405	0.9806
10.02	0.1062	1

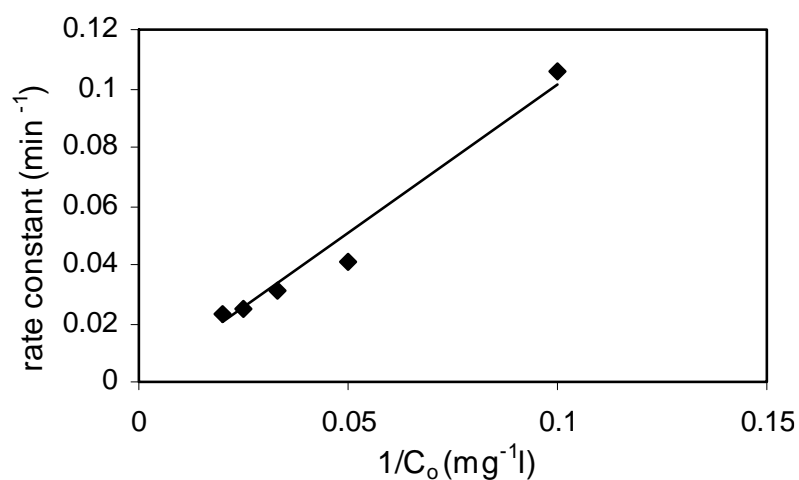


Fig. 5.2.6 Plot of rate constant vs reciprocal of initial concentration of J-acid

5.2.7 Effect of H₂O₂ concentration

The addition of powerful oxidizing species such as H₂O₂, K₂S₂O₈ to TiO₂ suspension is a well known procedure and in many cases leads to increase in the rate of photo-oxidation. Some experiments were carried out to elucidate the role of H₂O₂ concentration on the photodegradation of J-acid in the visible light/H₂O₂/sensitized TiO₂ system. A significant enhancement of degradation efficiency was observed when the

H₂O₂ concentration was increased from 0 to 1.5 ml L⁻¹ as shown in Fig. 5.2.7. Above this concentration, the rate of photodegradation decreases.

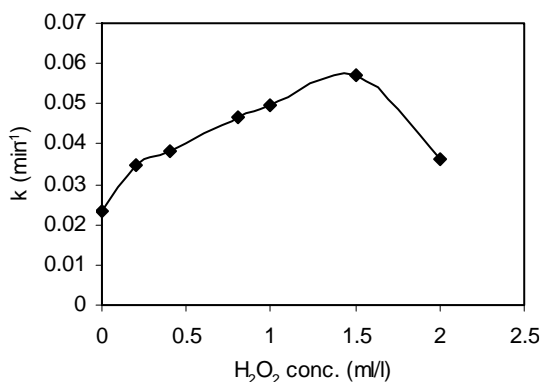


Fig. 5.2.7 Effect of addition of H₂O₂ addition on the degradation rate constant of J-acid

5.2.8 Comparison of degradation efficiency under photocatalytic and sonophotocatalytic conditions

Under the optimized concentrations of the sensitized catalyst concentration, the degradation of J-acid was carried out at an initial concentration of 50 mg L⁻¹ using photocatalytic conditions and sonophotocatalytic conditions to study the effect of ultrasound on the degradation rate as per the procedure given in section 3.4.2. As is observed from Fig 5.2.9 that 99.9% degradation takes place after 90 minutes in case of sonophotocatalysis and the degradation is about 87% in the same time under photocatalytic conditions.

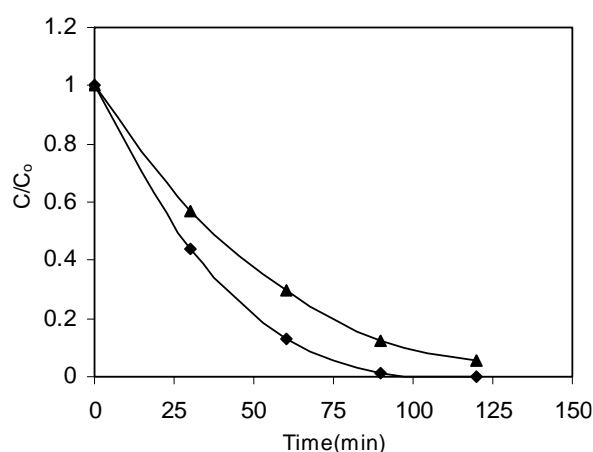


Fig. 5.2.8 Concentration versus time profile for the degradation of J acid (▲) under photocatalytic and (□) sonophotocatalytic conditions at initial conc. 50 mg L⁻¹ and catalyst conc. 0.25 mg L⁻¹

5.2.9 Mineralization of J-acid

Mineralization of J-acid was studied by studying the initial and final COD before and after the illumination reactions in visible light in the presence of sensitized TiO₂. The experiments were performed with 50 mg L⁻¹ of J-acid under optimized conditions using 0.25 g L⁻¹ of the catalyst at a normal pH of 5.7. The COD value decreased from initial 102 mg L⁻¹ to 32 mg L⁻¹ which indicates a good degree of mineralization.

5.2.10 Discussion

Although TiO₂ is a very popularly used photocatalyst, it suffers from the lack of visible light absorption. Photosensitization is widely used to extend the photo-response of TiO₂ into the visible region (Cho and Choi, 2001b). Visible light excites the sensitizer molecules adsorbed on TiO₂ and subsequently inject electrons to conduction band (CB) of TiO₂. In this case the electron induces the photocatalytic activation via formation of superoxide radical ion. No positive hole is formed in the valence band. The positive hole formed in UV light irradiation consumes hydroxyl ion to produce hydroxyl radical, and the pH of the solution changes (Moon et al., 2003). Results of the present study clearly show that the photocatalytic degradation of aqueous solution of J-acid with the Rose Bengal sensitized TiO₂ in the presence of visible light is successfully achieved. Change in COD further confirms the degradation of the dye intermediate to a satisfactory level.

One practical problem in using TiO₂ as a photocatalyst is the undesired electron/hole recombination, which in the absence of proper electron acceptor or donor, is extremely efficient and thus represents the major energy-wasting step thus limiting the achievable quantum yield (Saqib and Muneer, 2003a). One strategy to inhibit electron-hole pair recombination is to add other (irreversible) electron acceptors to the reaction. They could have several different effects such as, (1) increase the number of trapped electrons and, consequently, avoid recombination (2) to generate more radicals and other oxidizing species (3) to increase the oxidation rate of intermediate compounds and (4) to avoid problems caused by low oxygen concentration. It is pertinent to mention here that in highly toxic wastewater where the degradation of organic pollutants is the major concern, the addition of inorganic ions to enhance the organic degradation rate may often be justified. In this connection, we have studied the effect of electron acceptors such as hydrogen peroxide on the photocatalytic degradation of the J-acid.

It is necessary to determine the minimum amount of catalyst required to degrade the maximum amount of the dye intermediate at a particular experimental condition. For this, the experiments were conducted by varying the catalyst concentration from 0.05 g L⁻¹ to 0.35 g L⁻¹. Fig. 5.2.2 shows that without any catalyst the degradation of J-acid is insignificant. From Fig. 5.2.4 it is observed that the degradation first increases and then decreases slowly with the increase in catalyst concentration. Maximum degradation was obtained at a catalyst concentration of 0.25 g L⁻¹. This observation indicates that beyond this optimum concentration, other factors affect the degradation rate of J-acid. At high TiO₂ concentration, particles aggregate which reduces the interfacial area between the reaction solution and the photocatalyst. This way, the number of active sites on the catalyst surface is decreased. The increase in opacity and light scattering by the particles may be the other reasons for the decrease in the degradation rate.

Using Rose Bengal sensitized Degussa P25 as the photocatalyst, the photomineralization of J-acid in the aqueous suspensions of sensitized TiO₂ was studied in the pH range between 3 to 11. The degradation rate for the mineralization of J-acid as a function of reaction pH is shown in Fig. 5.2.5. These observations can be explained by the fact that in this case the adsorption is negligible. Since TiO₂ is sensitized by Rose Bengal which has number of electron withdrawing groups, the degradation of J-acid occurs via photo-reduction according to Eq. 5.2.1 rather than by photo-oxidation leading to the formation of OH radicals which diffuse more rapidly in alkaline medium than in the acidic medium as reported in the literature (Saquib and Muneer, 2003b).



In this case, the photosensitizer (the dye) served as an electron scavenger on the TiO₂ surface, i.e., to produce the positive hole. The degradation of the organic pollutants could then be mediated by a series of reactions initiated by the hydroxyl radical generated through the oxidation of water molecule by the positive hole (Eq. 5.2.1). This suggests that the hydroxyl ion in basic solution acts as a precursor of hydroxyl radical (Epling and Lin, 2002) which has a very active potential for decomposing organic compounds.

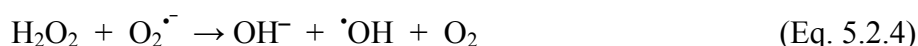
The influence of initial concentration of the dye intermediate solution on the photocatalytic degradation rate is an important aspect of the study. The effect of initial

concentration on the photocatalytic degradation of J-acid is shown in Fig. 5.2.6. The results of all the concentration profiles can be explained by the following equation:

$$C = C_0 \exp (-kt) \quad (\text{Eq. 5.2.2})$$

The rate constant 'k' in the above equation decreased with the increase in initial concentration of J-acid when other parameters are kept constant. Therefore, the degradation rate was pseudo first order with respect to concentration within experimental range. A decrease in reaction rate with increase in substrate concentration is due to the constancy of the percent amount of substrate interacting on the semiconductor. As the J-acid concentration increased, the quantity of intermediates formed by the degradation of J-acid increased as well, competing through side reactions with the parent dye intermediate decomposition. Fig. 5.2.6 shows that the degradation rate constant is proportional to the reciprocal of the initial concentration of J-acid and follows the Langmuir-Hinshelwood law irrespective of whether the process is occurring at the surface, in solution or at the interface.

The enhanced degradation rate in the presence of H₂O₂ could be rationalized as it has two functions in the process of photocatalytic degradation (Poulios and Tsachpinis, 1999). It accepts the photogenerated electron from the conduction band and thus promotes the charge separation Eq. 5.2.3, and it also forms •OH radicals according to Eq. 5.2.4.



When H₂O₂ is in excess, it may act as a hole or •OH scavenger or react with TiO₂ and form peroxo compounds, which are detrimental to the photocatalytic action.

Sonochemical reaction conditions in environmental remediation processes provide pollutant destruction either directly via activating thermal decomposition reactions, or indirectly by the production and/or enhancement of hydroxyl radical yields in advanced oxidation processes. The high-energy chemistry generated by ultrasound waves in liquid medium promotes the oxidative destruction of target contaminants. Use of ultrasound as a catalyst for water and wastewater treatment and solar detoxification for environmental applications is reported in literature (Ince et al., 2001; Hua and Hoffmann, 1997). This study reveals the acceleration of the degradation of J-acid by dye sensitized TiO₂ under

visible light has been achieved by ultrasonication. Mainly ultrasound contributes through cavitation to the scission of H_2O_2 produced by both photocatalysis and sonolysis. This increases the amount of reactive radical species inducing oxidation of the substrate and degradation of intermediates and is mainly responsible for the observed synergy.

Chapter 6

PHOTOCATALYTIC TREATMENT OF TEXTILE EFFLUENT UNDER SUNLIGHT

This chapter deals with the photocatalytic degradation as a method for pretreatment of the effluent from a textile industry containing various dyes and their intermediates which are non-biodegradable using a shallow pond slurry reactor. The process was optimized by varying various parameters like catalyst loading, initial pH, H₂O₂ as an oxidant and A/V ratio. Chemical oxygen demand (COD) changes during the process were determined.

6.1 Photocatalytic Degradation of Textile Effluent Using Shallow pond slurry reactor

The photocatalytic degradation of dye effluent obtained from a nearby textile industry in the presence of sunlight was studied using TiO₂ as a photocatalyst. Factors influencing the COD removal were studied in the subjects such as the effect of the pH, initial concentration, catalyst variation, H₂O₂ concentration and A/V ratio. To study the degradation of the effluent, the procedure given in section 3.4.3 was adopted. Schematic diagram of laboratory scale set up for shallow pond reactor which was used for the degradation of the effluent is shown in Fig. 3.3.

6.2 Textile Effluent Characteristics

Raw wastewater was collected from S.R. Industries (Textile Unit), Derra Bassi, Punjab, India located 80-90 km from Patiala on Zirakpur-Ambala road. Wastewater was taken from the flow equalization tank and analyzed for its various parameters. The color of the effluent was violet. The results of the various parameters are shown in Table 6.1. Thus these parameters show that the wastewater is highly polluted and needs to be subjected to some pretreatment so as to safely discharge the water.

Table 6.1 Characteristics of raw textile effluent from S.R. Industries

Parameters	Before Treatment (mg L ⁻¹)
COD	550-650
TS	4100
TSS	256
TDS	3844
BOD ₅ /COD	0.2-0.25
pH	10.3

6.3 Absorption Spectra for Raw Effluent

The absorption spectra of the raw sample were taken which showed several peaks in the UV and visible region as shown in Fig 6.1. This clearly indicates the presence of several organic chromophoric compounds in the wastewater and degradation studies for the complete mineralization is needed. This confirms the low biodegradability value (BOD₅/COD =0.2) for the effluent.

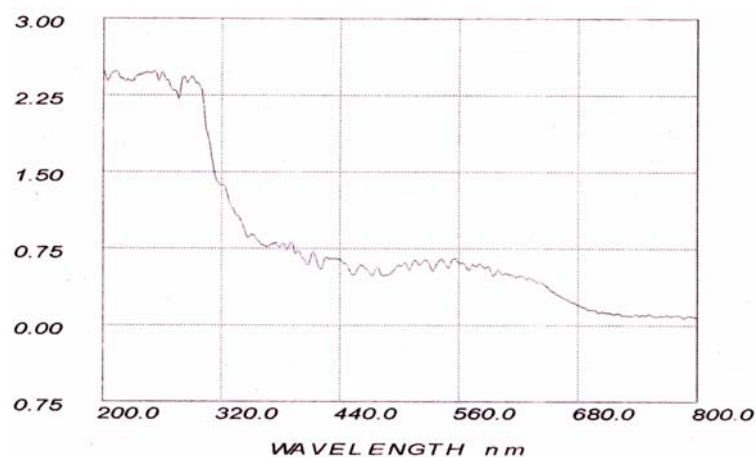


Fig. 6.1 Absorption Spectra of Raw Effluent

6.4 Solar Photocatalytic Pretreatment

After characterization of the waste sample, its photocatalytic treatment was done. Photocatalytic treatment depends upon catalyst concentration, operating pH, oxidant

addition and dilution factor. Depending upon these factors, optimized reaction conditions were calculated and used throughout the process.

6.4.1 Sample Preparation

Wastewater collected from the textile industry was highly concentrated and to get the values within range, the sample was diluted in the ratio of 1:1. Distilled water was used for all the dilutions. Initial pH of the sample was checked.

6.4.2 Radiation Conditions in Punjab, India during Summers

The solar photocatalytic treatment requires the effective exposure of samples to sunlight so as to collect solar radiations for treatment of the effluents. In Punjab, during summers we can have good intensity of sunlight. The amount of UV radiation, which can be used for TiO₂ photocatalysis on a summer day (April, May, June) is up to a maximum of about 30-37 W m⁻². The variation of solar intensities with time during the experimental days is shown in Fig. 6.2.

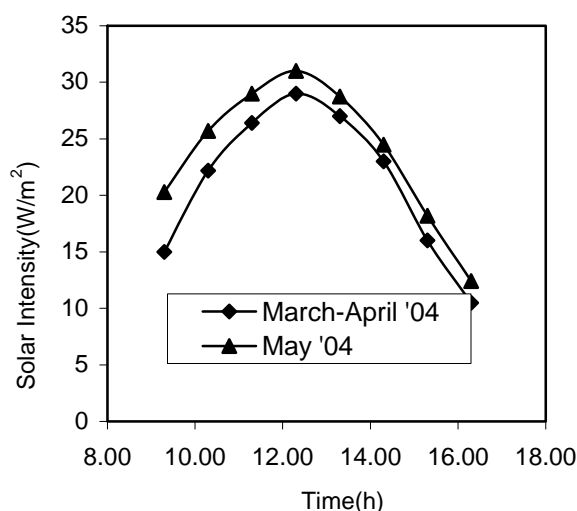


Fig. 6.2 Intensities of solar radiations during experimental days

6.4.3 Experiments with TiO₂

Catalyst (TiO₂) concentration was varied from 1.0 g L⁻¹ to 7.0 g L⁻¹ during photocatalytic reactions under sunlight. It was observed that the rate increases with increase in catalyst concentration and becomes constant above a certain level as shown Fig. 6.3 and it is seen that the optimum amount of TiO₂ is found to be 3.0 g L⁻¹. This concentration of TiO₂ has been taken for the subsequent experiments for studying the

effect of oxidant addition and pH of the solution. In Fig. 6.3 it is observed that the COD continuously decreases from 512 to 80 mg L⁻¹ on increasing the catalyst concentration from 1.0 g L⁻¹ to 7.0 g L⁻¹. An optimum of catalyst concentration has to be taken when the decrease in COD level are to be within acceptable limits. Use of higher concentration of catalyst will increase the cost of the process and decrease the permeability of sunlight.

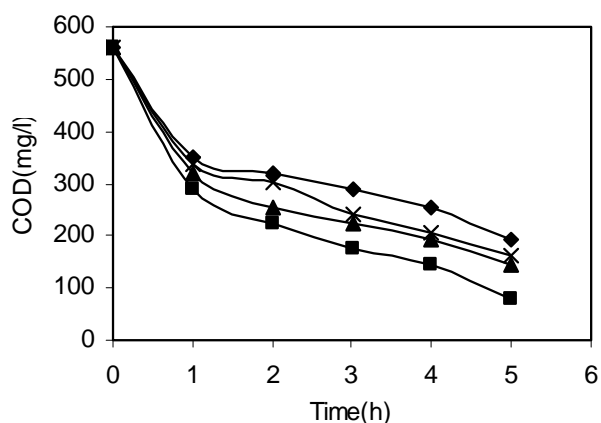


Fig. 6.3 Effect of catalyst concentration on the COD reduction,
 ◆: 0.1% TiO₂, ■: 0.3% TiO₂, ▲: 0.5% TiO₂, x: 0.7% TiO₂

6.4.4 Effect of initial pH

The wastewater from the textile industries usually has high pH values (10.3). Further, the generation of hydroxyl radicals is also a function of pH. Thus, pH plays an important role both in the characteristics of textile wastes and generation of hydroxyl radicals. Hence, attempts have been made to study the influence of pH in the degradation of dye in the pH range of 4.0 – 10.3.

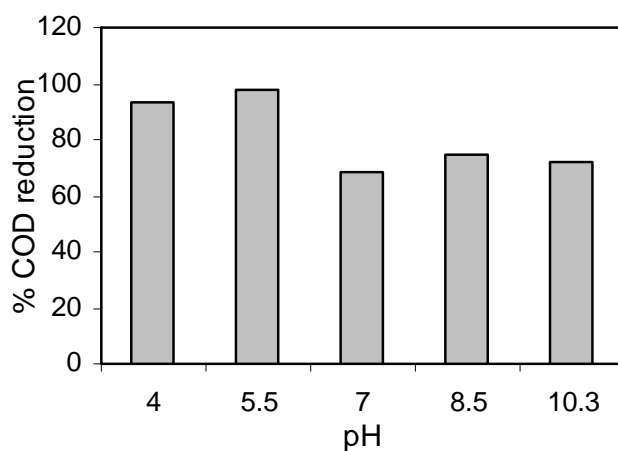


Fig. 6.4 Effect of pH on the % degradation of the effluent (0.3% catalyst loading)

In our experiments as shown in Fig 6.4, maximum degradation was observed at pH 5.5. Other pH values also responded to good degradation rates but the final pH after photocatalytic treatment which was the deciding factor for determining the optimum pH, was found to be 7.0. This is important because after photocatalytic treatment, the water can be subjected to biological treatment where the pH of the wastewater should be neutral.

Table 6.2 Showing change in pH values of the treated water by photocatalysis

pH before treatment	pH after treatment
4.0	7.4
5.5	7.0
7.0	8.5
8.5	8.2
10.3	8.5

It is clear from Table 6.2 that optimum pH should be at 5.5 because maximum degradation was achieved at this pH and final pH came out to be 7, which was suitable for the subsequent biological treatment process.

6.4.5 Effect of Oxidant addition

Another important parameter which affects the degradation of wastewater significantly is concentration of H_2O_2 , therefore it is important to study the effect of H_2O_2 so as to determine the optimum H_2O_2 concentration for the effective degradation to take place. From the experiments conducted by varying the hydrogen peroxide concentration from 0.5 to 3.0 ml L^{-1} of the effluent, the best results were obtained when oxidant addition came out to be 2.0 ml L^{-1} of the effluent and have been taken as the optimum amount required for the maximum degradation of pollutants as is clear from Fig. 6.5.

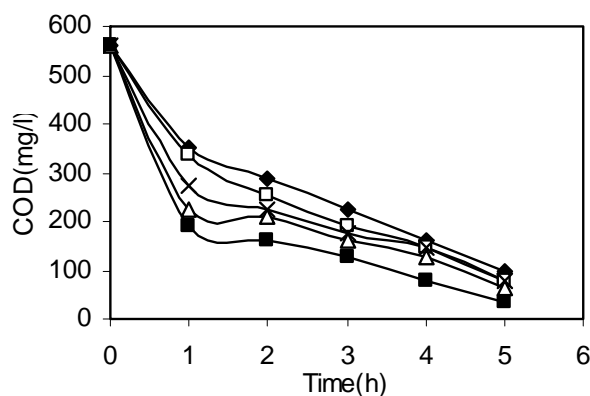


Fig. 6.5 Effect of oxidant addition (H_2O_2) on the COD reduction at 3.0 g L^{-1} of catalyst loading, ◆: no H_2O_2 , □: 0.5ml, Δ: 1 ml, ■: 2ml, x: 3ml

6.4.6 Effluent characteristics after Solar Photocatalytic Pretreatment

During photocatalytic pretreatment, reaction conditions were optimized for getting the economical benefits of the process. Effluent characteristics were determined after photocatalytic pretreatment as shown in Table 6.3 under optimized conditions i.e. at TiO_2 concentration of 3.0 g L^{-1} , 2 ml of oxidant addition and at a pH of 5.

Table 6.3 Characteristics of the wastewater after solar Photocatalytic treatment

Parameter	After Photocatalytic Treatment (mg L^{-1}) (Optimized Conditions)
COD	50-60(after 5h)
BOD ₅ /COD	0.7-0.8
TDS	1742
TS	1742
TSS	0
pH	7.0

6.4.7 Color Removal

Color which is mainly due to the azo dyes is usually the first contaminant to be recognized in wastewater. Color removal from wastewater is often more important than the removal of soluble colorless organic substances, a major fraction of which contributes

to the COD and BOD besides disturbing the ecological system of the receiving waters. Photocatalytic treatment is the most effective method which is used for the color removal as well as the degradation of the dyes present in the effluent as shown in Fig 6.6.



Fig. 6.6 Color removal after photocatalytic treatment

6.4.8 Absorption Spectra of Effluent after Photocatalytic Treatment

Fig. 6.7 shows the UV-Vis spectrum of the effluent as a function of time during photocatalytic degradation. The absorption peaks corresponding to the dyes diminish and finally disappear during the photocatalytic process indicating the complete degradation of the dyes. Moreover, no new absorption bands especially those of aromatic species or other similar intermediates appear in either the visible or ultraviolet regions.

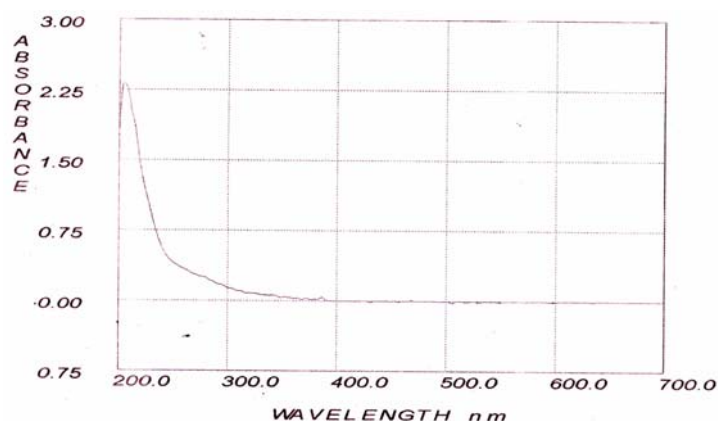


Fig. 6.7 Absorption spectra of effluent after photocatalytic treatment

6.4.9 Effect of different catalysts

The photocatalytic degradation of the textile effluent was investigated in aqueous suspensions containing TiO_2 , ZnO and Hombikat UV 100 as a photocatalyst under

optimized conditions. As shown in Fig. 6.8 maximum degradation takes place when ZnO is used as a photocatalyst.

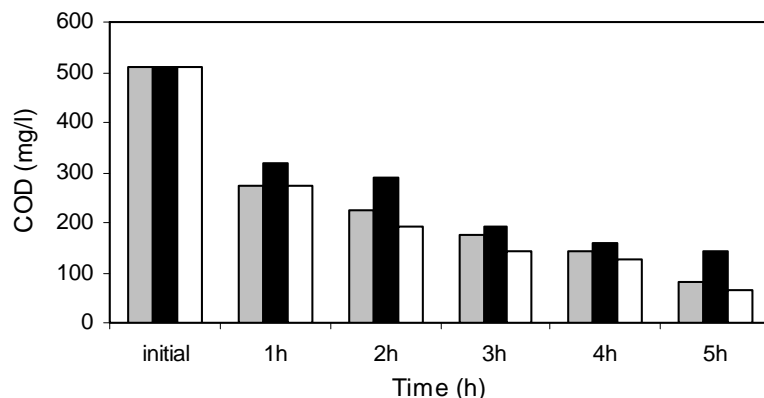


Fig. 6.8 Effect of different catalysts; ■ UV 100; ■ TiO₂; □ ZnO

6.4.10 Recycling of TiO₂

The catalyst's lifetime is an important parameter of the photocatalytic process, due to the fact that its use for a longer period of time leads to a significant cost reduction of the treatment. For this reason, the catalyst was recycled four times as shown in Fig. 6.9. After the optimized conditions for the degradation of the effluent were determined, the catalyst was recovered by filtration and activated at 100°C and again used to study its recyclability. As shown in Fig. 6.9, TiO₂ can be recycled effectively which makes the process cost effective. The process was repeated until reasonable COD reduction upto 54% was achieved after the fourth cycle.

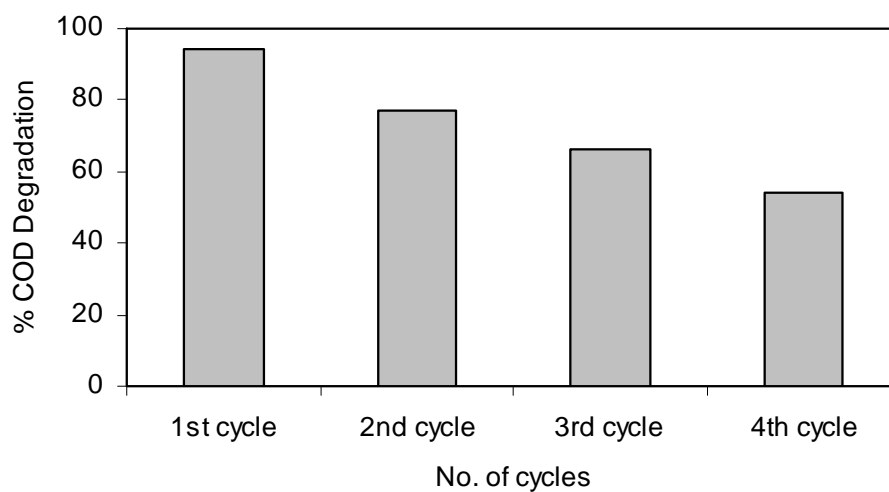


Fig. 6.9 Recycling of TiO₂

6.4.11 Effect of A/V ratio of the reactor

The ratio of area to volume (A/V) is critical for the shallow pond reactor as the photocatalytic oxidation reaction depends on area available for the irradiation of light. More area and less depth enhance the rate of degradation as the penetration of UV rays into the solution increases. Hence, the reaction rate increases with increasing aperture to volume ratio of the shallow pond type reactor as shown in Fig.6.10. As A/V ratio is increased from $0.45 \text{ cm}^2 \text{ ml}^{-1}$ to $1.14 \text{ cm}^2 \text{ ml}^{-1}$, the COD reduction is increased from 68.7 to 93.7% in 5 h for the textile dye effluent.

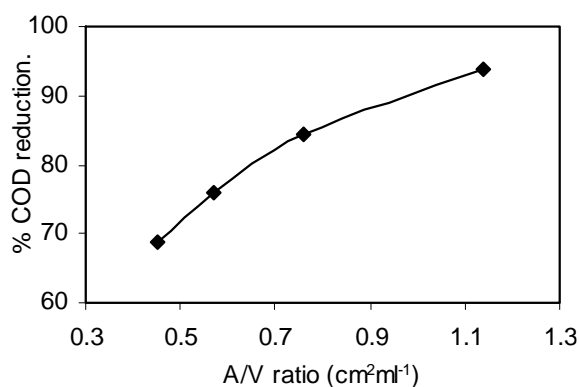


Fig. 6.10 Effect of A/V ratio on COD reduction

6.5 Discussion

The dyeing and finishing industry is the major polluters in the industrial sector (Arslan et al., 2000; Sauer et al., 2002). The current practice in textile mills is to discharge the wastewater into the local environment without any treatment. Due to the use of reactive azo dyes, up to 30% of the used dyestuff remains in the spent dye-bath after the dyeing process (Muruganandham and Swaminathan, 2004b) which is an important source of environmental contamination. This wastewater causes serious impact on natural water bodies and land in the surrounding area. High values of COD and BOD, presence of particulate matter and sediments, oil and grease in the effluent causes depletion of dissolved oxygen, which has an adverse effect on the marine ecological system. Effluents from mills also contain chemicals which are dark in color, leading to the turbidity of the water body which hampers the photosynthesis process, causing alteration in the habitat. The improper handling of hazardous chemicals in textile water also have some serious impact on the health and safety of workers putting them into the high-risk bracket for

contracting skin diseases like chemical burns, irritation, ulcers, etc. and even leads to respiratory problems.

Since solar light is an abundant natural energy source, photo-degradation of pollutants using TiO_2 with solar light can make it an economically viable process. The artificial light sources need high electrical power which is costly and hazardous. Photobleaching of some dyes by solar light irradiation using TiO_2 as a photocatalyst has been successfully achieved (Muruganandham and Swaminathan, 2004b).

The chemical oxygen demand (COD) was chosen as the parameter to characterize effluent from a high volume textile producer. COD is an indication of the overall oxygen load that a wastewater will impose on an effluent stream. COD is equal to the amount of dissolved oxygen that a sample will absorb from a hot acidic solution containing potassium dichromate and mercuric ions.

The amount of catalyst is one of the main parameters for the degradation studies. It is necessary to find out the optimum loading for efficient removal of the dye in order to avoid the use of excess catalyst. Several authors have investigated the reaction rate as a function of catalyst loading in the photocatalytic degradation process (San et al., 2002, Gouvea et al., 2000, Muneer and Bahnemann, 2002). As is shown in Fig. 6.3, the effect of catalyst concentration is studied by varying the amount of TiO_2 from 1.0 g L^{-1} to 7.0 g L^{-1} .

As the concentration of catalyst is increased, the number of photons absorbed and the number of pollutant molecules absorbed are increased owing to an increase in the number of TiO_2 particles. The density of particles in the area of illumination also increases and so the rate is enhanced. Above a certain level, the substrate available is not sufficient for adsorption by the increased number of TiO_2 particles. Hence, the additional catalyst amount is not involved in the catalytic activity and the rate does not increase with an increase in the amount of catalyst beyond a certain limit. Surface active sites also decrease due to aggregation of TiO_2 particles at high concentrations. This observation is in agreement with the observations reported in literature (Toor et al., 2006) and an amount of 3.0 g L^{-1} has been taken for the subsequent experiments for studying the effect of oxidant addition and pH of the solution.

The wastewater from textile industries usually has a wide range of pH values. Generally, pH plays an important role both in the characteristics of textile wastes and generation of hydroxyl radicals (Neppolian et al., 2002a). Hence, attempts have been made to study another very important parameter, the influence of pH in the degradation of the textile effluent at pH values in the range 4.0–10.3. The pH significantly affects TiO₂ activity, including the charge on the particles, the size of the aggregates it forms and the position of the conductance and valence bands. Extensive experimental data has been published dealing with the effect of pH on photocatalytic degradation of various organic compounds (Arslan et al., 2000). For charged substrates, a significant dependency of the photocatalytic degradation efficiency upon the pH value has often been observed, since the overall surface charge and hence the adsorption properties of TiO₂ particles depend strongly on solution pH (Bahnemann et al., 1994). Alkaline pH is favorable for the degradation of the cationic substrates, while negatively charged particles are effectively degraded in the acidic media when the photocatalyst surface is positively charged. In fact, in the degradation of the effluent, it is not the initial pH but it is the final pH which is the deciding pH, since the wastewater after the photocatalytic pretreatment has to be subjected to the biological treatment where the pH of the wastewater should be neutral so that effective biodegradation takes place leading to complete mineralization. As is clear from the experimental results, the photocatalytic treatment is carried out at an initial pH of 5.5, the final pH obtained after the degradation is 7.0 which shows that water can directly be subjected to the biodegradation so that further mineralization can take place.

One possible way to increase the reaction rate would be to increase the concentration of OH radicals because these species are widely considered to be promoters of photocatalytic degradation. The addition of hydrogen peroxide to the heterogeneous system increases the concentration of OH radicals, since it inhibits the electron-hole recombination according to Eq. 4.1.9.

Hydrogen peroxide is considered to have two functions in the process of photocatalytic degradation. It accepts a photo generated electron from the conduction band and thus promotes the charge separation, and also forms OH radical, according to Eq. 4.1.9. However, at high concentration of H₂O₂, it also acts as a scavenger as shown in the Eqs. 4.1.10 and 4.1.11.

Color is another important factor in the textile wastewater which contributes to the high COD values. The traditional techniques used for color removal are activated carbon (charcoal), filtration and coagulation. The use of charcoal is technically easy but has high waste disposal cost. Although filtration potentially provides pure water as the final product, it is possible for low molar mass dyes to pass through the filter system. Coagulation using alums, ferric salts or limes is a low cost process, but all these methods have a major disadvantage of simply transferring the pollutants to another phase rather than destroying them. Biological treatment is a proven technology and cost effective, however it has been reported that the majority of dyes are only adsorbed on the sludge and not degraded. Photocatalytic treatment is the most effective method which is used for the color removal as well as the degradation of the dyes present in the effluent as shown in Fig 6.6.

The ratio of BOD₅/COD in wastewater is normally used to express the biodegradability of the wastewater. When the ratio of BOD₅/COD is more than 0.3, the wastewater has a better biodegradability whereas if the ratio is less than 0.3, the wastewater is difficult to be biodegraded (Chun and Yizhang, 1999). It is clear from Table 6.1 and Table 6.3 that the COD value of the effluent decreases significantly thereby increasing the BOD₅/COD ratio from 0.2-0.25 to 0.7-0.8. The results clearly suggest that the textile wastewater which was initially non biodegradable becomes biodegradable after photocatalytic pretreatment which further helps in the complete mineralization of the intermediates formed during the photocatalytic process.

Effect of various photocatalysts on the degradation rate of the textile effluent is studied as shown in Fig. 6.8. TiO₂-P25 and ZnO is found to be more efficient as compared to UV-100. Although ZnO is the most efficient catalyst but it has the disadvantage of undergoing photo-corrosion under illumination in acidic conditions, therefore, the degradation studies have been carried out using TiO₂-P25 as a photocatalyst. The degradation process can be carried out under all the pH range varying from acidic to alkaline conditions. The high photoreactivity of TiO₂-P25 as compared to UV-100 is due to the slow recombination of electron-hole pair and large surface area of TiO₂.

The ratio of area to volume (A/V) is critical for the shallow pond reactor as the photocatalytic oxidation reaction depends on area available for the irradiation of light. More area and less depth enhance the rate of degradation as the penetration of UV rays into the solution increases. Hence, the reaction rate increases with increasing aperture to volume ratio of the shallow pond type reactor as shown in Fig. 6.10. Dependence on A/V ratio for the rate of degradation of 4-chlorophenol in shallow pond reactor has also been reported by Klausner et al., (1994).

Keeping in mind the economics of photocatalytic process, TiO_2 was recycled efficiently four times with 54% photoefficiency. One of the reasons for the decrease in efficiency of the recycled catalyst is due to deposition of photosensitive hydroxides on the photocatalysts surface blocking its active sites.

Chapter 7

CONCLUSIONS AND RECOMMENDATIONS

The photocatalytic degradation of RR dye 198, J-acid and textile effluent using artificial UV light/visible light/sunlight/sonolysis singly or in combination as radiation sources has been achieved. The observations of these investigations clearly demonstrate the importance of choosing the optimum degradation parameters to obtain a high degradation rate, which is essential for any practical application of photocatalytic oxidation processes using different photocatalysts like anatase TiO₂, dye sensitized TiO₂, ZnO and Hombikat UV-100. Use of shallow pond slurry reactor has the advantage of low cost and use of existing ponds for biological treatment further facilitates the technology.

Heterogenous photocatalytic oxidation process using UV light and oxygen could be efficiently applied for the degradation of non-biodegradable azo RR dye 198. It is observed that adsorption plays a major role in the photodegradation of the model compound and the photodegradation kinetics follow the Langmuir-Hinshelwood model. The results clearly delineate the important role of the selection of the optimum reaction conditions in achieving the highest level of degradation efficiency for RR dye 198. The rate of photodegradation under UV light was found to be maximum in the acidic medium with optimum TiO₂ concentration of 0.3 g L⁻¹ at low dye concentrations with good recyclization of catalyst. Optimum H₂O₂ concentration for the degradation of RR dye 198 under UV light was found to be 5ml L⁻¹. The experiments under sunlight show that higher photodegradation efficiency can be achieved under the same optimized conditions. Thus, this can be used as an efficient technology for solar photocatalytic degradation of the colored wastewater discharged from the textile industry is under Indian climatic conditions.

This study reveals that further the acceleration of the degradation of RR dye 198 by the process of dye sensitized TiO₂ under visible light can be achieved by ultrasonication. Mainly ultrasound contributes through cavitation to the scission of H₂O₂ produced by both photocatalysis and sonolysis. This increases the amount of reactive radical species inducing oxidation of the substrate and degradation of intermediates and is mainly responsible for the observed synergy. The photo-degradation kinetics follows the Langmuir-Hinshelwood model and depends on the TiO₂ concentration and pH. Maximum

degradation was achieved with catalyst loading 0.3 g L^{-1} under acidic conditions at low initial conc. and $0.5 \text{ ml L}^{-1} \text{ H}_2\text{O}_2$ concentration under visible light using sonophotocatalytic conditions. These results show that a conventional dye can be used as a photosensitizer of TiO_2 functioning under visible light which has been demonstrated by the degradation of phenol. It is also evident that the reaction takes place via formation of singlet oxygen, superoxide and hydroxyl radicals. This methodology has additional advantage for harnessing the visible component of the solar energy for the degradation of organic pollutants in water.

Dye intermediate, J-acid was degraded under UV irradiation using TiO_2 as photocatalyst to determine the optimum conditions of catalyst, initial substrate, pH and electron acceptors so that effective degradation can be achieved. Degradation was observed to be maximum at 0.3 g L^{-1} of catalyst loading, 6.5 pH and 0.4 g L^{-1} of ammonium persulphate or 4 ml L^{-1} of H_2O_2 concentration. The first order kinetic model can be used to describe the photocatalytic degradation of J-acid. The COD of the solution decreased from 102 mg L^{-1} to 4 mg L^{-1} which accounts for 95.8% reduction in 2.30 h. The catalyst was effectively recycled four times. The results of degradation under sunlight were comparable with those under UV irradiation.

J-acid was also degraded under visible light by using dye sensitized TiO_2 . The degradation of J-acid is efficiently carried out in the presence of Rose Bengal sensitized TiO_2 using an immersion well type photoreactor. The investigations demonstrate the possibility of using dye fixed TiO_2 semiconductor which is inexpensive under optimized conditions of 0.25 g L^{-1} of catalyst in alkaline medium at low concentration for the photodetoxification of J-acid. Further enhancement in the rate was observed with the addition of H_2O_2 and becomes maximum at 1.5 ml L^{-1} of dosage of H_2O_2 . This methodology can further be extended to the solar detoxification where visible light being the major component facilitates its commercial application.

It has been concluded that this process can be used as an efficient and environmental friendly technique for effluent treatment of industrial wastewater containing organic compounds and dyes from textile industry. The textile dye effluent was successfully degraded by the photocatalytic oxidation process under solar light in a shallow pond slurry reactor. The decolorization of the effluent, COD reduction by 90%

and increase in BOD₅/COD ratio of the effluent to 0.7 after photocatalytic pretreatment indicates the enhancement of the biodegradability of the treated water. This process can be coupled with the existing biological treatment process leading to complete mineralization of organic pollutants. The optimization of the photocatalytic process shows that the degradation should be carried with 0.3% TiO₂ at pH 5.5 in the presence of 2 ml L⁻¹ of H₂O₂ to get the best results. This technology will be very useful for countries like India where for more than 3/4th time of the year we have bright sunlight, as an inexpensive source of energy. This work has significant socio-economic importance, and will improve the quality of environment and adoption at industrial scale by textile industries.

The methodology adopted in this study demonstrates the efficiency of photocatalytic treatment as a pre- or post- treatment method to existing biological treatment method for textile wastewaters containing biorecalcitrant, non-biodegradable pollutants. Development of this technology is of importance in the Indian context as sunlight is in abundance and presently the existing technology in textile industry is not efficient for treating the wastewaters resulting in discharge of colored water into rivers and public sewage system which is a health hazard.

Future research is needed for the development of more efficient catalysts for harnessing solar energy which are low cost and effective. Designing of reactors and solar collectors for photocatalytic treatment needs to be developed so that they can be used by both small and large scale textile industries in combination with the existing technology ultimately leading to recycling of water as large amount of water is utilized in textile industry. Further research to extend sonophotocatalytic technology to the industrial scale is needed. It can be achieved by fitting transducers on the base of the wastewater tanks in the industries.

In light of these conclusions the textile industries need to review and incorporate these measures within their respective H&S and environmental polices which should be strictly governed.

REFERENCES

- Abdullah, M., G. Low, R.W. Matthews, 1990.** Effects of common inorganic anions on the rates of photocatalytic oxidation of organic carbon over illuminated titanium dioxide. *J. Phys. Chem.*, 94, 6820-6825.
- Abrahart, E.N., 1997 (2nd Ed.),** *Dyes and their intermediates*, Chemical Publishing Co., New York.
- Akyol, A., M. Bayramoglu, 2005.** Photocatalytic degradation of Remazol Red F3B using ZnO catalyst. *J. Haz. Mat.*, 124 (1-3) 241-246.
- Alaton, I.A., 2004.** Homogenous photocatalytic degradation of a disperse dye and its dye bath analogue by silicadodecatungstic acid. *Dyes and Pigments*, 60(2)167-176.
- Alaton, I. A., I.A. Balcioglu, 2001.** Photochemical heterogeneous photocatalytic degradation of waste vinylsulphone dyes: a case study with hydrolysed Reactive Black 5. *J. Photochem. Photobiol. A: Chem.*, 141, 247–254.
- Al-Ekabi, H., N. Serpone, E. Pelizzetti, C. Minero, M.A. Fox, R.B. Draper, 1989.** Kinetic studies in heterogeneous photocatalysis, titania-mediated degradation of 4-chlorophenol alone and in a three-component mixture of 4-chlorophenol, 2, 4-dichlorophenol, and 2, 4, 5-trichlorophenol in air-equilibrated aqueous media. *Langmuir*, 5, 250-255.
- Alfano, O.M., D. Bahnemann, A.E. Cassano, R. Dillert, R. Goslich, 2000.** Photocatalysis in water environments using artificial and solar light. *Catal. Today*, 58, 199-230.
- Alfano, O.M., M.I. Cabrera, A.E. Cassano, 1997.** Photocatalytic reactions involving hydroxyl radical attack, reaction kinetics formulation with explicit photon absorption effects. *J. Catal.*, 172, 370-379.
- Alvaro, M., E. Carbonell, M. Espla, H. Garcia, 2005.** Iron phthalocyanine supported on silica or encapsulated inside zeolite Y as solid photocatalysts for the degradation of phenols and sulfur heterocycles. *Appl. Catal. B: Environ.*, 57(1)37-42.
- An, T., H. Gu, Y. Xiong, W. Chen, X. Zhu, G. Sheng, J. Fu, 2003.** Decolourization and COD removal from reactive dye containing wastewater using sonophotocatalytic technology. *J. Chem. Technol. & Biotechnol.*, 78 (11) 1142-1148.

- Andreozzi, R., V. Caprio, A. Insola, G. Longo, V. Tufano, 2000.** Photo-catalytic oxidation of 4-nitrophenol in aqueous TiO₂ slurries: an experimental validation of literature kinetic models. *J. Chem. Technol. Biotechnol.*, 75, 131-136.
- Andreozzi, R., V. Caprio, A. Insola, R. Martota, 1999.** Advanced oxidation processes (AOP) for water purification and recovery. *Cat. Today*, 53, 51-59.
- Anielak, A. Maria, 1996.** Disposal of textile industry wastewaters. *Environ. Prot. Engg.*, 22(3-4) 71-88.
- Anpo, M., 2000.** Use of visible light. Second-generation TiO₂ photocatalysts prepared by the application of an advanced metal ion-implantation method. *Pure Appl. Chem.*, 72(9)1787-1792.
- Arslan, I., A. Isil, A. Balcioglu, 2001.** Photochemical and heterogeneous photocatalytic degradation of waste vinylsulphone dyes: a case study with hydrolysed Reactive Black 5. *J. Photochem. Photobiol. A: Chem.*, 141, 247-254.
- Arslan, I., I.A. Balcioglu, D.W. Bahnemann, 2000.** Heterogeneous photocatalytic treatment of simulated dyehouse effluents using novel TiO₂-photocatalysts. *Appl. Catal. B: Environ.*, 26, 193-206.
- Augugliaro, V., C. Baiocchi, A.B. Prevot, E.G. Lopez, V. Loddo, S. Malato, G. Marci, L. Palmisano, M. Pazzi, E. Pramaura, 2002.** Azo-dyes photocatalytic degradation in aqueous suspension of TiO₂ under solar irradiation. *Chemosphere*, 49(10) 1223-1230.
- Bahnemann, D.W., J. Cunningham, M.A. Fox, E. Pelizzetti, P. Pichat, N. Serpone, G.R. Helz, R.G. Zepp, D.G. Crosby, 1994.** *Acquatic and Surface Photochemistry*, CRC Press, Boca Raton, Florida, 261-316.
- Bahnemann, D.W., C. Kormann, M.R. Hoffmann, 1987.** Preparation and characterization of quantum size zinc oxide: fluorescence and non-linear optical effects. *J. Phys. Chem.*, 91, 3789-3798.
- Balcioglu, A, I.A. Alaton, M. Otker, R. Bahar, N. Bakar, M. Ikiz, 2003.** Application of advanced oxidation processes to different industrial wastewaters: I. *J. Environ. Sci. Health, Part A*, 38(8)1587-1596.
- Baran, W., A. Makowski, W. Wardas, 2003.** The influence of FeCl₃ on the photocatalytic degradation of dissolved azo dyes in aqueous TiO₂ suspensions. *Chemosphere*, 53, 87-95.

- Barbeni, M., E. Pramauro, E. Pelizzetti, E. Borgarello, N. Serpone, 1985.** Photodegradation of pentachlorophenol catalyzed by semiconductor particles. *Chemosphere*, 14, 195-208.
- Bardos, E., S. H. Czili, A. Horvath, 2003.** Photocatalytic oxidation of oxalic acid enhanced by silver deposition on a TiO₂ surface. *J. Photochem. Photobiol. A: Chem.*, 154, 195-201.
- Bauer, C., P. Jacques, A. Kalt, 2001.** Photooxidation of an azo dye induced by visible incident on the surface of TiO₂. *J. Photochem. Photobiol. A: Chem.*, 140(1) 87-92.
- Behnajady, M.A., N. Modirshahla, N. Daneshvar, M. Rabbani, 2007.** Photocatalytic degradation of an azo dye in a tubular continuous-flow photoreactor with immobilized TiO₂ on glass plates. *Chemical Engg. Journal*, 127(1-3)167-176.
- Behnajady, M.A., N. Modirshahla, H. Fathi, 2006.** Kinetics of decolorization of an azo dye in UV alone and UV/H₂O₂ processes. *J. Haz. Mat.*, 36(3) 816-821.
- Bessekhouad, Y., N. Chaoui, M. Trzpit, N. Ghazzal, D. Robert, J.V. Weber, 2006.** UV-vis versus visible degradation of Acid Orange II in a coupled CdS/TiO₂. *J. Photochem. Photobiol. A: Chem.*, 183(1-2)218-224.
- Bhatkhande, D.S., V.G. Pangarkar, A.C.M. Beenackers, 2002.** Photocatalytic degradation for environmental applications - A Review. *J. Chem. Technol. & Biotech.*, 77(1)102-116.
- Birnie M., S. Riffat, M. Gillott, 2006.** Photocatalytic reactors: design for effective air purification. *Int. J. Low Carbon Tech.*, 1(1)47-58.
- Blake, D.M., 2001.** Bibliography on the photocatalytic removal of hazardous compounds from water and air. National Renewable Energy Laboratory, Technical Report NREL/TP-510-31319.
- Blake, D.M., 1994.** Bibliography on the photocatalytic removal of hazardous compounds from water and air. NREL Report #NREL/ TP-430-6084. Available from NTIS, Springfield, VA.
- Blake, D.M., H.F. Link, K. Eber, 1992.** Solar photocatalytic detoxification of water. *Advances in Solar Energy*, K. W. Boer (Editor), American Solar Energy Society, Boulder, CO., 7, 167-210.
- Brandi, R.J., G. Rintoul, O. M. Alfano, A.E. Cassano, 2002.** Photocatalytic reactors reaction kinetics in a flat plate solar simulator. *Catal. Today*, 76, 161-175.
- Brown, G.T., J.R. Darwent, 1984.** Photoreduction of methylorange sensitized by colloidal TiO₂. *J. Chem. Soc., Faraday Trans*, 80, 1631-1637.

- Butler, E. C., A.P. Davis, 1993.** Photocatalytic oxidation in aqueous titanium dioxide suspensions: the influence of dissolved transition metals. *J. Photochem. Photobiol. A: Chem.*, 70, 273-283.
- Cabrera, M.I., O.M. Alfano, A.E. Cassano, 1994.** Novel reactor for photocatalytic kinetic studies. *Ind. Engg. Chem. Res.*, 33, 3031-3042.
- Caliman, A.F., I. Balasanian, 2005.** Reactors for application in heterogeneous photocatalysis. *Environ. Engg. Manag. J.*, 4 (3)371-391.
- Cangcang, C., H. Dewan, 1998.** Application of fixed bed reactor to photodegradation of soluble dye 4BS (Red) with solar light. *Huanjing Wuran Yu Fangzhi*, 20(4), 17-19.
- Carey, J.H., J. Lawrence, H.M. Tosine, 1976.** Photodechlorination of PCB's in the presence of titanium dioxide in aqueous suspensions. *Bull. Environ. Contam. Toxicol.*, 16, 697-701.
- Carraway, E.R., A.J. Hoffman, M.R. Hoffmann, 1994.** Photocatalytic oxidation of organic acids on quantum-sized semiconductor colloids. *Environ. Sci. Technol.*, 28, 786-793.
- Chakrabarti, S., B.K. Dutta, 2004.** Photocatalytic degradation of model textile dyes in wastewater using ZnO as semiconductor catalyst. *J. Haz. Mat. B*, 112, 269-278.
- Chan, A.H.C., C.K. Chan, J.P. Barford, J.F. Porter, 2003.** Solar photocatalytic thin film cascade reactor for treatment of benzoic acid containing wastewater. *Wat. Res.*, 37, 1125-1135.
- Chatterjee, D., S.D. Gupta, N.N. Rao, 2006.** Visible light assisted photodegradation of halocarbons on the dye modified TiO₂ surface using visible light. *Sol. Ener. Mat. Sol. Cells*, 90(7-8) 1013-1020.
- Chatterjee, D., A. Mahata, 2002.** Visible light induced photodegradation of organic pollutants on the dye adsorbed TiO₂ surface. *J. photochem. Photobiol. A: Chem.*, 153,199-204.
- Chatterjee, D., A. Mahata, 2001a.** Photoassisted detoxification of organic pollutants on the surface modified TiO₂ semiconductor particulate system. *Catal. Communications*, 2, 1-3.
- Chatterjee, D., B. Ruj, A. Mahata, 2001b.** Adsorption and photocatalysis of colour removal from waste water using flyash and sunlight. *Catal. Comm.*, 2, 113-117.
- Chatterjee, D., A. Mahata, 2001c.** Demineralization of organic pollutants on the dye modified TiO₂ semiconductor particulate system using visible light. *Appl. Catal. B: Environ.*, 33, 119-125.

- Chen, Y., A.V. Vorontsov, P.G. Smirniotis, 2003.** Enhanced photocatalytic degradation of dimethyl methylphosphonate in the presence of low-frequency ultrasound. *Photochem. Photobiol. Sci.*, 2, 694-698.
- Chen, C., W. Zhao, J. Li, J. Zhao, 2002a.** Formation and identification of intermediates in the visible-light-assisted photodegradation of sulforhodamine-B dye in aqueous TiO₂ dispersion. *Environ. Sci. Technol.*, 36, 3604-3611.
- Chen, C.Y., Smirniotis, Panagiotis, 2002b.** Enhancement of photocatalytic degradation of phenol and chlorophenols by ultrasound. *Ind. Engg. Chem. Res.*, 41 (24) 5958-5965.
- Chen, D., A.K. Ray, 1998.** Photodegradation kinetics of 4-nitrophenol in TiO₂ suspension. *Wat. Res.*, 32, 3223-3234.
- Cheng M., W. Ma, C. Chen, J. Yao, J. Zhao, 2006.** Photocatalytic degradation of organic pollutants catalyzed by layered iron (II) bipyridine complex-clay hybrid under visible irradiation. *Appl. Catal. B: Environ.*, 65(3-4)217-226.
- Chiron, S., A.F. Alba, A. Rodriguez, E. Garcia-Calvo, 2000.** Pesticide chemical oxidation: state of art. *Wat. Res.*, 34, 366-377.
- Cho, Y., W. Choi, 2001b.** Visible light-induced degradation of Carbon tetrachloride on Dye-sensitized TiO₂. *Environ. Sci. Technol.*, 35, 966-970.
- Cho, S., W. Choi, 2001a.** Solid-phase photocatalytic degradation of PVC-TiO₂ polymer composites. *J. Photochem. Photobiol. A: Chem.*, 143,221-228.
- Chun, H., W. Yizong, T. Hongxiao, 2001.** Preparation and characterization of surface bond-conjugated TiO₂/SiO₂ and photocatalysis for azo dyes. *J. Appl. Catal. B: Environ.*, 30, 277-285.
- Chun, H., W. Yizhong, 1999.** Decolorization and biodegradability of photocatalytic treated azo dyes and wool textile wastewater. *Chemosphere*, 39(12) 2107-2115.
- Comparelli, R., P.D. Cozzoli, M.L. Curri, A. Agostiano, G. Mascolo, G. Lovecchio, 2004.** Photocatalytic degradation of methyl-red by immobilized nanoparticles of TiO₂ and ZnO. *Wat. Sci. Technol.*, 49(4) 183-188.
- Crittendon, J.C., Y. Zhang, D.W. Hand, D.L. Perram, 1995.** Destruction of organic compounds in water using fixed bed photocatalysts. *Solar Engineering. Proceedings of the 1995 ASME International Solar Engineering Conference*, 449-457.
- Daneshvar, N., M. Rabbani, N. Modirshahla, M.A. Behnajady, 2005.** Photooxidative degradation of Acid Red 27 in a tubular continuous-flow photoreactor: influence of operational parameters and mineralization products. 18(1-3) 155-160.

- Davis, A., O. Hao, 1991.** Reactor dynamics in the evaluation of photocatalytic oxidation kinetics. *J. Catal.*, 131, 285-288.
- Davydov, L., E.P. Reddy, P. France, P.G. Smirniotis, 2001.** Sonophotocatalytic degradation of organic contaminants in aqueous systems on TiO₂ powders. *Appl. Catal. B: Environ.*, 32,95-105.
- Desilvestro, J., M. Gratzel, L. Kavan, J. Moser, J. Augustynski, 1986.** Highly efficient sensitization of titanium dioxide. *J. Am. Chem. Soc.*, 107, 2988-2995.
- Djebbar, K., A. Zertal, T. Sehili, 2006.** Photocatalytic Degradation of 2,4-Dichlorophenoxyacetic Acid and 4-Chloro-2-Methylphenoxyacetic Acid in Water by using TiO₂. *Environ. Technol.*, 27(11)1191-1197.
- Domenech, X., 1993(Ed.).** Photocatalytic purification and treatment of water and air, Elsevier, Amsterdam, 337.
- Dukkanci, M., G. Gunduz, 2006.** Ultrasonic degradation of oxalic acid in aqueous solutions. *Ultrason. Sonochem.*, 13 (6) 517-522.
- Dvoranova, D., V. Brezova, M. Mazur, M. A. Malati, 2002.** Investigations of metal-doped titanium dioxide photocatalysts. *Appl. Catal. B: Environ.*, 37, 91-105.
- Epling, G.A., C. Lin, 2002.** Photoassisted bleaching of dyes utilizing TiO₂ and visible light. *Chemosphere*, 46, 561–570.
- Esplugas, S., J. Gimenez, S. Contreras, E. Pascual, M. Rodriguez, 2002.** Comparison of different advanced oxidation processes for phenol degradation. *Wat. Res.*, 36, 1034-1042.
- Fernandez, J., J. Kiwi, J. Baeza, J. Freer, C. Lizama, H.D. Mansilla, 2004.** Orange II photocatalysis on immobilized TiO₂. Effect of the pH and H₂O₂. *Appl. Catal. B: Environ.*, 48(3) 205-211.
- Fox, M.A., M.T. Dulay, 1993.** Heterogeneous Photocatalysis. *Chem. Rev.*, 93, 341-57.
- Freudenhammer, H., D. Bahnemann, L. Bousselmi, S.U. Geissen, A. Ghrabi, F. Saleh, A. Si-Salah, U. Siemon, A. Vogelpohl, 1997.** Detoxification and recycling of wastewater by solar-catalytic treatment. *Water Sci. Technol.*, 35, 149-154.
- Fujihira, M., Y. Satoh, T. Osa, 1982.** Heterogenous photocatalytic reaction on semiconductor materials and effect of pH and Cu²⁺ ion on the photo Fenton type reaction. *Bull. Chem. Soc. Jpn.*, 55, 666-676.
- Fujishima, A., T.N. Rao, D.A. Tryk, 2000.** Titanium dioxide photocatalysis. *J. Photochem. Photobiol. C: Photochem. Rev.*, 1, 1-21.

- Fung, P. C., K. M. Sin, S.M. Tsui, 2000.** Decolorization and degradation kinetics of reactive dye wastewater by a UV/ultrasonic/peroxide system. *Coloration Technol.*, 116(5-6) 170-173.
- Galindo, C., P. Jacques, A. Kalt, 2002.** Photochemical and photocatalytic degradation of an indigoid dye: a case study of Acid Blue 74. *J. Photochem. Photobiol. A: Chem.*, 141, 47-56.
- Gemeay, A.H., R.E. Gehad, E. Ghrabawy, A.B. Zaki, 2007.** Kinetics of the oxidative decolorization of Reactive Blue-19 by acidic bromate in homogeneous and heterogeneous media. *Dyes and Pigments*, 73(1) 90-97.
- Gerischer, H., F. Willig, 1976.** Reaction of excited dye molecules at electrode. *Review Top. Curr. Chem.*, 61, 31-38.
- Giles, C.H., A.P. D'Silva, I.A. Easton, 1974.** A general treatment and classification of the solute adsorption isotherm part II. Experimental interpretation. *J. Coll. Interf. Sci.*, 47,766-771.
- Gogate, P.R., A.B. Pandit, 2005.** A review and assessment of hydrodynamic cavitation as a technology for the future. *Ultrason. Sonochem.*, 12 (1-2) 21-27.
- Gogate, P.R., A.B. Pandit, 2004a.** A review of imperative technologies for wastewater treatment I: oxidation technology in ambient conditions. *Advances in Environmental Research*, 8 (3-4) 501-551.
- Gogate, P.R., A.B. Pandit, 2004b.** A review of imperative technologies for wastewater treatment II: hybrid methods. *Advances in Environmental Research*, 8(3-4)553-597.
- Gogate, P.R., A.B. Pandit, 2004c.** Sonophotocatalytic reactors for wastewater treatment: A critical review. *AIChE*, 50 (5) 1051-1079.
- Gopalakrishnan, A.N., V. Mohan, 1997.** Solar photo sensitizer technology for dyeing waste reclamation. *Indian J. Environmental Protection*, 17, 268-271.
- Gopidas, K.R., M. Bohorquez, P.V. Kamat, 1990.** Photophysical and photochemical aspects of coupled semiconductors: charge-transfer processes in colloidal cadmium sulfide-titania and cadmium sulfide-silver (I) iodide systems. *J. Phys. Chem.*, 94, 6435-6440.
- Goswami, D.Y., 1997.** A review of engineering developments of aqueous phase solar photocatalytic detoxification and disinfection processes. *J. Sol. Energy Engg.*, 119, 101-107.

- Gouvea, C.A., K.F. Wypych, S.G. Moraes, N. Duran, N. Nagata and P.P. Zamora, 2000.** Semiconductor-assisted photocatalytic degradation of reactive dyes in aqueous solution. *Chemosphere*, 40, 443-440.
- Gratzel, M., R.F. Howe, 1990.** Electron paramagnetic resonance studies of doped titanium dioxide colloids. *J. Phys. Chem.*, 94, 2566-2572.
- Greenberg A.E., 1989** (17th Ed.). Standard methods for examination of water and wastewater, American Public Health Association.
- Gultekin, I., N.H. Ince, 2006.** Degradation of aryl-azo-naphthol dyes by ultrasound, ozone and their combination: Effect of \square -substituents, *Ultrason. Sonochem.*, 13 (3) 208-214.
- Guo, Z., Z. Zheng, S. Zheng, W. Hu, F. Ruo, 2005.** Effect of various sono-oxidation parameters on the removal of aqueous 2, 4-dinitrophenol. *Ultrason. Sonochem.*, 12 (6) 461-465.
- Gupta, A.K., A. Pal, C. Sahoo, 2006.** Photocatalytic degradation of a mixture of Crystal Violet (Basic Violet 3) and Methyl Red dye in aqueous suspensions using Ag^+ doped TiO_2 . *Dyes and Pigments*, 69 (3), 224-232.
- Harada, H., C. Hosoki, A. Kudo, 2001.** Overall water splitting by sonophotocatalytic reaction: the role of powdered photocatalyst and an attempt to decompose water using a visible-light sensitive photocatalyst. *J. Photochem. Photobiol. A: Chem.*, 141, 219-224.
- Hariharan, C., 2006.** Photocatalytic degradation of organic contaminants in water by ZnO nanoparticles. *Appl. Catal. A: General*, 304, 55-61.
- Hasnat, M.A., I.A. Siddiquey, A. Nuruddin, 2005.** Comparative photocatalytic studies of degradation of a cationic and an anionic dye. *Dyes and Pigments*, 66(3) 185-188.
- He, C., D. Shu, Y. Xiong, X. Zhu, X. Li, 2006.** Comparison of catalytic activity of two platinised TiO_2 films towards the oxidation of organic pollutants. *Chemosphere*, 63(2)183-191.
- Henglein, A., 1982.** Photochemistry of colloidal cadmium sulfide. 2. Effects of adsorbed methyl viologen and of colloidal platinum. *J. Phys. Chem.*, 86, 2291-2299.
- Herrera, F., A. Lopez, J. Kiwi, 2000.** Photochemically activated degradation of reactive dyes: statistical modeling of the reactor performance. *J. Photochem. Photobiol. A: Chem*, 135, 45-51.

- Herrmann, J.M., C. Guillard, J. Disdier, C. Lehaut, S. Malato, J. Blanco, 2002.** New industrial titania photocatalysts for the solar detoxification of water containing various pollutants. *Appl. Catal. B: Environ.*, 35, 281-294.
- Herrmann, J.M., 1999.** Heterogeneous photocatalysis: fundamentals and applications to the removal of various types of aqueous pollutants. *Catal. Today*, 53, 115-129.
- Herrmann, J.M., J. Disdier, P. Pichat, 1984.** Effect of chromium doping on the electrical and catalytic properties of powder titania under UV and visible illumination. *Chem. Phys. Lett.*, 108, 618-622.
- Heung, Y.H., M.A. Anderson, 1996.** Photocatalytic degradation of formic acid via metal-supported titania. *J. Environ. Engg.*, 122, 217-221.
- Hirano, K., H. Nitta, K. Sawada, 2005.** Effect of sonication on the photo-catalytic mineralization of some chlorinated organic compounds. *Ultrasonics Sonochemistry*, 12 (4) 271-276.
- Hoffmann, M.R., S.T. Martin, W. Choi, D.W. Bahnemann, 1995.** Environmental applications of semiconductor photocatalysis. *Chem. Rev.*, 95, 69-96.
- Hoffmann, A. J., E.R. Carraway, M.R. Hoffmann, 1994.** Photocatalytic production of H₂O₂ and organic peroxides on quantum-sized semiconductor colloids. *Environ. Sci. Technol.*, 28, 776-785.
- Houas, A., H. Lachheb, M. Ksibi, E. Elaloui, C. Guillard, J.M. Herrmann, 2001.** Photocatalytic degradation pathway of methylene blue in water. *Appl. Catal. B: Environ.*, 31, 145-157.
- Horvath, O., E. Bodnar, J. Hegyi, 2005.** Photoassisted oxidative degradation of surfactants and simultaneous reduction of metals in titanium dioxide dispersions. *Colloids and Surfaces A: Physicochemical and Engineering Aspects*, 265(1-3)135-140.
- Horvath, O., R. Huszank, 2003.** Degradation of surfactants by hydroxyl radicals photogenerated from hydroxoiron (III) complexes. *Photochem. Photobiol. Sci.*, 2, 960-966.
- Hu, C., Y. Lan, J. Qu, X. Hu, A. Wang, 2006.** Ag/AgBr/TiO₂ Visible light photocatalyst for destruction of Azo dyes and Bacteria. *J. Phys. Chem. B*, 110, 4066-4072.
- Hua, M.R. Hoffmann, 1997.** Optimization of ultrasonic irradiation as an advanced oxidation technology. *Environ. Sci. Technol.*, 31, 2237-2243.
- Iliev, V., 2002.** Phthalocyanine-modified titania-catalyst for photooxidation of phenols by irradiation with visible light. *J. Photochem. Photobiol. A: Chem.*, 151, 195-199.

- Ince, N.H., G. Tezcanli, R.K. Belen, I.G. Apikyan, 2001.** Ultrasound as a catalyser of aqueous reaction systems: The state of the art and environmental applications. *Appl. Catal. B: Environ.* 29, 167-176.
- Inel, Y., A. Okte, 1996.** Photocatalytic degradation of malonic acid in aqueous suspensions of TiO₂: an initial kinetic investigation of CO₂ photogeneration. *J. Photochem. Photobiol. A Chem.* 96, 175-180.
- Inoue, M., F. Okada, A. Sakurai, M. Sakakibara, 2006.** A new development of dyestuffs degradation system using ultrasound. *Ultrason. Sonochem.*, 13 (4) 313-320.
- Jackson, J.D., 1975.** *Classical Electrodynamics*; Wiley & Sons: New York, 424-429.
- Jang, Y.J., C. Simer, T. Ohm, 2006.** Comparison of zinc oxide nanoparticles and its nano-crystalline particles on the photocatalytic degradation of methylene blue. *Mater. Res. Bull.*, 41(1)67-77.
- Jiang, Y., C. Petrier, D. Waite, 2006.** Sonolysis of 4-chlorophenol in aqueous solution: Effects of substrate concentration, aqueous temperature and ultrasonic frequency. *Ultrason. Sonochem.*, 13 (5) 415-422.
- Kamat, P.V., 1993.** Photochemistry on non-reactive and reactive (semi-conductor) surfaces. *Chemical Rev.*, 93, 267–300.
- Kamat, P.V., M.A. Fox, 1983.** Photosensitization of TiO₂ colloids by erythrosin B in acetonitrile. *Chem. Phys. Lett.*, 102, 379-384.
- Kang, J.W., H.M. Hung, A. Lin, M.R. Hoffmann, 1999.** Sonolytic destruction of methyl tert-butyl ether by ultrasonic irradiation: The role of O₃, H₂O₂, frequency, and power density. *Environ. Sci. Technol.*, 33, 3199-3205.
- Kanmani, S., K. Thanasekaran, 2003.** Decolorization of industrial wastewaters of textile dyeing industry by photocatalysis. *Ind. J. Chem. Tech.*, 10, 53-59.
- Karakitsou, K.E., X.E. Verykios, 1993.** Effects of altrivalent cation doping of TiO₂ on its performance as a photocatalyst for water cleavage. *J. Phys. Chem.*, 97, 1184-1189.
- Karcher, S., A. Kornmuller, M. Jekel, 2002.** Anion exchange resins for removal of reactive dyes from textile wastewater. *Wat. Res.*, 36, 4717-4724.
- Karunakan, C., S. Senthivelon, 2005.** Solar Photocatalysis: Oxidation of aniline on CdS. *Sol. Energy*, 79(5) 505-512.
- Khalil, M.M.H., A.A. Abdel-Sha, M.S.A. Abdel-Mottaleb, 1999.** Photocatalytic degradation of some toxic analytical reagents with TiO₂. *International J. Photoenergy*, 1, 85-88.

- Kiriakidou, F., D.I. Kondarides, X.E. Verykios, 1999.** The effect of operational parameters and TiO₂ doping on the photocatalytic degradation of azo dyes. *Catal.Today*, 54, 119-130.
- Klausner, J.F., A.R. Martin, D.Y. Goswami, K.S. Schanze, 1994.** On the accurate determination of reaction rate constants in batch-type solar photocatalytic oxidation facilities. *J. Sol. Energ. Engg.*, 116, 19-24.
- Koh, I.O., X.C. Hamacher, K. Hicke, W. Thiemann, 2004.** Leachate treatment by the combination of photochemical oxidation with biological process. *J. Photochem. Photobiol. A: Chem.*, 162(2-3)261-271.
- Kohtani, S., K.A. Koshiko, K. Tokumura, Y. Ishigaki, A. Toriba, K. Haryakawa, R. Nakagaki, 2003.** Photodegradation of 4-alkylphenols using BiVO₄ photocatalyst under irradiation with visible light from a solar simulator. *Appl. Catal. B: Environ.*, 46, 573-586.
- Konstantinou, I.K., T.A. Albanis, 2003.** Photocatalytic transformation of pesticides in aqueous titanium dioxide suspension using artificial and solar light: intermediates and degradation pathways. *Appl. Catal. B: Environ.*, 42, 319-335.
- Kositzi, M., I. Poulios, S. Malato, J. Caceres, A. Campos, 2004.** Solar photocatalytic treatment of synthetic municipal wastewater. *Wat. Res.*, 38, 1147-1154.
- Kuo, W.S., P.H. Ho, 2006.** Solar photocatalytic decolorization of dyes in solution with TiO₂ film. *Dyes and Pigments*, 71(3) 212-217.
- Kusic, H., N. Koprivanac, A.L. Bozic, I. Selanec, 2006.** Photo-assisted Fenton type processes for the degradation of phenol: A kinetic study. *J. Haz. Mat.*, 137(1) 632-644.
- Lam, R.C.W., M.K.H. Leung, D.Y.C. Leung, L.L.P. Vrijmoed, W.C. Yam, S.P. Ng, 2007.** Visible-light assisted photocatalytic degradation of gaseous formaldehyde by parallel-plate reactor coated with Cr ion-implanted TiO₂ thin film. *Sol. Energ. Mater. Sol. Cells*, 91(1) 54-61.
- Lafi, W.K., Z. Al-Qodah, 2006.** Combined advanced oxidation and biological treatment processes for the removal of pesticides from aqueous solutions. *J. Haz. Mat.*, 137(1)489-497.
- Ledakowicz, S., M. Solecka, R. Zylla, 2001.** Biodegradation, decolorization and detoxification of textile wastewater enhanced by advanced oxidation processes. *J. Biotech.*, 89, 175-184.

- Lee, H.H.W., G. Chen, P.L. Yue, 2001.** Integration of chemical and biological treatments of textile industry wastewater: a possible zero-discharge system. *Wat. Sci. Technol.*, 44 (5)75-83.
- Legrini, O., E. Oliveros, A.M. Braun, 1993.** Photochemical processes for water treatment. *Chem. Rev.*, 93, 671-698.
- Lei, L., H.P. Chu, X. Hu, P.L. Yue, 1999.** Preparation of heterogeneous photocatalyst (TiO₂/alumina) by metallo-organic chemical vapour deposition. *Ind. Eng. Chem.*, 38.
- Linder, M., D.W. Bahnemann, B. Hirthe, W. D. Griebler, 1997.** Solar water detoxification: novel TiO₂ powders as highly active photocatalysts. *J. Sol. Energ. Engg.*, 119, 120-125.
- Linsebigler, A.L., G. Lu, J.T. Yates, 1995.** Photocatalysis on TiO₂ surfaces. *Chem. Rev.*, 95, 735- 758.
- Liu, R., H.M. Chiu, C.S. Shiau, R.Y.L. Yeh, Y.T. Hung, 2007.** Degradation and sludge production of textile dyes by Fenton and photo-Fenton processes. *Dyes and Pigments*, 73(1) 1-6.
- Liu, G., X. Li, J. Zhao, 2000.** Photo-oxidation pathway of Sulforhodamine-B dependence on the adsorption mode on TiO₂ exposed to visible light radiation. *Environ. Sci. Technol.*, 34, 3982-3990.
- Lizama, C., J. Freer, J. Baeza, H.D. Mansilla, 2002.** Optimized photodegradation of Reactive Blue 19 on TiO₂ and ZnO suspensions. *Catal. Today*, 76, 235-246.
- Lucas, M.S., J.A. Peres, 2006.** Decolorization of the azo dye Reactive Black 5 by Fenton and photo-Fenton oxidation. *Dyes and Pigments*, 71(3)236-244.
- Luo, Z., Q.H. Gao, 1992.** Decrease in the photoactivity of TiO₂ pigment on doping with transition metals. *J Photochem. Photobiol. A: Chem.*, 63,367-372.
- Lu, Y., N. Riyanto, N.K. Weavers, 2002.** Sonolysis of synthetic sediment particles: particle characteristics affecting particle dissolution and size reduction. *Ultrason. Sonochem.*, 9,181-188.
- Ma, C.W., W. Chu, 2001.** Photodegradation mechanism and rate improvement of chlorinated aromatic dye in non ionic surfactant solutions. *Wat. Res.*, 35 (2001) 2453-2459.
- Magrini, K.A., A.S. Watt, B. Rinehart, 1995.** Photocatalyst evaluation for solar-based aqueous organic oxidation. *Solar Engineering ASME*, 1, 415-420.

- Magrini, K.A., R.M. Goggin, A.S. Watt, A.M. Taylor, A.L. Baker, 1994.** Improving catalyst performance for solar-based photocatalytic oxidation of organics. Joint Solar Engg. Conference, ASME, 163-169.
- Mahamuni, N.N., A.B. Pandit, 2006.** Effect of additives on ultrasonic degradation of phenol. *Ultrason. Sonochem.*, 13 (2) 165-174.
- Malato, S., J. Blanco, A. Vidal, C. Richter, 2002.** Photocatalysis with solar energy at a pilot-plant scale: an overview. *Appl. Catal. B: Environ.*, 37, 1-15.
- Martin, S.T., H. Herrmann, W. Choi, M.R. Hoffmann, 1994a.** Time-resolved microwave conductivity (TRMC) 1. TiO₂ photoactivity and size quantization. *Trans. Faraday Soc.*, 90, 3315-3323.
- Martin, S.T., H. Herrmann, M.R. Hoffmann, 1994b.** Time-resolved microwave conductivity (TRMC) 2. TiO₂ photoactivity and size quantization. *Trans. Faraday Soc.*, 90, 3323-3330.
- Martin, S.T., C.L. Morrison, M.R. Hoffmann, 1994c.** Photochemical mechanism of size-quantized vanadium-doped TiO₂. *J. Phys. Chem.*, 98, 13695-13704.
- Martins, A. de O., V.M. Canalli, C.M.N. Azevedo, M. Pires, 2006.** Degradation of pararosaniline (C.I. Basic Red 9 monohydrochloride) dye by ozonation and sonolysis. *Dyes and Pigments*, 68(1-2) 227-234.
- Matthews, R.W., 1990.** Purification of water with near UV illuminated suspensions of titanium dioxide. *Water Resources*, 24, 653-660.
- Matthews, R.W., 1988.** Kinetics of photocatalytic oxidation of organic solutes over titanium dioxide. *J. Catal.*, 111,264-272.
- Matthews, R.W., 1987.** Photo-oxidation of organic impurities in water using thin films of titanium dioxide. *J. Phys. Chem.*, 91, 3328-3333.
- Mehrvar, M., W.A. Anderson, M. Moo-Young, 2000.** Photocatalytic degradation of aqueous tetrahydrofuran, 1, 4-dioxane, and their mixture with TiO₂. *Internat. J. Photoenergy*, 2, 141-146.
- Miller, L.W., M.I. Tejedor, M.A. Anderson, 1999.** Titanium dioxide coated waveguides for the photocatalytic oxidation of formic acid in water. *Environ. Sci. Technol.*, 33, 2070-2075.
- Mills, A., N. Elliott, I.P. Parkin, S. A. O'Neill, R.J. Clark, 2002a.** Novel TiO₂ CVD films for semiconductor photocatalysis. *J. Photochem. Photobiol. A: Chem.*, 151, 171-179.

- Mills, A., S.K. Lee, 2002b.** A web-based overview of semiconductor photochemistry based current commercial applications. *J. Photochem. Photobiol. A: Chem.*, 152, 233-247.
- Mills, A., J. Wang, 1998.** Photomineralisation of 4-chlorophenol sensitized by TiO₂ thin films. *J. Photochem. Photobiol. A: Chem.*, 118, 53-63.
- Mills, A., R.H. Davies, D. Worsley, 1993a.** Water purification by semiconductor photocatalysis. *Chem. Soc. Rev.*, 417- 425.
- Mills, A., S. Morris, 1993b.** Photomineralization of 4-chlorophenol sensitized by titanium dioxide: a study of the initial kinetics of carbon dioxide photogeneration. *J. Photochem. Photobiol. A: Chem.*, 71, 75-83.
- Minero, C., 1999.** Kinetic analysis of photoinduced reactions at the water semiconductor interface. *Catal. Today*, 54, 205-216.
- Minero, C., 1995.** A rigorous kinetic approach to model primary oxidative steps of photocatalytic degradations. *Sol. Energ. Mat. Sol.Cells*, 38, 421-430.
- Modirshahla, N., M.A. Behnajady, F. Ghanbary, 2007.** Decolourization and mineralization of C.I. Acid Yellow 23 by Fenton and photo-Fenton processes. *Dyes and Pigments*, 73(3)305-310.
- Modirshahla, N., M.A. Behnajady, 2006.** Photooxidative degradation of Malachite Green (MG) by UV/H₂O₂: Influence of operational parameters and kinetic modeling. *Dyes and Pigments*, 70(1)54-59.
- Mohamed, O.S., 2002.** Photocatalytic oxidation of selected fluorenols on TiO₂ semiconductor. *J. Photochem. Photobiol. A: Chem.*, 152, 229-232.
- Moon, J., C.Y. Yun, K.W. Chung, M.S. Kang, J. Yi, 2003.** Photocatalytic activation of TiO₂ under visible light using Acid Red 44. *Catal. Today*, 87, 77-86.
- Morsi, T.M., W.R. Budakowski, A.S. Aziz, K.J. Friesen, 2000.** Photocatalytic degradation of 1, 10-dichlorodecane in aqueous suspensions of titanium dioxide: a reaction of adsorbed chlorinated alkane with surface hydroxyl radicals. *Environ. Sci. Technol.*, 34, 1018-1022.
- Mrowetz, M., E. Selli, 2004.** Effects of iron species in the photocatalytic degradation of an azo dye in TiO₂ aqueous suspensions. *J. Photochem. Photobiol. A: Chem.*, 162, 89-95.
- Mrowetz, M., C. Pirola, E. Selli, 2003.** Degradation of organic water pollutants through sonophotocatalysis in the presence of TiO₂. *Ultrason. Sonochem.*, 10, 247-254.

- Mu, W., J.M. Herrmann, P. Pichat, 1989.** Room temperature photocatalytic oxidation of liquid cyclohexane into cyclohexanone over neat and modified TiO₂. *Catal. Lett.*, 3, 73-78.
- Muneer, M., D. Bahnemann, 2002.** Semiconductor-mediated photocatalyzed degradation of two selected pesticide derivatives, terbacil and 2, 4, 5-tribromoimidazole, in aqueous suspension. *Appl. Catal. B: Environ.*, 36, 95-111.
- Muneer, M., J. Theurich, D. Bahnemann, 2001.** Titanium dioxide mediated photocatalytic degradation of 1, 2-diethyl phthalate. *J. Photochem. Photobiol. A: Chem.*, 143, 213-219.
- Muneer, M., R. Philip, S. Das, 1997.** Photocatalytic degradation of waste water pollutants. titanium dioxide-mediated oxidation of a textile dye, Acid Blue 40. *Res. Chem. Intermed.*, 23, 233-246.
- Muruganandham, M., M. Swaminathan, 2006.** Photocatalytic decolorization and degradation of Reactive Orange 4 by TiO₂-UV process. *Dyes and Pigments*, 68(2-3) 133-142.
- Muruganandham, M., M. Swaminathan, 2004a.** Decolorization of Reactive Orange 4 by Fenton and photo-Fenton oxidation technology. *Dyes and Pigments*, 63(3)315-321.
- Muruganandham, M. and Swaminathan M., 2004b.** Solar photocatalytic degradation of a reactive azo dye in TiO₂-suspension. *Sol. Energ. Mat. Sol. Cells*, 81, 439-457.
- Muszkat, L., D. Raucher, M. Magaritz, D. Ronen, 1994.** in : U. Zoller (Ed.), *Groundwater Contamination and Control*, Marcel Dekker, New York, 257–271.
- Naffrechoux, E., S. Chanoux, C. Petrier, J. Suptil, 2000.** Sonochemical and photochemical oxidation of organic matter. *Ultrasonics Sonochemistry*, 7, 255-259.
- Nagaveni, K., G. Sivalingam, M.S. Hegde, G. Madras, 2004.** Solar photocatalytic degradation of dyes: high activity of combustion synthesized nano TiO₂. *Appl. Catal. B: Environ.*, 48, 83-93.
- Nasr, C., K. Vinodgopal, L. Fisher, S. Hotchandani, A.K. Chattopadhyay, P.V. Kamat, 1996.** Environmental photochemistry on semiconductor surfaces. Visible light induced degradation of a textile diazo dye, naphthol blue black, on titanium dioxide nanoparticles. *J. Phys. Chem.*, 100, 8436-8442.
- Neppolian, B., H.C. Choi, S. Sakthivel, B. Arabindoo, V. Murugesan, 2002a.** Solar light induced and TiO₂ assisted degradation of textile dye Reactive Blue 4. *Chemosphere*, 46, 1173-1181.

- Neppolian, B., H.C. Choi, S. Sakthivel, B. Arabindoo, V. Murugesan, 2002b.** Solar/UV-induced Photocatalytic degradation of three commercial textile dyes. *J. Haz. Mat.*, 89 (2-3) 303-317.
- Neppolian, B., M. V. Shankar, V. Murugesan, 2002c.** Semiconductor assisted photodegradation of textile dye. *J. Scientific and Industrial Research*, 61, 224-230.
- Neppolian, B., S. Sakthivel, B. Arabindoo, M. Palanichamy, V. Murugensan, 1998.** Degradation of textile dye by solar light using TiO₂ and ZnO photocatalysts. *J. Environ. Sci. Health: Part A*, 34(9)1829-1838.
- Neyens, E., J. Baeyens, 2003.** A review of classic Fenton's peroxidation as an advanced oxidation technique. *J. Haz. Mat.*, 98(1-3)33-50.
- Nishimoto, S., B. Ohtani, H. Kajiwara, T. Kagiya, 1985.** Correlation of the crystal structure of titanium dioxide prepared from titanium tetra-2-propoxide with the photocatalytic activity for redox reactions in aqueous propan-2-ol and silver salt solutions. *J. Chem. Soc., Faraday Trans. 1*, 81, 61-68.
- Nishio, J., M. Tokumura, H.T. Znad, Y. Kawase, 2006.** Photocatalytic decolorization of azo-dye with zinc oxide powder in an external UV light irradiation slurry photoreactor. *J. Haz. Mat.*, 138(1) 106-115.
- Noorjahan, M., M.P. Reddy, V.D. Kumari, B. Lavedrine, P. Boule, M. Subrahmanyam, 2003.** Photocatalytic degradation of H-acid over a novel TiO₂ thin film fixed bed reactor and in aqueous suspensions, *J. Photochem. Photobiol. A: Chem.*, 156,179-187.
- Oberg, V., D.Y. Goswami, G. Svedberg, 1993.** On photocatalytic detoxification of water containing volatile organic compounds. *Joint Solar Engg. Conference, ASME*, 147-153.
- Ohtani, B., S. Nishimoto, 1993.** Effect of surface adsorptions of aliphatic alcohols and silver ion on the photocatalytic activity of titania suspended in aqueous solutions. *J. Phys. Chem.*, 97,920-926.
- Okitsu K., K. Iwasaki, Yobiko Y., Bandow H., Nishimura R., Y. Maeda, 2005.** Sonochemical degradation of azo dyes in aqueous solution: a new heterogenous kinetics model taking into account the local concentration of OH radicals and azo dyes. *Ultrason. Sonochem.*, 12 (4) 255-262.
- Ollis, D.F, H. Al-Ekabi, 1993.** Photocatalytic purification and treatment of water and air. Vol. 3, Elsevier, Amsterdam.

- Ollis, D.F., E. Pelizzetti, N. Serpone, 1991.** Destruction of water contaminants. *Environ. Sci. Technol.*, 25, 1523-1529.
- Ollis, D.F., E. Pelizzetti, N. Serpone, 1989.** Heterogeneous Photocatalysis in the Environment: Application to Water Purification. *Photocatalysis: Fundamentals and Applications*, Wiley, NY.
- Ooka, C., H. Yoshida, M. Horio, K. Suzuki, T. Hattori, 2003.** Adsorptive and photocatalytic performance of TiO₂ pillared montmorillonite in degradation of endocrine disruptors having different hydrophobicity. *Appl. Catal. B: Environ.*, 41, 313-321.
- Oyama, T., A. Aoshima, S. Horikoshi, S. Hidaka, J. Zhao, N. Serpone, 2004.** Solar photocatalysis, photodegradation of a commercial detergent in aqueous TiO₂ dispersions under sunlight irradiation. *Sol. Energ.*, 77(5)525-532.
- Pandiyam, T., O.M. Rivas, J. O. Martinez, G. B. Amezcua, M.A. Martinez-Carrillo, 2002.** Comparison of methods for the photochemical degradation of chlorophenols. *J. Photochem. Photobiol. A: Chem.*, 146, 149-155.
- Pandurangan, A., P. Kamala, S. Uma, M. Palanichamy, V. Murugesan, 2001.** Degradation of basic yellow auramine O-A textile dye by semiconductor photocatalysis. *Ind. J. Chem. Technol.*, 8(6)496-499.
- Park, H., W. Choi, 2005.** Photocatalytic Reactivities of Nafion-Coated TiO₂ for the Degradation of Charged Organic Compounds under UV or Visible Light. *J. Phy. Chem. B*, 109(23)11667-11674.
- Parra, S., V. Sarria, S. Malato, P. Peringer, C. Pulgarin, 2000.** Photochemical versus coupled photochemical-biological flow system for the treatment of two biorecalcitrant herbicides: metobromuron and isoproturon. *Appl. Catal. B: Environ.*, 27, 153-168.
- Patrick, B., P.V. Kamat, 1992.** Photophysics and photochemistry of quantized ZnO colloids. *J. Phys. Chem.*, 96, 1423-1428.
- Peral, J., J. Munoz, X. Domenech, 1990.** Photosensitized CN⁻ oxidation over TiO₂. *J. Photochem. Photobiol. A: Chem.*, 55, 251-257.
- Peterson, M.W., J.A. Turner, A.J. Nozik, 1991.** Mechanistic studies of the photocatalytic behaviours of TiO₂ particles in a photochemical slurry cell and the relevance of photodetoxification reactions. *J. Phy. Chem.*, 95, 665.
- Poulios, I., I. Tsachpinis, 1999.** Photodegradation of the textile dye reactive black 5 in the presence of semiconducting oxides. *J. Chem. Technol. Biotechnol.*, 74, 349-357.

- Prevot, A.B., C. Baiocchi, M.C. Brussino, E. Pramauro, P. Savarino, V. Augugliaro, G. Marci, L. Palmisano, 2001.** Photocatalytic Degradation of Acid Blue 80 in Aqueous Solutions Containing TiO₂ Suspensions. *Environ. Sci. Technol.*, 35, 971-976.
- Pulgarin, C., M. Invernizzi, S. Parra, V. Sarria, R. Polania, P. Peringer, 1999.** Strategy for the coupling of photochemical and biological flow reactors useful in mineralization of biorecalcitrant industrial pollutants. *Catal. Today*, 53, 341-352.
- Puma, G.L., P.L. Yue, 1999.** Photocatalytic oxidation of chlorophenols in single-component and multi-component systems. *Ind. Eng. Chem. Res.*, 38, 3238-3245.
- Qamar, M., M. Saquib, M. Muneer, 2005.** Photocatalytic degradation of two selected dye derivatives, chromotrope 2B and Amido Black 10B, in aqueous suspensions of titanium dioxide. *Dyes and Pigments*, 65, 1-9.
- Qaradawi, S.A., S.R. Salman, 2002.** Photocatalytic degradation of methyl orange as a model compound. *J. Photochem. Photobiol. A: Chem.*, 148, 161-168.
- Rachel, A., M. Sarakha, M. Subrahmanyam, P. Boule, 2002.** Comparison of several titanium dioxides for the photocatalytic degradation of benzenesulfonic acids. *Appl. Catal. B: Environ.*, 37, 293-300.
- Rao, N.N., G. Bose, P. Khare, S.N. Kaul, 2006.** Fenton and Electro-Fenton Methods for Oxidation of H-Acid and Reactive Black 5. *J. Environ. Engg.*, 132 (3) 367-376.
- Rao, K.V.S., B. Lavedrine, P. Boule, 2003a.** Influence of metallic species on TiO₂ for the photocatalytic degradation of dyes and dye intermediates. *J. Photochem. Photobiol. A: Chem.*, 154, 189-193.
- Rao, K.V.S., A. Rachel, M. Subramanyam, P. Boule, 2003b.** Immobilization of TiO₂ on pumice stone for the photocatalytic degradation of dyes and dye industry pollutants. *Appl. Catal. B: Environ.*, 46(1) 77-85.
- Rao, M.V., K. Rajeshwar, V.R. Vernerker, J. Dubow, 1980.** Photosynthetic of H₂ and H₂O₂ on semiconducting oxide grain in aqueous solutions. *J. Phys.*, 84, 1987.
- Rathi, A., H.K. Rajor, R.K. Sharma, 2003.** Photodegradation of Direct Yellow 12 using UV/H₂O₂/Fe²⁺. *J. Haz. Mat. B*, 102, 231-241.
- Ray, A.K., A.C.M. Beenackers, 1997.** Novel swirl-flow reactor for kinetics studies of semiconductor photocatalysis. *AIChE Journal*, 43, 2571-2578.
- Reddy, M.P. et al., 2003.** *Indian Journal of Environmental Protection*, 23 (4), 438-445.

- Regina, P.M.M., P.S. Ticiane, C. Leonardo, H. Eduardo, R. Krishnan, 2005.** Mass transfer and photocatalytic degradation of leather dye using TiO₂/UV. *J. Appl. Electrochem.*, 35(7-8)821-829.
- Revtergardh, L.B., M. Iangphasuk, 1997.** Photocatalytic decolourization of reactive azo dye: A comparison between TiO₂ and CdS photocatalysis. *Chemosphere*, 35(3)585-596.
- Rideh, L., D.R. Wehrer, A. Zoulalian, 1997.** Photocatalytic degradation of 2-chlorophenol in TiO₂ Aqueous suspension: Modelling of reaction rate. *Ind. Eng. Chem. Res.*, 36, 4712-4718.
- Robert, D., S. Malato, 2002.** Solar photocatalysis: a clean process for water detoxification. *The Science of the Total Environment*, 291, 85-97.
- Robert, D., A. Piscopo, O. Heintz, J.V. Weber, 1999.** Photocatalytic detoxification with TiO₂ supported on glass fibre by using artificial and natural light. *Catal. Today*, 54, 291-296.
- Roselin, L.S., G.R. Rajarajeswari, R. Selvin, V. Sadasivan, B. Sivasankar, K. Rengaraj, 2002.** Sunlight/ZnO-mediated photocatalytic degradation of Reactive Red 22 using thin film flat bed flow photoreactor. *Sol. Energy*, 73(4), 281-285.
- Ross, H., J. Bendig, S. Hecht, 1994.** Sensitized photocatalytical oxidation of terbutylzoline. *Sol. Energ. Mat. Sol. Cells*, 33, 475-481.
- Saha, A.K., C. Malay, 2003.** Solar photocatalytic degradation of metal complex azo dyes and treatment of dye house waste. *Ind. J. Engg. Mater. Sci.*, 10(1), 69-74.
- Sahoo, C., A.K. Gupta, A. Pal, 2005.** Photocatalytic degradation of Crystal Violet (C.I. Basic Violet 3) on silver ion doped TiO₂. *Dyes and Pigments*, 66(3) 189-196.
- Sakthivel, S., M.V. Shankar, M. Palanichamy, B. Arabindoo, V. Murugesan, 2002.** Photocatalytic decomposition of leather dye comparative study of TiO₂ supported on alumina and glass beads. *J. Photochem. Photobiol. A: Chem.*, 148, 153-159.
- Sakthivel, S., B. Neppolian, M. Palanichamy, B. Arabindoo, V. Murugesan, 2001.** Photocatalytic degradation of leather dye over ZnO catalyst supported on alumina and glass surfaces. *Wat. Sci. Technol.*, 44(5) 211-218.
- San, N., A. Hatipolu, G. Kocturk, Z. Cinar, 2002.** Photocatalytic degradation of 4-nitrophenol in aqueous TiO₂ suspensions: theoretical prediction of the intermediates. *J. Photochem. Photobiol. A: Chem.*, 146, 189-197.

- Saquib, M., M. Muneer, 2003a.** TiO₂-mediated photocatalytic degradation of a triphenylmethane dye (gentian violet), in aqueous suspensions. *Dyes and Pigments*, 56, 37-49.
- Saquib, M., M. Muneer, 2003b.** Titanium dioxide mediated photocatalyzed degradation of a textile dye derivative, Acid Orange 8, in aqueous suspensions. *Desalination*, 155, 255-263.
- Saquib, M., M. Muneer, 2002.** Semiconductor mediated photocatalyzed degradation of an anthraquinone dye, Remazol Brilliant Blue R under sunlight and artificial light source. *Dyes and Pigments*, 53, 237-249.
- Saquib, M., T.M. Abu, M.M. Haque, M. Muneer, 2007.** Photocatalytic degradation of disperse blue 1 using UV/TiO₂/H₂O₂ process. *J. Environ. Manag.*, [In press, Available online 8 May 2007]
- Saria, V., S. Parra, N. Adler, P. Peringer, N. Benitez, C. Pulgarin, 2002.** Recent developments in the coupling of photoassisted and aerobic biological processes for the treatment of biorecalcitrant compounds. *Catalysis Today*, 76, 301-315.
- Sato, C., J. Yao, 2006.** Simultaneous and Sequential Photosonolysis of TCE and PCE, *J. Environ. Engg.*, 132 (1) 32-41.
- Sattler, C., L.D. Oliveira, M. Tzchirner, A.E.H. Machado, 2004.** Solar photocatalytic water detoxification of paper mill effluents. *Energy*, 29, 835-843.
- Sauer, T., G.C. Neto, H.J. Jose, R.F.P.M. Moreira, 2002.** Kinetics of photocatalytic degradation of reactive dyes in a TiO₂ slurry reactor. *J. Photochem. Photobiol. A: Chem.*, 149, 147-154.
- Schramm, J.D., I. Hua, 2001.** Ultrasonic irradiation of Dichlorvos decomposition mechanism. *Wat. Res.*, 35(3) 665-674.
- Schrank, S.G., H.J. José, R.F.P.M. Moreira, 2002.** Simultaneous photo-catalytic Cr (VI) reduction and dye oxidation in a TiO₂ slurry reactor. *J. Photochem. Photobiol. A: Chem.*, 147, 71-76.
- Scott, J.P., D.F. Ollis, 2006.** Integration of Chemical and Biological oxidation processes for water treatment: Review and recommendations. *Environ. Prog.*, 14(2)88-103.
- Selli, E., C.L. Bianchi, C. Pirola, M. Bertelli, 2005.** Degradation of methyl tert-butyl ether in water: effects of the combined use of sonolysis and photocatalysis. *Ultrason. Sonochem.*, 12 (5) 395-400.

- Selli, E., 2002.** Synergistic effects of sonolysis combined with photocatalysis in the degradation of an azo dye. *Phy. Chem. Chem. Phys.*, 4 (24) 6123-6128.
- Shankar, M.V., S.A.N. Venkatachalam, B. Arabindoo, V. Murugesan, 2004.** Novel thin-film reactor for photocatalytic degradation of pesticides in an aqueous solution. *J. Chem. Technol. Biotechnol.*, 79(11)1279-1285.
- Shchukin, D.G., D.V. Sviridov, A.I. Kulak, 1999.** Magneto rheological photocatalytic systems. *Internat. J. Photoenergy*, 1, 65-67.
- Shemer, H., N. Narkis, 2005.** Sonochemical removal of trihalomethanes from aqueous solutions. *Ultrason. Sonochem.*, 12 (6) 495-499.
- Shen, Y.S., D.K. Wang, 2002.** Development of photoreactor design equation for the treatment of dye wastewater by UV/H₂O₂ process. *J. Haz. Mat., B* 89, 267-277.
- Shirgaonkar, I.Z., A.B. Pandit, 1998.** Sonophotochemical destruction of aqueous solution of 2, 4, 6- trichoro phenol. *Ultrason. Sonochem.*, 5,53-61.
- Shu, H.Y., 2006.** Degradation of dyehouse effluent containing C.I. Direct Blue 199 by processes of ozonation, UV/H₂O₂ and in sequence of ozonation with UV/H₂O₂. *J. Haz. Mat.*, 33(1-3)92-98.
- Shu, H.Y., M.C. Chang, 2005.** Decolorization effects of six azo dyes by O₃, UV/O₃ and UV/H₂O₂ processes. *Dyes and Pigments*, 65(1)1-9.
- Singh, V., V. Sapehiya, G.L. Kad, 2003.** Ultrasonically activated oxidation of hydroquinones to quinines catalyzed by ceric ammonium nitrate doped on metal exchanged K-10 clay. *Synthesis*, 198-200.
- Sirisuk, A., C.G. Hill Jr., M.A. Anderson, 1999.** Photocatalytic degradation of ethylene over thin films of titania supported on glass rings. *Catal. Today*, 54, 159-164.
- Sivekumar, T., K. Shanthi, 2001.** Photocatalytic studies on some textile reactive dyes using TiO₂. *Indian J. Environ. Prot.*, 21(2), 101-104.
- Soana, F., M. Sturini, L. Cermenati, A. Albini, 2000.** Titanium dioxide photocatalyzed oxygenation of naphthalene and some of its derivatives. *J. Chem. Soc., Perkin Trans.*, 2, 699 – 704.
- Solmaz, S.K.A., A. Birgul, G.E. Ustun, T. Yonar, 2006.** Colour and COD removal from textile effluent by coagulation and advanced oxidation processes. *Coloration Technology*, 122(2), 102-109.
- Spiewak, I., R. Benmair, R. Messalem, O. Radchenko, 1998.** Water detoxification and disinfection using high solar concentration and homogeneous photocatalysts. *Proceedings of the Indian Academy of Sciences: Chemical Sciences*, 110, 229-238.

- Styliidi, M., I.K. Dimitris, X.E. Verykios, 2003.** Pathways of solar light-induced photocatalytic degradation of azo dyes in aqueous TiO₂ suspensions. *Appl. Catal. B: Environ.*, 40, 271-286.
- Subrahmanyam, M., K.V.S. Rao, M.R. Babu, B. Srinivas, 1998.** Photocatalytic degradation of textile dyes using TiO₂ based catalysts. *Ind. J. Environ. Protect.*, 18, 266-272.
- Sun, Z., Y. Chen, Q. Ke, Y. Yang, J. Yuan, 2002.** Photocatalytic degradation of cationic azo dye by TiO₂/bentonite nanocomposite. *J. Photochem. Photobiol. A: Chem.*, 149, 169-174.
- Suslick, K.S., 1999.** Application of ultrasound to materials chemistry. *Annu. Rev. Mater. Sci.*, 29, 295-326.
- Swaminathan, K., S. Sandhya, S.A. Carmalin, K. Pachhade, Y.V. Subrahmanyam, 2003.** Decolorization and degradation of H-acid and other dyes using ferrous-hydrogen peroxide system. *Chemosphere*, 50(5)619-625.
- Tada, H., M. Yamamoto, S. Ito, 2000.** MgO_x submonolayer formation on TiO₂ and its effect on the photocatalytic oxidation of sodium dodecylbenzenesulfonate. *J. Electrochemical Soc*, 147, 613-616.
- Tanaka, K., T. Hisanaga, K. Harada, 1989.** Photocatalytic degradation of organohalide compounds in semiconductor suspension with added hydrogen peroxide. *New J. Chem.*, 13, 5.
- Tezcanli-Guyer, G., N.H. Ince, 2004.** Individual and combined effects of ultrasound, ozone and UV irradiation: a case study with textile dyes. *Ultrasonics*, 42 (1-9) 603-609.
- Theron, P., P. Pichat, C. Guillard, C. Petrier, T. Chopin, 1999.** Degradation of phenyltrifluoromethylketone in water by separate or simultaneous use of TiO₂ photocatalysis and 30 or 515 KHz ultrasound. *Phys. Chem. Chem. Phys.*, 1(19)4663-4668.
- Toor, A.P., A. Verma, C.K. Jotshi, P.K. Bajpai, V. Singh, 2006.** Photocatalytic degradation of Direct Yellow 12 dye using UV/TiO₂ in a shallow pond slurry reactor. *Dyes and Pigments*, 68, 53-60.
- Turchi, C.S., D.F. Ollis, 1989.** Mixed reactant photocatalysis: intermediates and mutual rate inhibition. *J. Catal.*, 119, 483-496.
- Vajnhandl, S., A.M.L. Marechal, 2005.** Ultrasound in textile dyeing and the decolouration/mineralization of textile dyes. *Dyes and Pigments*, 65 (2) 89-101.

- Venkatadri, R., R.W. Peters, 1993.** Chemical oxidation technologies: ultraviolet light/hydrogen peroxide, fenton's reagent and titanium dioxide assisted photocatalysis. *Haz. waste and Haz. Mater.*, 10, 107-149.
- Vinodgopal, K., P.V. Kamat, 1995.** Electrochemically assisted photocatalysis using nanocrystalline semiconductor thin films. *Solar Energy Materials and Solar Cells*, 38 (1-4), 401-410.
- Vlachopoulos, N., P. Liska, J. Augustynski, M. Gratzel, 1988.** Very efficient visible light energy harvesting and conversion by spectral sensitization of high surface area polycrystalline titanium dioxide films. *J. Am. Chem. Soc.*, 110, 1216-1218.
- Vogelpohl, A., S.M. Kim, 2004.** Advanced oxidation processes (AOP's) in wastewater treatment. *J. of Indust. Engg. Chem.*, 10(1)33-40.
- Vrachnou, E., N. Vlachopoulos, M. Gratzel, 1987.** Efficient visible light sensitization of TiO₂ by surface complexation with ferrocyanide. *J. Chem. Soc., Chem. Commun.*, 12, 868-870.
- Wang, S., Z.H. Zhu, 2005a.** Sonochemical treatment of fly ash for dye removal from wastewater. *J. of Haz. Mat.*, 26(1-3) 91-95.
- Wang, J., B. Guo, X. Zhang, Z. Zhang, J. Han, J. Wu, 2005b.** Sonocatalytic degradation of methyl orange in the presence of TiO₂ catalysts and catalytic activity comparison of rutile and anatase. *Ultrason. Sonochem.*, 12 (5) 331-337.
- Wang, G.S., S.T. Hsieh, C.S. Hong, 2000.** Destruction of humic acid in water by UV light-catalysed oxidation with hydrogen peroxide. *Wat. Res.*, 34, 3882-3887.
- Warman, J.M., M.P.D. Hass, P. Pichat, N. Serpone, 1991.** Effect of isopropyl alcohol on the surface localization and recombination of conduction-band electrons in degussa P25 titania: a pulse-radiolysis time-resolved microwave conductivity study. *J. Phys. Chem.*, 95, 8858-8861.
- Wu, C.H., H.W. Chang, J.M. Chem, 2006.** Basic dye decomposition kinetics in a photocatalytic slurry reactor. *J. Haz. Mat.*, 137(1)336-343.
- Wu, C., X. Liu, D. Wei, J. Fan, L. Wang, 2001.** Photosonochemical degradation of phenol in water. *Wat. Res.*, 35(16) 3927-3933.
- Wu, S., 1999a.** Principles of advanced chemical oxidation processes and their application in wastewater treatment of pulp and paper industry. *Chung-kuo Tsao Chih/China Pulp and Paper*, 18, 43-49.

- Wu, T., T. Lin, J. Zhao, H. Hidaka, N. Serpone, 1999b.** TiO₂-Assisted photodegradation of dyes. 9. Photooxidation of a Squarylium Cyanine dye in aqueous dispersions under visible light irradiation. *Environ. Sci. Technol.*, 33, 1379-1387.
- Xiaodan, Y., W. Qingyin, J. Shicheng, G. Yihang, 2006.** Nanoscale ZnS/TiO₂ composites: Preparation, characterization, and visible-light photocatalytic activity. *57(4-5)*333-341.
- Xu, M.W., Bao S.J. and Zhang X.G., 2005.** Enhanced photocatalytic activity of magnetic TiO₂ photocatalyst by silver deposition. *Materials Letters*, 59(17)2194-2198.
- Xu, Y., C.H. Langford, 2000.** Variation of Langmuir adsorption constant determined for TiO₂ photocatalyzed degradation of acetophenone under different light intensity. *J. Photchem. Photobiol. A: Chem.*, 133, 67-71.
- Xu, Y., Langford C.H., 1997.** Photoactivity of Titanium Dioxide Supported on MCM41, Zeolite X, and Zeolite Y. *J. Phys. Chem. B.*, 101, 3115-3121.
- Yang, T.C.K., S.F. Wang, S.H.Y. Tsai, S.Y. Lin, 2001.** Intrinsic photo-catalytic oxidation of the dye adsorbed on TiO₂ photocatalysts by diffuse reflectance infrared fourier transform spectroscopy. *Appl. Catal. B*, 30, 293-301.
- Yang, J., D. Li, Z. Zhang, Q. Li, H. Wang, 2000.** A study of the photocatalytic oxidation of formaldehyde on Pt/Fe₂O₃/TiO₂. *J. Photochem. Photobiol. A: Chem.*, 137, 197-202.
- Yano, J., J. Matsuura, H. Ohura, S. Yamasaki, 2005.** Complete mineralization of propyzamide in aqueous solution containing TiO₂ particles and H₂O₂ by the simultaneous irradiation of light and ultrasonic waves. *Ultrason. Sonochem.*, 12 (3) 197-203.
- Yoshida, M.M., V.C. Martinez, P.A. Madrid, A.A. Elguezabal, 2002.** Thin films of photocatalytic TiO₂ and ZnO deposited inside tubing by spray pyrolysis. *Thin Solid Films*, 419, 60-64.
- Zamostny, P., Z. Belohlav, 2002.** Identification of kinetic models of heterogenously catalysed reactions. *Appl. Catal. A: General*, 225, 291-299.
- Zeng, L., W.M. James, 2006.** Degradation of pentachlorophenol in aqueous solution by audible-frequency sonolytic ozonation. *J. Haz. Mat.*, 35(1-3) 218-225.
- Zhang, H., Duan L., D. Zhang, 2006.** Decolorization of methyl orange by ozonation in combination with ultrasonic irradiation. *J. of Haz. Mat.*, 138 (2) 53-59.

Zhang, M., T. An, X. Hu, C. Wang, G. Sheng, J. Fu, 2004. Preparation and photocatalytic properties of a nanometer ZnO-SnO₂ coupled oxide. *Appl. Catal. A: General*, 260(2)215-222.

Zhao, J., T. Wu, R. Wu, K. Oikawa, H. Hidaka, N. Serpone, 1998. Photoassisted degradation of dye pollutants. 3. Degradation of the cationic dye rhodamine 8 in aqueous anionic surfactant/TiO₂ dispersions under visible light irradiation: Evidence for the need of substrate adsorption on TiO₂ particles. *Environ. Sci. Technol.*, 32, 2394-2400.

Zhou, M., J. Yu, B. Cheng, 2006. Effects of Fe-doping on the photocatalytic activity of mesoporous TiO₂ powders prepared by an ultrasonic method. *J. Haz. Mat.*, 137(3)1838-1847.

Zheng, H., Y. Pan, X. Xiang, 2007. Oxidation of acidic dye Eosin Y by the solar photo-Fenton processes. *J. Haz. Mat.*, 141(3)457-464.

Zielinska, B., J. Grzechulska, A.W. Morawski, 2003. Photocatalytic decomposition of textile dyes on TiO₂-Tytanpol A11 and TiO₂-Degussa P25. *J. Photochem. Photobiol. A: Chem.*, 157, 65-70.

Zorn, M.E., D.T. Tompkins, W.A. Zeltner, M.A. Anderson, 2000. Catalytic and photocatalytic oxidation of ethylene on titania-based thin films. *Environ. Sci. Technol.*, 34, 5206-5210.

LIST OF PUBLICATIONS

PUBLICATIONS

1. **Kaur S., Singh V., 2007.** TiO₂ mediated Photocatalytic degradation studies of Reactive Red 198 by UV irradiation, J. of Haz. Mat., 141, 230-236.
2. **Kaur S., and Singh V., 2007.** Visible light induced sonophotocatalytic degradation of Reactive Red dye 198 using dye sensitized TiO₂, Ultrason. Sonochem., 14(5)531-537.

CONFERENCES

1. **Sumandeep Kaur,** Vasundhara Singh, *Sonophotocatalytic degradation of Reactive Red dye*, A poster presented at the 6th CRSI Symposium held at IIT Kanpur, 6-8 Feb 2004.
2. **Sumandeep Kaur,** Vasundhara Singh, *Ultrasound induced degradation of organic pollutants on the Dye-sensitized TiO₂ under visible light*, A poster presented at the 7th CRSI Symposium held at Kolkata, 4-6 Feb 2005.
3. **Sumandeep Kaur,** Vineet Kumar, Vasundhara Singh, *Photocatalytic degradation of J-acid of Dye sensitized TiO₂ under visible light*, A poster presented at the 8th CRSI Symposium held at IIT Bombay, 3-5 Feb 2006.